

Cover Page



Universiteit Leiden



The following handle holds various files of this Leiden University dissertation:

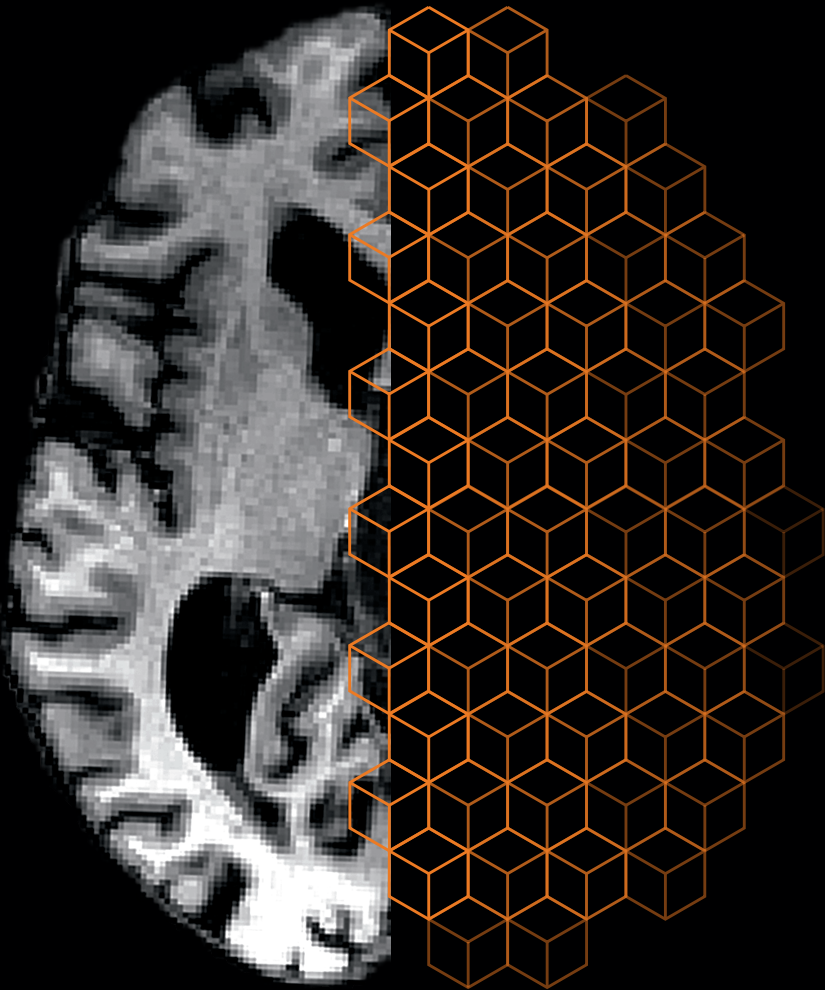
<http://hdl.handle.net/1887/74010>

Author: Coppen, E.M.

Title: Structure and function of the cerebral cortex in Huntington's disease

Issue Date: 2019-06-05

Structure and function of the cerebral cortex in Huntington's disease



Emma Coppen

Structure and function of the cerebral cortex in **Huntington's disease**

Emma Coppen

ISBN: 978-94-6375-384-5

Cover design: Lars de Groot

Lay-out: Esther Beekman (www.estherontwerpt.nl)

Printed by: Ridderprint, Ridderkerk

Cover: The cover of this thesis depicts a transversal T1 MRI image from a Huntington's disease patient that participated in one of the studies at the Leiden University Medical Center that is described in this thesis.

Printing of this thesis was financial supported by the University of Leiden, the Netherlands, Stichting Alkemade-Keuls, ChipSoft B.V and Vereniging van Huntington.

© 2019 Emma Coppen

All rights reserved. No part of this dissertation may be reprinted, reproduced, or utilized in any form or by any electronic, mechanical, or other means, now known or hereafter invented, including photocopying and recording or any information storage or retrieval system, without prior written permission of the author.

Structure and function of the cerebral cortex in **Huntington's disease**

Proefschrift

ter verkrijging van
de graad van Doctor aan de Universiteit Leiden,
op gezag van Rector Magnificus prof. mr. C.J.J.M. Stolker,
volgens besluit van het College voor Promoties
te verdedigen op woensdag 5 juni 2019
klokke 16.15 uur

door
Emma Marja Coppen

geboren te Amsterdam
1987

Promotor

Prof. dr. R.A.C. Roos

Copromotor

Dr. J. van der Grond

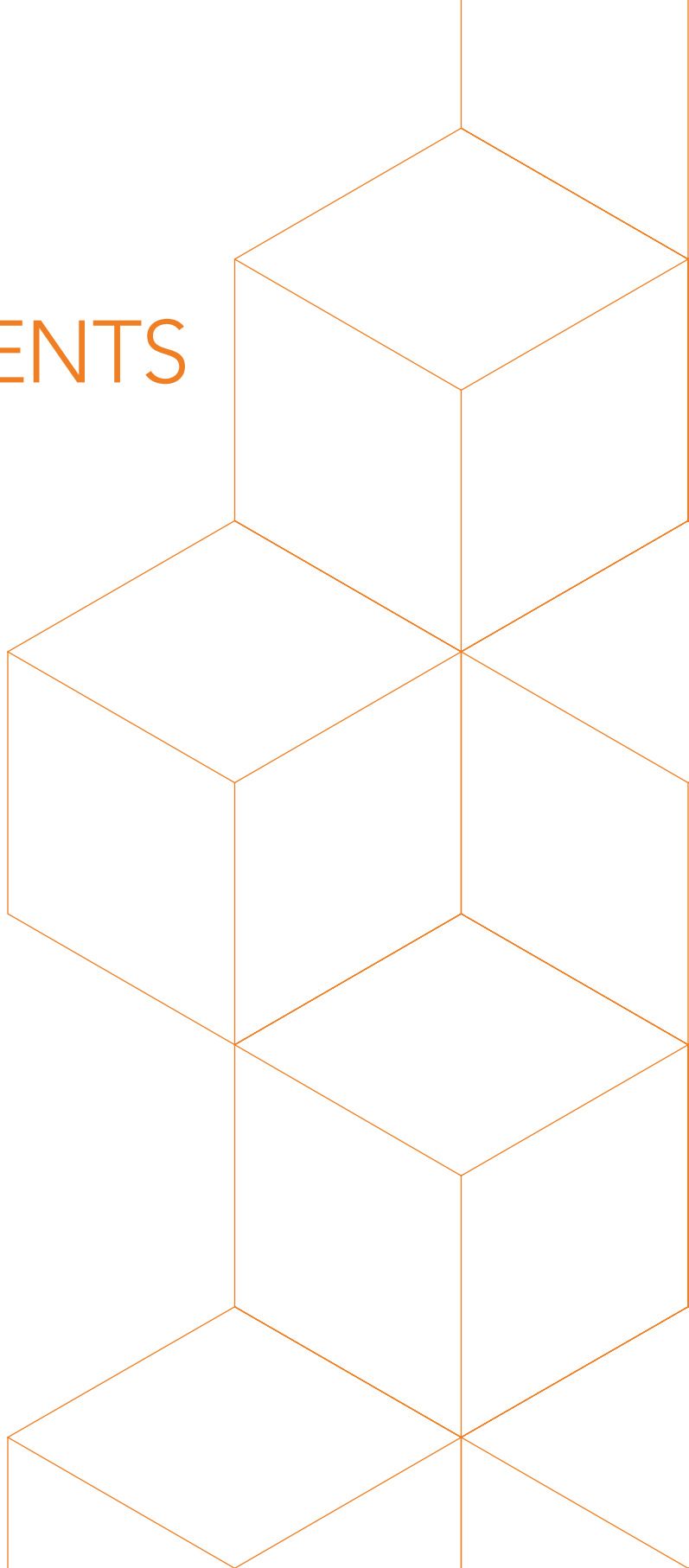
Leden promotiecommissie

Prof. dr. J. G. van Dijk

Prof. dr. H.A.M. Middelkoop

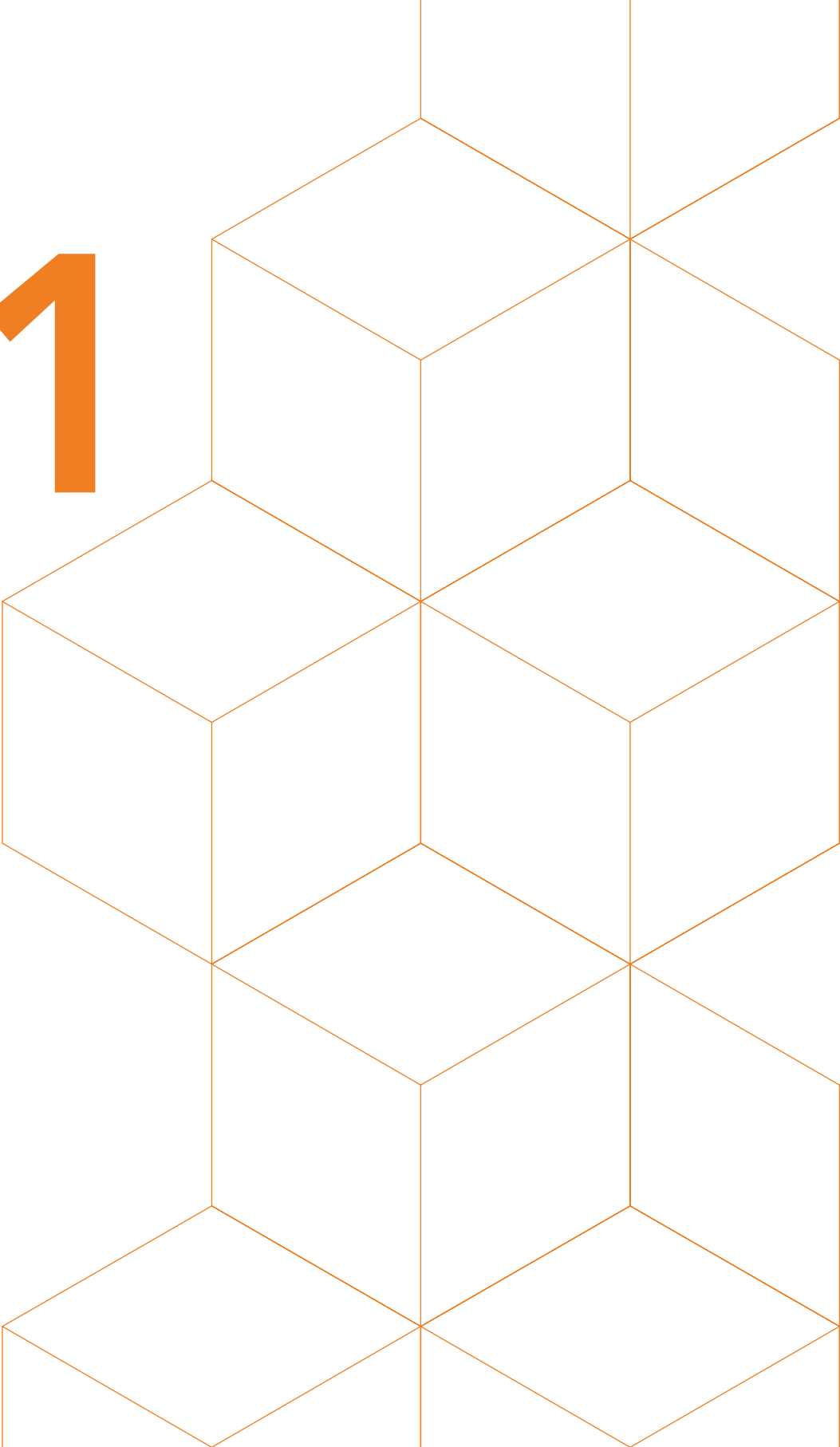
Prof. dr. M.A.J. de Koning-Tijssen (Rijksuniversiteit Groningen)

CONTENTS

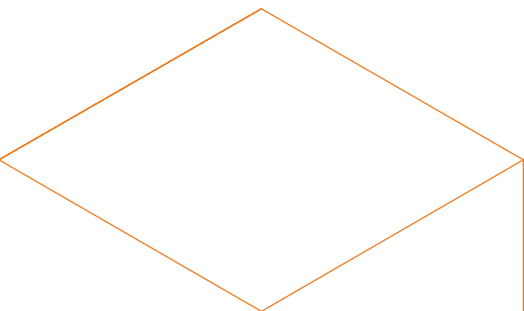


Chapter 1	General introduction	9
Chapter 2	Grey matter volume loss is associated with specific clinical motor signs in Huntington's disease <i>Parkinsonism and Related Disorders. 2018 Jan;46:56-61</i>	19
Chapter 3	Early grey matter changes in structural covariance networks in Huntington's disease <i>NeuroImage: Clinical. 2016 Oct;12:806-814</i>	37
Chapter 4	Patterns of corticostriatal degeneration in early Huntington's disease patients <i>Submitted</i>	63
Chapter 5	The visual cortex and visual cognition in Huntington's disease: an overview of current literature <i>Behavioural Brain Research. 2018 May;351:63-74</i>	79
Chapter 6	Structural and functional changes of the visual cortex in early Huntington's disease <i>Human Brain Mapping. 2018 Dec;39:4776-4786</i>	111
Chapter 7	The visual pathway in Huntington's disease; a diffusion tensor imaging and neurophysiological study <i>Submitted</i>	139
Chapter 8	Summary, discussion and future perspectives	157
Samenvatting		170
List of publications		176
Dankwoord		178
Curriculum Vitae		180

1



General introduction



Huntington's disease (HD) is a progressive autosomal dominant inherited neurodegenerative disorder, with an estimated prevalence of 5 – 10 per 100,000 in the Caucasian population.^{1,2} In the Netherlands, there are approximately 1,700 individuals with genetically confirmed HD and 6,000 to 9,000 individuals that potentially have the disease but have not been tested.

In 1993, it was discovered that HD is caused by a cytosine-adenine-guanine (CAG) trinucleotide repeat expansion located on the short arm of chromosome 4p16.3 in the Huntingtin gene, which encodes the huntingtin protein.³ Expanded repeat lengths above 36 units cause a mutation in the Huntingtin gene, which inevitably leads to clinical signs of HD, whereas in the normal population the repeat length ranges from 6 to 35 units.² When the disease progresses, the mutant huntingtin aggregates within different compartments of nerve cells (e.g., in the nucleus, cytoplasm and axons), resulting in cell toxicity and neuronal dysfunction.^{2,4}

There is currently no effective treatment available to delay or prevent disease progression. As a result, physicians are focused on improving daily functioning by reducing symptom severity to maintain a good quality of life for the patient and their caregivers.⁵

CLINICAL FEATURES

HD is characterized by progressive motor dysfunction, cognitive decline and behavioral changes,^{1,2} and is often accompanied by weight loss and sleep disturbances.^{6,7} Still, the presence and severity of symptoms is very heterogeneous among individuals. Disease onset varies between the ages of 30 and 50 years with a mean disease duration of 17 to 20 years, although the disease can also occur in early childhood (juvenile HD) or later in life (late onset HD).^{1,8} Longer CAG repeat lengths are associated with early clinical disease onset and more rapid progression.^{1,2} Clinical disease onset is typically defined by the manifestation of characteristic motor signs, which are divided into involuntary movements such as chorea, dystonia, and tics, and impaired voluntary movements resulting in hypokinesia and apraxia.^{1,9} Chorea is the most recognized sign and can be described as unwanted, irregular movements of the extremities and facial jerking.⁹ The occurrence and severity of choreiform movements can vary from subtle movements of the eyebrows or upper face to more generalized contractions of the trunk and limbs.⁹ Dystonia is often present in more advanced stages of the disease and is defined as intermittent muscle contractions leading to abnormal posture of the trunk and extremities.¹⁰ Ultimately, motor symptoms will interfere with speech, swallowing, and gait stability.¹

In general, HD gene carriers are considered to be clinically manifest based on the presence of motor signs that are related to HD, whereas premanifest HD gene carriers are defined as individuals with a confirmed expanded CAG repeat before the occurrence of substantial motor signs.¹¹ Still, cognitive deterioration can already be present before the onset of motor symptoms, which progresses throughout the course of the disease and eventually results in dementia.¹¹ Frequently reported early cognitive deficits include impairments in executive functioning (i.e., difficulties with planned behavior, attentional deficits and disinhibition), psychomotor speed, and emotion recognition.^{2,11,12} The majority of HD gene carriers additionally experience behavioral changes during their lifetime.¹³ Depression, irritability, aggression, obsessive-compulsive behavior, and apathy are the most frequently reported neuropsychiatric symptoms in HD.¹³

Patients become increasingly dependent in daily life, which interferes with social activities. Eventually, severe motor disturbances and behavioral changes are often the main reasons for nursing home placement.¹⁴

NEUROPATHOLOGY

Progressive neurodegeneration bilateral in the striatum, i.e., caudate nucleus, putamen, and nucleus accumbens, is the main neuropathological feature of HD.¹⁵ Striatal degeneration is caused by an extensive loss of medium spiny projection neurons that form the main efferent output of the striatum towards cortical brain regions.^{4,15} The presence of neuronal loss and reactive astrogliosis is, therefore, often suggested as an explanation for the clinical signs in HD.^{15,16} Neuronal loss progresses along a dorsal-ventral and medial-lateral gradient, with the most early microscopic changes occurring in the body and tail of the caudate nucleus.^{4,15} In addition to striatal atrophy, post-mortem studies have shown severe widespread cortical atrophy.^{4,17–20} In advanced disease stages, brain weight is often reduced to 1,000 – 1,100 grams while the average normal brain weight is 1,300 to 1,500 grams.²⁰

Still, it remains uncertain if cortical degeneration precedes or is secondary to striatal neuronal loss in HD and how this relates to the clinical features of HD.

BRAIN STRUCTURE AND FUNCTION

Magnetic Resonance Imaging (MRI) is a non-invasive and objective approach to quantify *in vivo* alterations in brain structure and function. In general, structural imaging modalities such as T1-weighted images and diffusion tensor imaging (DTI), measure global and regional brain volume and the microstructure of white matter fiber tracts, while functional imaging modalities assess neural activity and cell (dys-)function by detecting changes in cerebral blood flow in rest or when performing tasks.

For the diagnosis of HD, genetic testing is the gold standard. Therefore, MRI is not of diagnostic value in clinical practice. Occasionally, MRI is used to exclude other disorders in case of an atypical presentation or absent family history of HD.²¹

In HD research, MRI is primarily used as a tool to evaluate the natural progression of the disease and to find biomarkers that can be used as an outcome measure in clinical trials.^{21,22} Structural imaging studies have mainly focused on changes in striatal volume and consistently observed atrophy of both caudate nucleus and putamen.^{22,23} Striatal atrophy is even found a decade before predicted disease onset in premanifest HD gene carriers,²⁴ with a relatively linear rate of decline throughout the course of the disease.²⁵ As a result, striatal volume is now frequently used as a marker for disease severity, to predict time to diagnosis, or as an outcome measure in clinical intervention trials.

In addition to striatal atrophy, volumes of other subcortical and cortical brain regions are also vulnerable for degeneration early in the disease,^{11,26,27} but have been studied less extensively. In clinical manifest disease stages, early cortical atrophy is thought to originate in the superior and posterior cerebral cortex, primarily in the parietal and occipital lobes, and spreads throughout the entire cortex in more advanced stages.^{11,26} Atrophy of the pallidum and nucleus accumbens is found in premanifest stages of the disease,²⁷ but there is some controversy regarding cortical involvement in this stage. Several studies report cortical volume loss in premanifest HD gene carriers which is primarily localized in the posterior frontal, parietal and occipital brain regions,^{11,28} whereas other studies report no changes, or even an increase of cortical grey matter volume in premanifest HD compared to controls.^{29,30}

There is additional evidence that besides brain atrophy, the clinical manifestation of HD also results from neuronal dysfunction, tissue repair, and circuitry reorganization that can be measured using task-based or resting-state functional MRI.³¹ Here, changes in the blood-oxygen-level-dependent (BOLD) signal are used to discriminate between brain regions with altered activations. In HD, functional imaging studies

showed reduced brain activity (e.g., cellular dysfunction) in heterogeneous cortical and subcortical areas after cognitive task performance (such as working memory and attentional tasks) and at rest.^{31–33} Changes in functional brain networks can even be found independent of brain atrophy, implying that cellular dysfunction precedes cell death in HD.³¹ However, the pattern of cortical dysfunction, the influence of structural and functional cortical degeneration on the clinical signs of HD, and associations with striatal atrophy are not yet identified.

AIMS OF THIS THESIS

The primary aim of this thesis is to examine alterations in the cerebral cortex in HD gene carriers. Different image modalities and approaches will be used to extend the knowledge on both structural and functional cortical brain changes in early disease stages and their relation to the clinical features of HD.

First, to examine the influence of brain changes on the motor phenotype in HD, we aimed to identify associations between grey matter loss and motor symptoms in early stage HD patients (**chapter 2**). To further explore the cortical coherence, we aimed to investigate alterations in grey matter brain regions using a novel technique to identify structural covariance networks in controls, premanifest and manifest HD gene carriers (**chapter 3**). In **chapter 4**, we wanted to investigate corticostriatal circuitry in HD by assessing the pattern of cortical degeneration and the relationship with striatal degeneration in early manifest disease stages.

An overview of the current literature regarding brain structure and function of the visual cortex and visual cognitive impairment in HD is presented in **chapter 5**. Here, the aim was to summarize the findings on clinical visual cognitive deficits and underlying structural and functional changes in the posterior cerebral cortex in HD.

Based on the findings reported in chapter 5, we conducted a cross-sectional study in a cohort of controls, premanifest HD gene carriers and manifest HD gene carriers. The aim was to investigate changes in structure and function of the posterior cerebral cortex in different disease stages and examine the relation with visual cognitive impairments. The findings of this study are described in **chapters 6 and 7**. Conclusions, final remarks on the findings of this thesis, and future perspectives are presented in **chapter 8**.

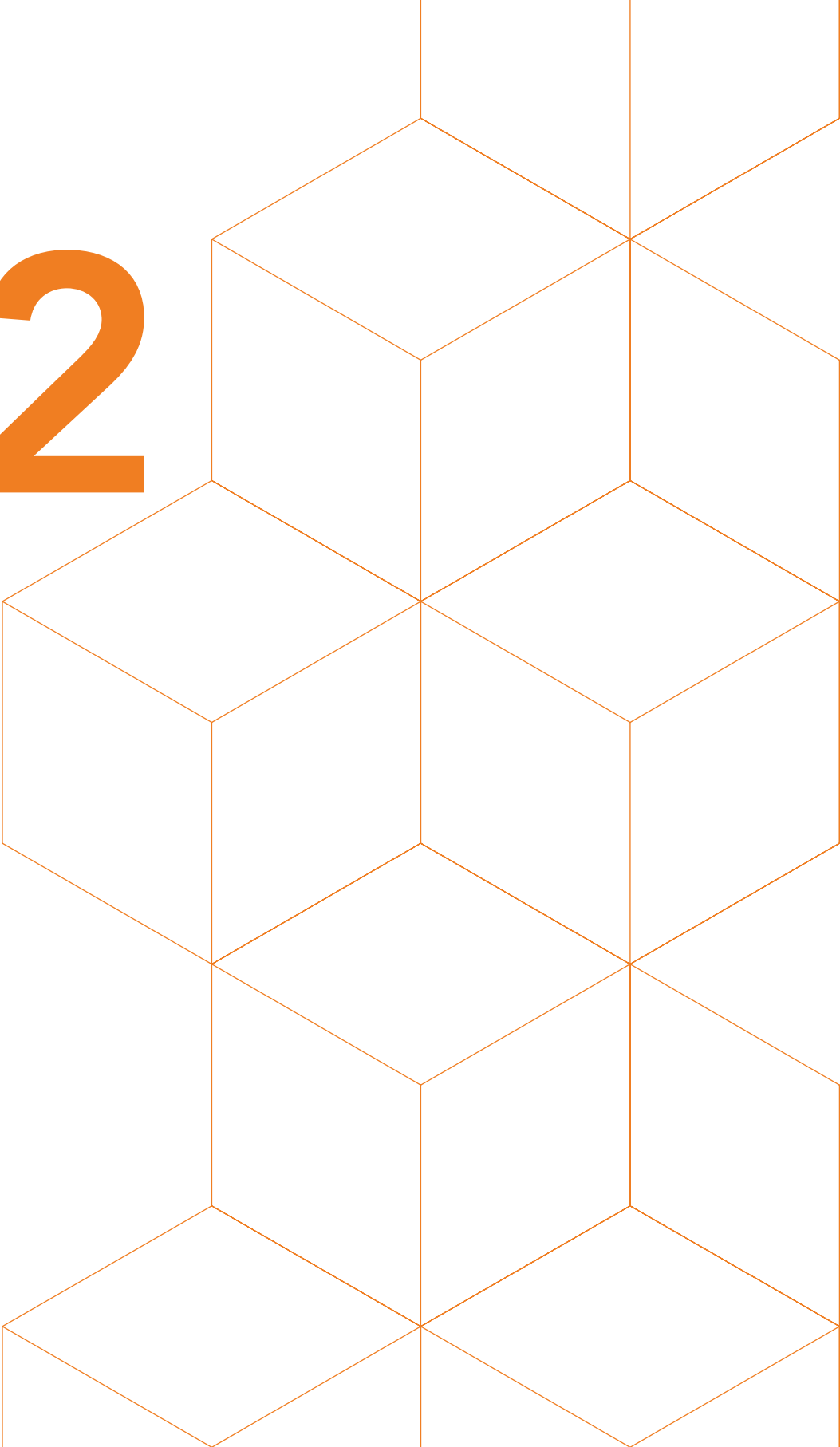
REFERENCES

1. Roos RAC. Huntington's disease: a clinical review. *Orphanet J Rare Dis.* 2010;5(1):40.
2. Bates GP, Dorsey R, Gusella JF, et al. Huntington disease. *Nat Rev Dis Prim.* 2015;1:1-21.
3. The Huntington's Disease Collaborative Research Group. A novel gene containing a trinucleotide repeat that is expanded and unstable on Huntington's disease chromosomes. *Cell.* 1993;72(6):971-983.
4. Rüb U, Seidel K, Heinsen H, Vonsattel JP, den Dunnen WF, Korf HW. Huntington's disease (HD): the neuropathology of a multisystem neurodegenerative disorder of the human brain. *Brain Pathol.* 2016;26:726-740.
5. Burgunder JM, Guttman M, Perlman S, Goodman N, van Kammen DP, Goodman L. An International Survey-based Algorithm for the Pharmacologic Treatment of Chorea in Huntington's Disease. *PLOS Curr Huntingt Dis.* 2011;Sep 2(Edition 1):1-24.
6. Aziz NA, van der Burg JMM, Landwehrmeyer GB, Brundin P, Stijnen T, Roos RAC. Weight loss in Huntington disease increases with higher CAG repeat number. *Neurology.* 2008;71:1506-1513.
7. Aziz NA, Anguelova GV, Marinus J, Lammers GJ, Roos RAC. Sleep and circadian rhythm alterations correlate with depression and cognitive impairment in Huntington's disease. *Park Relat Disord.* 2010;16:345-350.
8. Rosenblatt A, Kumar BV, Mo A, Welsh CS, Margolis RL, Ross CA. Age, CAG repeat length, and clinical progression in Huntington's disease. *Mov Disord.* 2012;27(2):272-276.
9. Jankovic J, Roos RAC. Chorea associated with Huntington's disease: To treat or not to treat? *Mov Disord.* 2014;29(11):1414-1418.
10. Albanese A, Bhatia K, Bressman SB, et al. Phenomenology and classification of dystonia : A consensus update. *Mov Disord.* 2013;28(7):863-873.
11. Tabrizi SJ, Langbehn DR, Leavitt BR, et al. Biological and clinical manifestations of Huntington's disease in the longitudinal TRACK-HD study: cross-sectional analysis of baseline data. *Lancet Neurol.* 2009;8(9):791-801.
12. Dumas EM, van den Bogaard SJA, Middelkoop HAM, Roos RAC. A review of cognition in Huntington s disease. *Front Biosci.* 2013;S5:1-18.
13. van Duijn E, Craufurd D, Hubers AAM, et al. Neuropsychiatric symptoms in a European Huntington's disease cohort (REGISTRY). *J Neurol Neurosurg Psychiatry.* 2014;85(12):1411-1418.
14. Wheelock VL, Tempkin T, Marder K, et al. Predictors of nursing home placement in Huntington disease. *Neurology.* 2003;60(6):998-1001.
15. Vonsattel JP, Myers RH, Stevens TJ, Ferrante RJ, Bird ED, Richardson EP. Neuropathological classification of Huntington's disease. *J Neuropathol Exp Neurol.* 1985;44(6):559-577.

16. Reiner A, Albin RL, Anderson KD, D'Amato CJ, Penney JB, Young AB. Differential loss of striatal projection neurons in Huntington disease. *Proc Natl Acad Sci U S A*. 1988;85(15):5733-5737.
17. de la Monte S, Vonsattel J, Richardson E. Morphometric demonstration of atrophic changes in cerebral cortex, white matter and neostriatum in Huntington's disease. *J Neuropathol Exp Neurol*. 1988;47(5):516-525.
18. Lange H. Quantitative changes of telencephalon, diencephalon, and mesencephalon in Huntington's chorea, postencephalitic, and idiopathic parkinsonism. *Verh Anat Ges*. 1981;75:923-925.
19. Nana AL, Kim EH, Thu DCV, et al. Widespread heterogeneous neuronal loss across the cerebral cortex in Huntington's disease. *J Huntingtons Dis*. 2014;3:45-64.
20. Waldvogel HJ, Kim EH, Thu DCV, Tippett LJ, Faull RLM. New perspectives on the neuropathology in Huntington's disease in the human brain and its relation to symptom variation. *J Huntingtons Dis*. 2012;1:143-153.
21. van den Bogaard SJA, Roos RAC. Chapter 19 Imaging in Huntington's disease. In: Saba L, ed. *Imaging in Neurodegenerative Disorders*. First Edit. Oxford University Press; 2015:303-315.
22. Bohanna I, Georgiou-Karistianis N, Hannan AJ, Egan GF. Magnetic resonance imaging as an approach towards identifying neuropathological biomarkers for Huntington's disease. *Brain Res Rev*. 2008;58(1):209-225.
23. Aylward EH. Magnetic resonance imaging striatal volumes: A biomarker for clinical trials in Huntington's disease. *Mov Disord*. 2014;29(11):1429-1433.
24. Aylward EH, Liu D, Nopoulos PC, et al. Striatal volume contributes to the prediction of onset of Huntington disease in incident cases. *Biol Psychiatry*. 2012;71(9):822-828.
25. Aylward EH, Nopoulos PC, Ross CA, et al. Longitudinal change in regional brain volumes in prodromal Huntington disease. *J Neurol Neurosurg Psychiatry*. 2011;82(4):405-410.
26. Rosas HD, Salat DH, Lee SY, et al. Cerebral cortex and the clinical expression of Huntington's disease: complexity and heterogeneity. *Brain*. 2008;131(4):1057-1068.
27. van den Bogaard SJA, Dumas EM, Acharya TP, et al. Early atrophy of pallidum and accumbens nucleus in Huntington's disease. *J Neurol*. 2011;258(3):412-420.
28. Nopoulos PC, Aylward EH, Ross CA, et al. Cerebral cortex structure in prodromal Huntington disease. *Neurobiol Dis*. 2010;40(3):544-554.
29. Kipps CM, Duggins AJ, Mahant N, Gomes L, Ashburner J, McCusker EA. Progression of structural neuropathology in preclinical Huntington's disease: a tensor based morphometry study. *J Neurol Neurosurg Psychiatry*. 2005;76(5):650-655.
30. Paulsen JS, Magnotta VA, Mikos AE, et al. Brain structure in preclinical Huntington's disease. *Biol Psychiatry*. 2006;59(1):57-63.
31. Paulsen JS. Functional imaging in Huntington's disease. *Exp Neurol*. 2009;216(2):272-277.

32. Wolf RC, Grön G, Sambataro F, et al. Brain activation and functional connectivity in premanifest Huntington's disease during states of intrinsic and phasic alertness. *Hum Brain Mapp.* 2012;33(9):2161-2173.
33. Dumas EM, van den Bogaard SJA, Hart EP, et al. Reduced functional brain connectivity prior to and after disease onset in Huntington's disease. *NeuroImage Clin.* 2013;2(1):377-384.

2

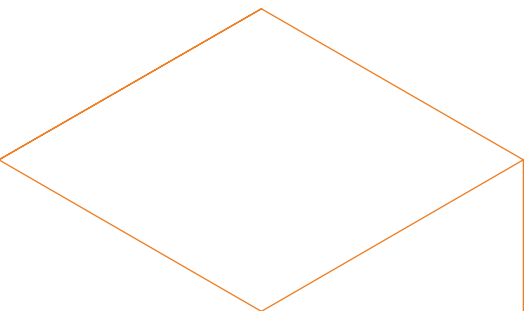


Grey matter volume loss is associated with specific clinical motor signs in **Huntington's disease**

Emma M. Coppen *, Milou Jacobs *,
Annette A. van den Berg-Huysmans,
Jeroen van der Grond, Raymund A.C. Roos

Parkinsonism and Related Disorders. 2018 Jan; 46:56-61

*These authors contributed equally



ABSTRACT

Background: Motor disturbances are clinical hallmarks of HD and involve chorea, dystonia, hypokinesia and visuomotor dysfunction. Investigating the association between specific motor signs and different regional volumes is important to understand the heterogeneity of HD.

Objectives: To investigate the motor phenotype of Huntington's disease (HD) and associations with subcortical and cortical grey matter volume loss.

Methods: Structural T1-weighted MRI scans of 79 HD patients and 30 healthy controls were used to calculate volumes of seven subcortical structures including the nucleus accumbens, hippocampus, thalamus, caudate nucleus, putamen, pallidum and amygdala. Multiple linear regression analyses, corrected for age, gender, CAG, MRI scan protocol and normalized brain volume, were performed to assess the relationship between subcortical volumes and different motor subdomains (i.e., eye movements, chorea, dystonia, hypokinesia/rigidity and gait/balance). Voxel-based morphometry analysis was used to investigate the relationship between cortical volume changes and motor signs.

Results: Subcortical volume loss of the accumbens nucleus, caudate nucleus, putamen, and pallidum were associated with higher chorea scores. No other subcortical region was significantly associated with motor symptoms after correction for multiple comparisons. Voxel-based cortical grey matter volume reductions in occipital regions were related with an increase in eye movement scores.

Conclusion: In HD, chorea is mainly associated with subcortical volume loss, while eye movements are more related to cortical volume loss. Both subcortical and cortical degeneration has an impact on motor impairment in HD. This implies that there is a widespread contribution of different brain regions resulting in the clinical motor presentation seen in HD patients.

1. INTRODUCTION

Huntington's disease (HD) is an autosomal-dominant, neurodegenerative disorder characterized by progressive motor disturbances, cognitive impairment and psychiatric symptoms. The clinical diagnosis of HD is based on the presence of motor signs, and can involve chorea, dystonia and/or hypokinesia.¹ Oculomotor dysfunction, such as saccadic eye movements or gaze paralysis, can also be prominent in premanifest and early HD.² The clinical HD phenotype is heterogeneous and different motor signs can also co-exist.³ Longitudinal analysis of motor signs showed that choreatic movements decrease over time, whereas hypokinetic-rigid signs slightly increase.⁴ This suggests that different motor symptoms can be more pronounced during different disease stages. The Unified HD Rating Scale Total Motor Score (UHDRS-TMS)⁵ is the gold standard to evaluate motor functioning in HD and establish the clinical diagnosis. Here, several motor domains including chorea, dystonia, gait, rigidity, and eye movements are examined, with higher total scores indicating more motor dysfunction.

Although striatal atrophy is the main neuropathological finding in HD, neuronal loss has been identified in many other extrastriatal brain regions.⁶ In these regions, it has been shown that grey matter volume reductions may also be associated with decreased global motor and functional scores.⁷⁻¹¹

Instead of focusing on global motor functioning, we aimed to investigate associations between separate motor domains and grey matter volume changes. To monitor HD signs in clinical practice and intervention trials, it is important to further understand the pathophysiology underlying the HD phenotype, because this can vary among patients.

2. METHODS

2.1 Participants

A total of 79 patients with manifest HD and 30 healthy controls who visited the outpatient clinic at the department of Neurology of the Leiden University Medical Center (LUMC) between January 2008 and June 2016 were included. All manifest HD had a genetically confirmed CAG repeat length of ≥ 39 and an UHDRS-TMS of more than 5, confirming the diagnosis and clinical motor presence of HD. The local ethical committee approved this study and written informed consent was obtained from all participants.

Distinctive items of the UHDRS motor scale were added for each participant to establish total scores per motor subdomain based on previous studies,^{4,12,13} representing five domains of motor functioning. For further details, see supplementary Table S1.

2.2 MRI image acquisition

All participants underwent MRI scanning on a 3 Tesla MRI scanner (Philips Achieva, Best, the Netherlands). For each participant, a structural three-dimensional T1-weighted image was acquired. Imaging parameters of the scan protocols were: TR = 7.7 ms, TE = 3.5 ms, flip angle = 8°, FOV 24 cm, matrix size 224 x 224 cm and 164 sagittal slices to cover the entire brain with a slice thickness of 1.0 mm with no gap between slices. This resulted in a voxel size of 1,07 mm x 1,07 mm x 1,0 mm.

2.3 Image post-processing

Functional Magnetic Resonance Imaging of the Brain (FMRIB) Software Library (FSL, version 5.0.8, Oxford, United Kingdom) was used for data analysis of all structural T1-weighted images.¹⁴ Brain tissue volume, normalized for individual head size, was estimated with SIENAX.¹⁵ Using SIENAX, brain and skull images were extracted from the single whole-head input data. Then, the brain image is affine-registered to Montreal Neurological Institute (MNI) 152-space standard image,¹⁶ using the skull image to determine the registration scaling. This volumetric scaling factor was used to normalize for head size. Next, tissue-type segmentation with partial volume estimation was performed in order to calculate the total volume of normalized brain tissue, including separate estimates of volumes of grey matter, white matter, peripheral grey matter and ventricular CSF for each HD patient. Visual inspection of the registration and segmentation was performed for each brain-extracted image.

2.4 Subcortical volumes

Absolute volumes of seven subcortical structures (i.e., nucleus accumbens, hippocampus, thalamus, caudate nucleus, putamen, pallidum and amygdala) were measured using FMRIB's integrated registration and segmentation tool (FIRST).¹⁷ Here, all non-brain tissue was removed from the T1-weighted images using a semi-automated brain extraction tool that is implemented in FSL.¹⁸ After registration of the images to the MNI 152-standard space image, using linear registration with 12° of freedom, segmentation of the subcortical regions was carried out using mesh models that were constructed from manually segmented images provided by the Center for Morphometric Analysis (CMA), Massachusetts General Hospital, Boston. Then, the volume for each structure was separately estimated. Visual inspection was performed for each output image during the registration and segmentation steps.

2.5 Voxel-based morphometry

To investigate voxel-wise differences in grey matter volume between HD patients and controls, voxel-based morphometry (VBM) analysis was performed as implemented in FSL.¹⁹

First, brain extracted T1-weighted images were segmented into different tissue types (i.e., grey matter, white matter or cerebrospinal fluid). Each segmented image has values that indicate the probability of a given tissue type. Then, the grey matter images were aligned to the 2 mm MNI-152 standard space image using non-linear registration. The resulting images were averaged to create a study-specific grey matter template. Subsequently, all native grey matter images were non-linearly registered to this study-specific template and 'modulated' to correct for local enlargements and contractions due to the non-linear component of the spatial transformation.²⁰ The modulated grey matter images were finally smoothed with an isotropic Gaussian kernel with a sigma of 3 mm and analyzed using a general linear model in FSL for statistical inference.

Brain structures that showed a significant difference between groups were identified using the Harvard-Oxford atlas integrated in FSL.

2.6 Statistical analyses

Group differences between HD patients and controls were analyzed using parametric (independent sample t-test) and non-parametric tests (χ^2 -test) when applicable. To analyze group differences in the VBM output, a general linear model was constructed in FSL to compare controls with manifest HD using two-tailed t-statistics with age, gender, normalized brain volume and MRI scan protocol as covariates. Voxel-wise non-parametric permutation testing with 5000 permutations was performed using FSL randomise.²¹ The Threshold-Free Cluster Enhancement (TFCE) technique was used to correct for multiple comparisons with family wise error,²² with a p -value < 0.05 as significant threshold. The regions that showed significant differences between HD patients and controls were selected for further analyses in the HD group only.

The following analyses, investigating the relationship between separate motor subdomains, subcortical and cortical brain volumes, were performed in HD patients only. Multiple linear regression analyses were used to investigate the relationship between the separate motor subdomains and subcortical brain volumes. Analyses were accounted for age, gender, CAG repeat length, normalized brain volume, and MRI scan protocol. To correct for multiple comparisons the p -value for statistical significance was set at $p < 0.008$ (0.05/6) for analyses of subcortical volumes. To assess the relationship between clinical motor scores and cortical grey matter changes in HD patients, a general linear model was constructed using a design matrix in FSL with

each clinical motor domain separately, correcting for age, gender, CAG repeat length, normalized brain volume, and MRI scan protocol. FSL-Randomise was used for voxel-wise non-permutation testing,²¹ using the regions that showed significant grey matter changes between controls and HD patients as a grey matter mask. Again, the TFCE technique was used to correct for multiple comparisons with family wise error,²² with a p -value < 0.05 as significant threshold. Statistical analyses were performed using IBM SPSS 23.0 for Windows.

3. RESULTS

Group characteristics and comparisons between HD patients and controls are reported in Table 1. There were no significant differences in age and gender between both groups. HD patients had a significantly higher mean UHDRS-TMS compared to the control group.

3.1 Subcortical volumes

The mean volumes of the accumbens nucleus, caudate nucleus, putamen, pallidum, thalamus and hippocampus were significantly lower in manifest HD compared to controls (Table 1). Since the mean volume of the amygdala did not differ between HD patients and controls, this structure was not included in further analyses in HD patients only.

After correction for multiple comparisons, there was a significant association between the UHDRS chorea score and UHDRS-TMS with the accumbens nucleus, caudate nucleus, putamen and pallidum in HD patients (Table 2). Thalamus and hippocampus volumes did not show any association with UHDRS motor subdomains.

3.2 Cortical grey matter volume

To assess differences in cortical grey matter volume between HD patients and controls, regional volumetric VBM analysis was performed. Significant grey matter volume reduction in HD patients was found in the motor cortex, visual cortex, and in the frontal and temporal lobes (Figure 1 and supplementary Table S2).

In HD patients, VBM analysis showed that after correction for covariates and multiple comparisons, higher eye movement scores and UHDRS-TMS were associated with cortical volume loss of occipital regions (Figure 2 and supplementary Table S3).

TABLE 1 Clinical and volumetric group differences between HD patients and controls

	HD (n= 79)	Controls (n=30)	p-value
Clinical characteristics			
Age	46.5 (9.7; 28 – 65)	48.9 (8.4; 35 – 65)	0.229
Gender m/f (%m)	30/49 (38.0%)	14/16 (46.7%)	0.409
CAG	44.1 (2.4; 40 – 51)	NA	NA
Disease duration	3.3 (3.0; 0 – 13)	NA	NA
Disease burden	382.1 (77.8; 234 – 551)	NA	NA
UHDRS-TMS	17.8 (10.8; 6 – 45)	2.6 (2.4; 0 – 7)	<0.001
UHDRS chorea	5.2 (4.8; 0 – 18)	NA	NA
UHDRS hypokinetic-rigid	4.6 (3.2; 0 – 12)	NA	NA
UHDRS dystonia	0.2 (0.6; 0 – 3)	NA	NA
UHDRS eye movements	4.9 (3.2; 0 – 13)	NA	NA
UHDRS gait/balance	1.8 (1.4; 0 – 6)	NA	NA
Subcortical structures			
Accumbens nucleus	732.0 (188.0)	930.5 (207.0)	<0.001
Caudate nucleus	4942.2 (997.5)	6695.4 (839.0)	<0.001
Amygdala	2208.0 (528.5)	2163.4 (379.4)	0.673
Putamen	7093.0 (1229.1)	9280.0 (1289.7)	<0.001
Pallidum	2749.8 (555.8)	3338.5 (471.4)	<0.001
Thalamus	13958.0 (1551.3)	14844.2 (1383.7)	<0.005
Hippocampus	7195.4 (1016.0)	7682.1 (818.3)	0.021

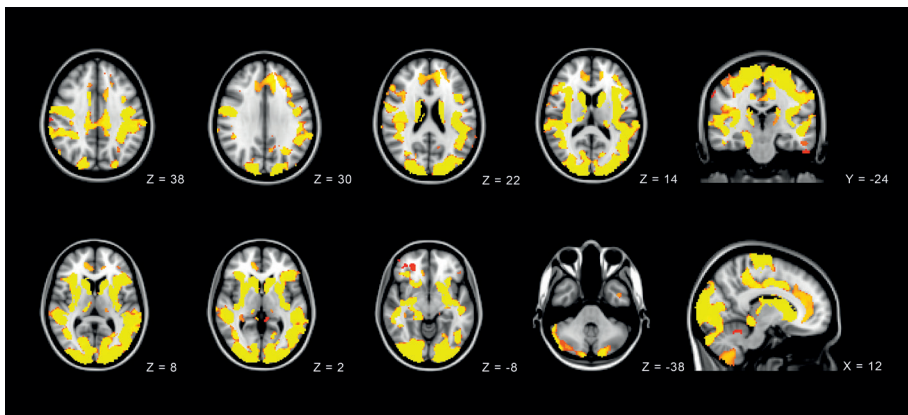
Data are mean (SD; range) or number (%) for gender. Volumes of subcortical structures are expressed in mm³. Mean disease duration is based on a smaller sample size (n=65) due to missing data. Independent sample t-test was used to compare groups, except for gender (χ^2 -test). Statistically significant p-values are highlighted in bold ($p < 0.05$). NA = Not applicable; CAG = Cytosine-Adenine-Guanine; HD = Huntington's Disease; UHDRS = Unified Huntington's Disease Rating Scale; TMS = Total Motor Score.

TABLE 2 Relationship between UHDRS motor subdomains and subcortical brain volumes

	Accumbens nucleus	Caudate nucleus	Putamen	Pallidum	Thalamus	Hippocampus
UHDRS-TMS	-0.283	-0.316	-0.279	-0.312	-0.096	-0.265
UHDRS chorea	-0.260	-0.346	-0.275	-0.273	-0.045	-0.172
UHDRS hypokinetic-rigid	-0.180	-0.118	-0.175	-0.156	-0.052	-0.179
UHDRS dystonia	-0.075	-0.033	-0.012	0.076	0.056	0.047
UHDRS eye movements	-0.188	-0.212	-0.171	-0.239	-0.169	-0.240
UHDRS gait/balance	-0.097	-0.056	-0.112	-0.214	-0.057	-0.245

Reported data are standardized coefficients (standardized beta) from the multiple linear regression analysis. Analyses were accounted for age, gender, CAG, MRI scan protocol, and normalized brain volume. Statistically significant values are printed in bold (corrected for multiple comparisons, $p < 0.008$). UHDRS = Unified Huntington’s Disease Rating Scale; TMS = Total Motor Score

FIGURE 1 Voxel based morphometry analysis between manifest HD and controls



Brain regions that showed significant differences in grey matter volume in manifest HD compared to controls by means of voxel-based morphometry (VBM) are presented. Age, gender, MRI study protocol and normalized brain volume were included as covariates in the statistical model. Identified grey matter regions are overlaid on sagittal, transversal and coronal slices of Montreal Neurological Institute (MNI)-152 standard space T1-weighted images. Corresponding MNI x-, y-, z- coordinates are displayed. A threshold of $p < 0.05$ (corrected with TFCE family wise error) is used.

4. DISCUSSION

Our study showed that specific clinical motor signs in manifest HD are related to volume loss in different grey matter brain regions. Higher UHDRS chorea scores were particularly related to volume loss of subcortical structures, especially the accumbens nucleus, caudate nucleus, putamen and pallidum, whereas cortical brain regions did not. These findings suggest that volume loss in the subcortical regions are more involved in the development of chorea than cortical atrophy. It is well known that the medium-sized spiny neurons located in the striatum, that comprises of the caudate nucleus and putamen, are the most affected cells in HD.²³ As these neurons are involved in motor control, this might explain the association we found between striatal volume loss and the UHDRS chorea score.

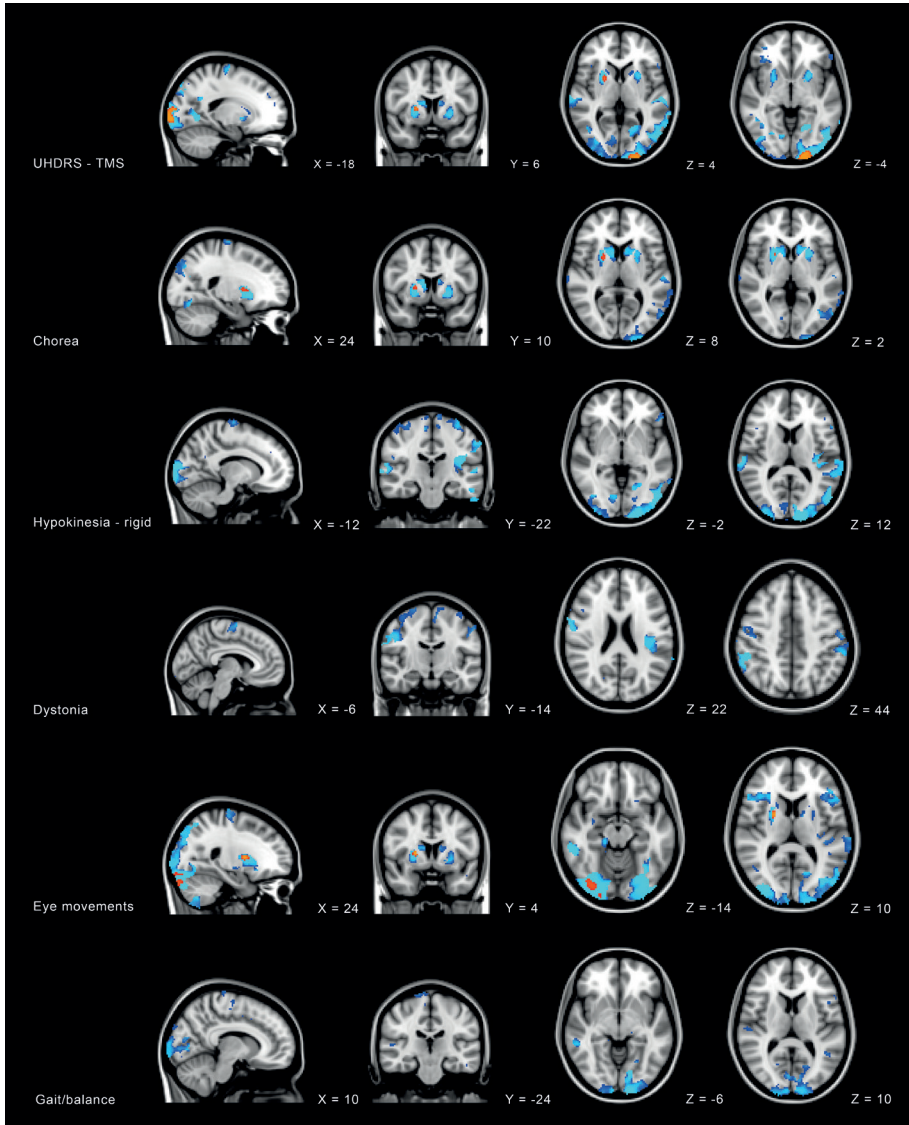
In premanifest HD, general motor functioning is related to volume loss of the putamen, caudate nucleus and pallidum.^{7,10,11} Increased choreatic movements have been associated with striatal atrophy in premanifest HD.²⁴ However, to our knowledge, no studies have been performed that examined motor domains separately in relation with both subcortical and cortical changes. In addition to striatal volume loss, we observed a correlation between volume loss of the pallidum and higher UHDRS chorea scores.

It is suggested that changes in the pallidum might be due to the loss of striato-pallidal fibers projecting from striatal medium spiny neurons, implying that volume loss of the pallidum is not due to cell loss within the pallidum.¹¹

Besides subcortical grey matter volume changes, we also investigated the association with cortical regions in patients with HD. Here, cortical grey matter volume loss was particularly associated with oculomotor dysfunction, but not with choreatic signs. Our findings are in contrast with results reported in a previous study where no correlations were found between cortical grey matter and motor functioning in premanifest HD.¹¹ A possible explanation might be that this previous study calculated lobular cortical volumes instead of investigating relationships with cortical volumes using a voxel-based technique. Another explanation could be that the HD patients included in our study were in a more advanced disease stage with more motor impairments, suggesting that involvement of cortical regions is more pronounced later in the disease. Still, UHDRS dystonia and hypokinetic-rigid scores did not show any significant correlations with subcortical volumes in our study.

The motor cortex, visual cortex, and cortical regions in the frontal and temporal lobes showed significant decrease in grey matter volume in manifest HD compared to controls by means of voxel-based morphometry. These identified regions are consistent with

FIGURE 2 Correlations between clinical motor scores and grey matter loss in manifest HD



VBM analyses showing significant correlations between increased motor scores and reduction in grey matter volume. A threshold of $p < 0.05$ is used. Brain regions in blue are uncorrected for multiple testing and red-yellow brain regions are corrected with TFCE family wise error. Results are overlaid on sagittal, transversal and coronal slices of Montreal Neurological Institute (MNI)-152 standard space T1-weighted images. Corresponding MNI x-, y-, z- coordinates are displayed. UHDRS – TMS = Unified Huntington’s Disease Rating Scale – Total Motor Score.

findings in previous voxel-based studies.^{11,25-28} Additionally, we observed volume loss in visual cortical regions, which were associated with higher eye movement scores in HD gene carriers. It is known that fronto-striatal and occipital regions are important for oculomotor control and visual processing,^{29,30} providing a possible explanation for the observed correlations in these specific motor domains. These results are comparable to other studies observing associations between volume changes and quantitative motor functioning.^{27,28}

It has also been reported that more prominent bradykinesia and dystonia are related to cortical thinning of the anterior frontal regions, including the premotor and supplementary motor cortex.^{9,28} In addition, finger tapping has been related to striatal and cortical atrophy.^{24,28} Although we investigated changes in subcortical and cortical regions separately, there is a known interplay between the basal ganglia and cerebral cortex. Especially changes of the basal ganglia-thalamo-frontal circuits are known to contribute to hyperkinetic movements such as chorea.^{11,23}

We did not find an association between some of the motor domains and grey matter regions, such as the cingulate gyrus. Since we aimed to focus on the clinical hallmark of HD, which is the presence of motor signs, this absent association might be caused by the fact that these brain regions are also involved in other domains than motor control. It has been reported that cortical brain atrophy, specifically in frontal, parietal and occipital lobes is related to a decline in cognitive functioning.^{9,27,30} Future studies investigating the relationship between cognitive and psychiatric symptoms of HD and volume reductions of the brain are necessary to further understand the pathogenesis of HD.

The lack of a relationship between dystonia and subcortical volumes in our study might also be caused by the relatively low scores on this item in our cohort of early stage HD patients. A further limitation of this study is the relatively smaller sample size of the control group, which could potentially influence the results. A larger sample size of the control group is preferred in future studies.

In conclusion, patients with HD can present with a heterogeneous motor phenotype, consisting of chorea, dystonia, hypokinesia and/or balance disturbances. Our results demonstrate that chorea, which is the clinical hallmark of HD, is strongly associated with subcortical volume loss of the striatum and pallidum and not with cortical atrophy. Oculomotor dysfunction, however, seems to be more related to cortical volume changes, especially in occipital regions. Thus, there is a widespread contribution of different brain regions resulting in the overall clinical motor presentation seen in HD patients. We showed that not only subcortical volume loss is involved in the expression of motor disturbances, but also, although to a much lesser extent, cortical degeneration.

REFERENCES

1. Roos RAC. Huntington's disease: a clinical review. *Orphanet J Rare Dis.* 2010;5(1):40.
2. Blekher TM, Yee RD, Kirkwood SC, et al. Oculomotor control in asymptomatic and recently diagnosed individuals with the genetic marker for Huntington's disease. *Vision Res.* 2004;44:2729-2736.
3. Thompson P, Berardelli A, Rothwell J., et al. The coexistence of bradykinesia and chorea in Huntington's disease and its implications for theories of basal ganglia control of movement. *Brain.* 1988;111:223-244.
4. Jacobs M, Hart EP, van Zwet EW, et al. Progression of motor subtypes in Huntington's disease: a 6-year follow-up study. *J Neurol.* 2016;263(10):2080-2085.
5. Huntington Study Group. Unified Huntington's disease rating scale: reliability and consistency. *Mov Disord.* 1996;11(2):136-142.
6. de la Monte S, Vonsattel J, Richardson E. Morphometric demonstration of atrophic changes in cerebral cortex, white matter and neostriatum in Huntington's disease. *J Neuropathol Exp Neurol.* 1988;47(5):516-525.
7. Jurgens CK, van de Wiel L, van Es ACGM, et al. Basal ganglia volume and clinical correlates in "preclinical" Huntington's disease. *J Neurol.* 2008;255(11):1785-1791.
8. Gómez-Ansón B, Alegret M, Muñoz E, et al. Prefrontal cortex volume reduction on MRI in preclinical Huntington's disease relates to visuomotor performance and CAG number. *Park Relat Disord.* 2009;15(3):213-219.
9. Rosas HD, Salat DH, Lee SY, et al. Cerebral cortex and the clinical expression of Huntington's disease: complexity and heterogeneity. *Brain.* 2008;131(4):1057-1068. doi:10.1093/brain/awn025.
10. van den Bogaard SJA, Dumas EM, Acharya TP, et al. Early atrophy of pallidum and accumbens nucleus in Huntington's disease. *J Neurol.* 2011;258(3):412-420.
11. Aylward EH, Harrington DL, Mills JA, et al. Regional atrophy associated with cognitive and motor function in prodromal Huntington disease. *J Huntingtons Dis.* 2013;2:477-489.
12. Marder K, Zhao H, Myers RH, et al. Rate of functional decline in Huntington's disease. *Neurology.* 2000;54:452-458.
13. Mahant N, McCusker E., Byth K, Graham S. Huntington's disease: clinical correlates of disability and progression. *Neurology.* 2003;61:1085-1092.
14. Smith SM, Jenkinson M, Woolrich MW, et al. Advances in functional and structural MR image analysis and implementation as FSL. *Neuroimage.* 2004;23:S208-S219.
15. Smith SM, Zhang Y, Jenkinson M, et al. Accurate, robust, and automated longitudinal and cross-sectional brain change analysis. *Neuroimage.* 2002;17(1):479-489.

16. Jenkinson M, Bannister P, Brady M, Smith S. Improved optimization for the robust and accurate linear registration and motion correction of brain images. *Neuroimage*. 2002;17(2):825-841.
17. Patenaude B, Smith SM, Kennedy DN, Jenkinson M. A Bayesian model of shape and appearance for subcortical brain segmentation. *Neuroimage*. 2011;56(3):907-922.
18. Smith SM. Fast robust automated brain extraction. *Hum Brain Mapp*. 2002;17(3):143-155.
19. Ashburner J, Friston KJ. Voxel-Based Morphometry—The Methods. *Neuroimage*. 2000;11(6):805-821.
20. Good C, Johnsrude I, Ashburner J, Henson R, Friston K, Frackowiak R. A voxel-based morphometric study of ageing in 465 normal adult human brains. *Neuroimage*. 2001;14(1):21-36.
21. Winkler AM, Ridgway GR, Webster MA, Smith SM, Nichols TE. Permutation inference for the general linear model. *Neuroimage*. 2014;92:381-397.
22. Smith SM, Nichols TE. Threshold-free cluster enhancement: addressing problems of smoothing, threshold dependence and localisation in cluster inference. *Neuroimage*. 2009;44(1):83-98.
23. Reiner A, Albin RL, Anderson KD, D'Amato CJ, Penney JB, Young AB. Differential loss of striatal projection neurons in Huntington disease. *Proc Natl Acad Sci U S A*. 1988;85(15):5733-5737.
24. Biglan KM, Ross CA, Langbehn DR, et al. Motor abnormalities in premanifest persons with Huntington's disease: The PREDICT-HD study. *Mov Disord*. 2009;24(12):1763-1772.
25. Kassubek J, Juengling FD, Kioschies T, et al. Topography of cerebral atrophy in early Huntington's disease: a voxel based morphometric MRI study. *J Neurol Neurosurg Psychiatry*. 2004;75(2):213-220.
26. Tabrizi SJ, Langbehn DR, Leavitt BR, et al. Biological and clinical manifestations of Huntington's disease in the longitudinal TRACK-HD study: cross-sectional analysis of baseline data. *Lancet Neurol*. 2009;8(9):791-801.
27. Scahill RI, Hobbs NZ, Say MJ, et al. Clinical impairment in premanifest and early Huntington's disease is associated with regionally specific atrophy. *Hum Brain Mapp*. 2013;34(3):519-529.
28. Bechtel N, Scahill RI, Rosas HD, et al. Tapping linked to function and structure in premanifest and symptomatic Huntington disease. *Neurology*. 2010;75(24):2150-2160.
29. Lobel E, Kahane P, Leonards U, et al. Localization of human frontal eye fields: anatomical and functional findings of functional magnetic resonance imaging and intracerebral electrical stimulation. *J Neurosurg*. 2001;95:804-815.
30. Johnson EB, Rees EM, Labuschagne I, et al. The impact of occipital lobe cortical thickness on cognitive task performance: An investigation in Huntington's Disease. *Neuropsychologia*. 2015;79:138-146.

SUPPLEMENTARY MATERIAL

TABLE S1 Subscales of five motor domains based on the Unified Huntington’s Disease Rating Scale (UHDRS)

Motor sum scores	Description	Items from UHDRS	Range
Chorea	Chorea	12	0 – 28
Dystonia	Dystonia	11	0 – 20
Eye movements	Ocular, saccades	1, 2, 3	0 – 24
Hypokinesia/rigidity	Finger tapping, pronate/supinate, bradykinesia, rigidity	6, 7, 9, 10	0 – 28
Gait/balance	Gait, tandem walking, retropulsion	13, 14, 15	0 – 12

Motor domains are based on previous studies.^{5, 14, 15} Scores of each individual item of the UHDRS were summed to create the specific motor domains.
UHDRS = Unified Huntington’s Disease Rating Scale

TABLE S2 Grey matter differences in manifest HD compared to controls

	MNI coordinates (mm)			t-value	p-value
	x	y	z		
Frontal lobe					
Precentral gyrus	14	-14	76	6.65	<0.001
Supplementary motor cortex	10	-22	66	6.17	<0.001
Frontal orbital cortex	24	42	-8	3.21	0.043
Frontal pole	36	44	-6	3.10	0.044
Temporal lobe					
Inferior temporal gyrus	48	-36	-14	6.37	<0.001
Middle temporal gyrus	-46	-58	6	6.06	<0.001
Parietal lobe					
Postcentral gyrus	-20	-34	72	3.16	<0.001
Supramarginal gyrus	66	-22	42	3.37	0.045
Cingulate gyrus	-8	-38	2	3.51	0.043
Occipital lobe					
Occipital pole	26	-92	0	7.34	<0.001
Occipital fusiform gyrus	22	-80	-10	7.11	<0.001
Lateral occipital cortex	-30	-94	4	6.91	<0.001

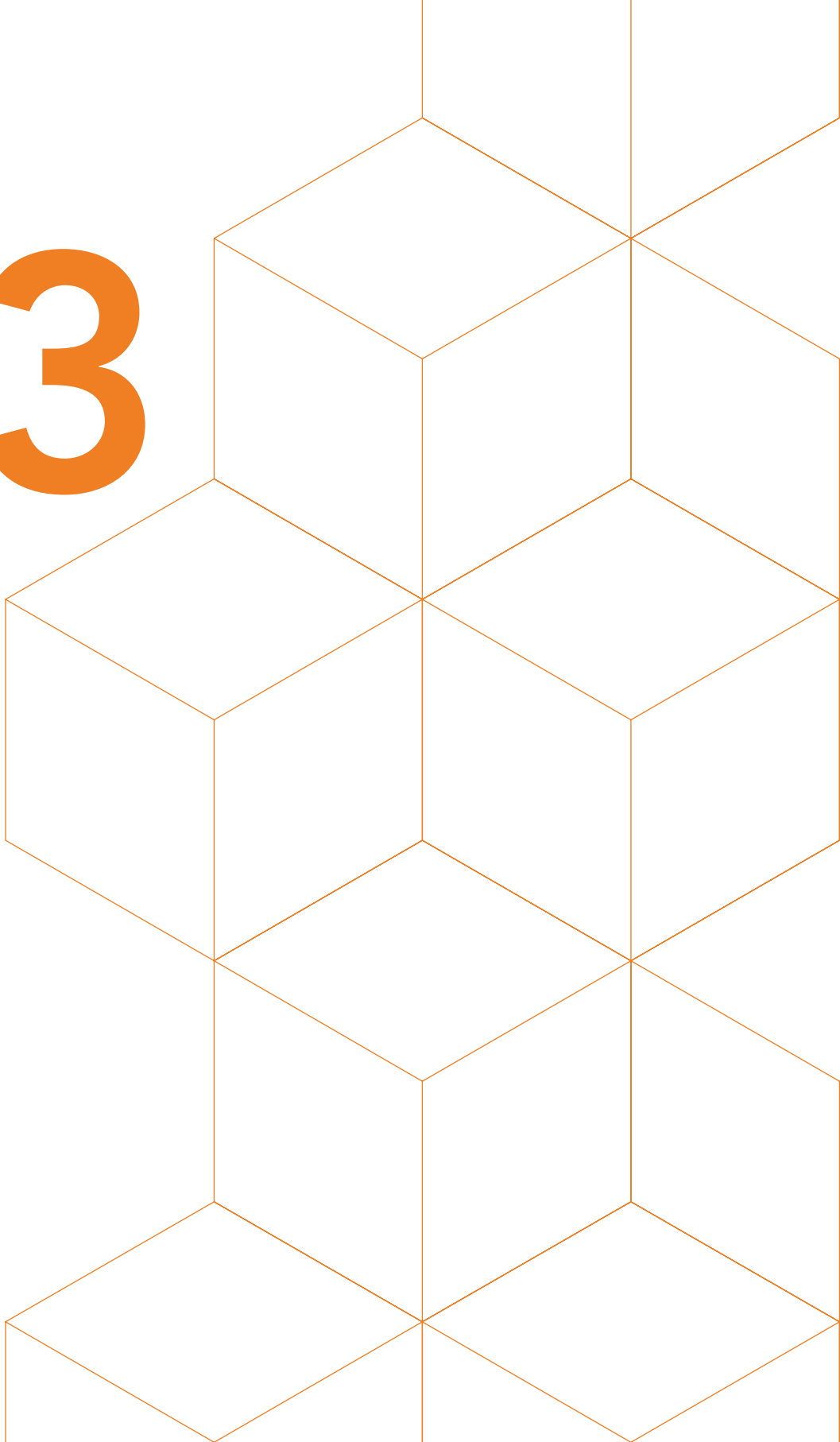
Anatomical regions that showed a significant difference in grey matter volume between manifest HD and controls using voxel-based morphometry. All anatomical regions were identified using the Harvard-Oxford Subcortical and Cortical atlases and the cluster tool implemented in FSL. T-statistics and corresponding p-values are presented (with a family wise corrected p-value of $p < 0.05$)

TABLE S3 Correlations between anatomical regions and clinical scores in HD patients

	Anatomical region	Voxel size	MNI coordinates (mm)			t-value	p-value
			x	y	z		
UHDRS-TMS	Left occipital pole	403	-16	-100	-2	1.05	0.019
	Right putamen	33	22	4	6	1.47	0.024
Chorea	Right putamen	23	22	4	6	1.32	0.038
Eye movements	Lateral occipital cortex	172	20	-92	-28	0.92	0.036
	Occipital fusiform gyrus	141	32	-84	-16	0.95	0.036
	Right putamen	41	22	2	8	1.65	0.016

Voxel-wise identified anatomical regions that showed a negative correlation with clinical scores in HD patients, i.e. an increase in clinical score is correlated with a decrease in grey matter volume. All anatomical regions were identified using the Harvard-Oxford Subcortical and Cortical atlases and the cluster tool implemented in FSL. T-statistics and corresponding *p*-values are presented (with a TFCE-family wise corrected *p*-value of $p < 0.05$).

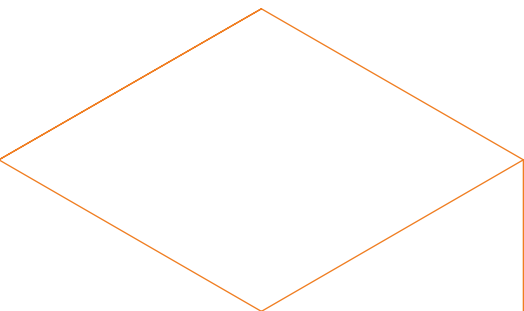
3



Early grey matter changes in structural covariance networks in Huntington's disease

Emma M. Coppen, Jeroen van der Grond, Anne Hafkemeijer, Serge A.R.B. Rombouts, Raymund A.C Roos

NeuroImage: Clinical. 2016 Oct;12:806-814



ABSTRACT

Background: Progressive subcortical changes are known to occur in Huntington's disease (HD), a hereditary neurodegenerative disorder. Less is known about the occurrence and cohesion of whole brain grey matter changes in HD.

Objectives: We aimed to detect network integrity changes in grey matter structural covariance networks and examined relationships with clinical assessments.

Methods: Structural magnetic resonance imaging data of premanifest HD ($n = 30$), HD patients ($n = 30$) and controls ($n = 30$) was used to identify ten structural covariance networks based on a novel technique using the co-variation of grey matter with independent component analysis in FSL. Group differences were studied controlling for age and gender. To explore whether our approach is effective in examining grey matter changes, regional voxel-based analysis was additionally performed.

Results: Premanifest HD and HD patients showed decreased network integrity in two networks compared to controls. One network included the caudate nucleus, precuneus and anterior cingulate cortex (in HD $p < 0.001$, in pre-HD $p = 0.003$). One other network contained the hippocampus, premotor, sensorimotor, and insular cortices (in HD $p < 0.001$, in pre-HD $p = 0.023$). Additionally, in HD patients only, decreased network integrity was observed in a network including the lingual gyrus, intracalcarine, cuneal, and lateral occipital cortices ($p = 0.032$). Changes in network integrity were significantly associated with scores of motor and neuropsychological assessments. In premanifest HD, voxel-based analyses showed pronounced volume loss in the basal ganglia, but less prominent in cortical regions.

Conclusion: Our results suggest that structural covariance might be a sensitive approach to reveal early grey matter changes, especially for premanifest HD.

1. INTRODUCTION

Huntington's disease (HD) is an autosomal dominant inherited neurodegenerative disorder, caused by a cytosine-adenine-guanine (CAG) trinucleotide repeat expansion on chromosome four in the Huntingtin (HTT) gene.¹ The clinically manifest phase of the disease is characterized by motor disturbances, cognitive decline and psychiatric symptoms (such as apathy, depression, irritability, and obsessive-compulsive behavior), with a mean age at onset of 30 to 50 years.²

HD gene carriers that have been tested positive for the CAG expansion are diagnosed as manifest HD based on the presence of typical motor disturbances that mainly involve chorea, dystonia, bradykinesia and rigidity.²

Recent neuroimaging studies revealed pronounced neuropathological changes in subcortical structures, which primarily involve atrophy of the caudate nucleus and putamen.³ This decline in striatal volume is already detectable in premanifest gene carriers, years before onset of motor disturbances.⁴⁻⁶ Local subcortical grey matter volume changes in HD are commonly examined using a voxel-based approach,⁷⁻¹³ but only few neuroimaging studies have investigated the occurrence of volume changes in the cerebral cortex. Still, neuropathological studies on HD report the presence of widespread cortical atrophy in addition to striatal atrophy.¹⁴ Reported voxel-wise subcortical volume changes in HD are, however, more prominent than cortical changes and the amount of cortical changes varies across voxel-based studies.^{15,16}

As voxel-based methods, such as voxel-based morphometry (VBM) analysis, provide whole-brain results for individual regions by studying voxels separately, a multivariate network-based analysis might give more information about inter-regional dependencies between grey matter voxels. As neurodegeneration is probably a network-based process involving several brain regions and is not regional specific,¹⁷ examining such approach might be particularly interesting in HD. Recently, a novel technique is developed to study disease-specific inter-regional network changes in grey matter by using structural covariance networks independent of a-priori defined regions.^{18,19} Structural covariance networks are based on the observation that grey matter regions in the brain co-vary in morphometric characteristics. Therefore, structural covariance networks might be a valuable tool in investigating the topological organization of the brain.¹⁸

Previous studies in premanifest HD showed that cognitive impairment and psychiatric symptoms can present prior to motor disturbances.^{5,20} Additionally, subcortical changes are already detectable in this stage of the disease.^{21,22} Whether or not abnormal grey matter changes are present in premanifest HD, we hypothesize that we may be able

to reveal morphological characteristics that vary reciprocally between cortices or between the cortex and the subcortical grey matter regions using structural covariance networks. Such changes in a given patient population address for abnormality in the reciprocal relationship that is due to disturbance in normal development or aging. Using structural covariance networks in such an unrestricted exploratory way can give more insight into the pathophysiological processes underlying HD.

Network integrity scores can be defined as the strength of an individuals' expression in each identified anatomical network and can therefore indirectly provide information about grey matter changes. Network integrity scores can change as covariance can diminish when the existing correlation drops due to the variation within a normal range. Therefore, network integrity can change regardless of atrophy and might provide a more sensitive biomarker for tracking disease progression than direct measurement of volume changes in HD.

Thus, the aim of this study is to investigate network integrity changes in grey matter structural covariance networks in HD and examine the relationship between the identified networks and clinical assessments. Furthermore, we compared our inter-regional findings with regional volumetric voxel-based analysis on the same data, as this approach is most often used to examine volume loss in HD.¹⁶

2. METHODS

2.1 Participants

Thirty premanifest gene carriers (pre-HD), 30 HD patients and 30 healthy controls who participated in the TRACK-HD study at the Leiden University Medical Center study site, were included. Both pre-HD and HD patients required a positive genetic test with 40 CAG repeats or more. Participants were considered pre-HD with a total motor score (TMS) of 5 or less on the motor assessment of the Unified Huntington's Disease Rating Scale (UHDRS)²³ and a disease burden score ($\text{age} \times [\text{CAG repeat length} - 35.5]$) of > 250 .²⁴ HD patients were included with an UHDRS-TMS score > 5 and a Total Functional Capacity (TFC) score greater than or equal to 7 points. Partners and gene-negative relatives were recruited as healthy controls. The control group was age and gender matched to the combined pre-HD and HD patients. The Medical Ethical Committee of the Leiden University Medical Center approved this study and written informed consent was obtained from all participants. For additional details about the study design and exclusion criteria, see Tabrizi et al. (2009).⁴

2.2. Clinical assessments

The UHDRS-TMS was used to measure the degree of motor disturbances, ranging from 0 to 124, with higher scores indicating more increased motor impairment. The TFC assesses global impairments in daily functioning, ranging from 0 to 13, with lower scores indicating more impaired function. Cognitive scores included the total scores of the Mini Mental State Examination (MMSE), Symbol Digit Modality Test (SDMT), Stroop word reading test and Trail-Making Test (TMT) A and B. The TMT score was derived by subtracting the completion time of TMT-A from TMT-B, thus minimizing the potential effect of motor speed and disturbances. For more details on all clinical assessments.⁴

2.3. MRI image acquisition

From January until August 2008, all participants underwent structural magnetic resonance imaging (MRI) scanning. Quality control of all images was performed by IXICO, London, United Kingdom. Imaging was performed on a 3 Tesla MRI scanner (Philips Achieva, Best, the Netherlands) using a standard 8-channel whole-head coil. Three-dimensional T1-weighted images were acquired with the following parameters: TR = 7.7 ms, TE = 3.5 ms, flip angle = 8 °, FOV 24 cm, matrix size 224 x 224 cm and 164 sagittal slices to cover the entire brain with a slice thickness of 1.0 mm with no gap between slices. This resulted in a voxel size of 1,07 mm x 1,07 mm x 1,0 mm.

2.4. Data analysis

2.4.1. Image post-processing

All T1-weighted images were analyzed using the software provided by FMRIB's software library (FSL, version 5.0.8, Oxford, United Kingdom).²⁵

First, all non-brain tissue was removed from structural T1-weighted images using a semi-automated brain extraction tool implemented in FSL.²⁶ Before being aligned to the 2 mm MNI (Montreal Neurological Institute)-152 standard space image²⁷ using non-linear registration,²⁸ voxel-based morphometry (VBM) analysis was used as implemented in FSL.²⁹ First, tissue-type segmentation was performed. The segmented images have values that indicate the probability of a given tissue type (i.e. grey matter, white matter or cerebrospinal fluid). To correct for the partial volume effect (i.e. voxels containing more than one tissue type), the tissue type segmentation was carried out with partial volume estimation. The segmented images have values that indicate the probability of a given tissue type. The resulting grey matter segmented images were averaged to create a study-specific grey matter template and 'modulated' to correct for local enlargements and contractions due to the non-linear component of the

spatial transformation.³⁰ During the modulation step, each voxel of every registered grey matter image was multiplied by the Jacobian of the warp field. This defines the direction (larger or smaller) and the amount of modulation. The modulated grey matter images were finally smoothed with an isotropic Gaussian kernel with a sigma of 3 mm. For the network-based data-driven analysis, Multivariate Exploratory Linear Optimized Decomposition into Independent Components (MELODIC)^{31,32} was used with the modulated grey matter images of all participants as a four-dimensional dataset. This statistical technique with independent component analysis (ICA) defines fully automated spatial component maps of maximal statistical independence, which is commonly used to study functional network integrity. When applied on structural grey matter images, this method defines spatial components based on the co-variation of grey matter patterns among all participants.^{18,19,33} Then, ICA provides for each participant a score ('network integrity score'), which can be negative or positive, describing the strength of the individual expression in each network,^{31,33} with high scores indicating strong individual expression of the identified network. In general, there is no consensus on the optimal number of components, which may be depending on the data size and the research question.³⁴ In our study, choosing less than ten components caused loss of spatial information due to merging of components, whereas selecting more components created additional components consisting of considerable noise. Therefore, we choose to set the number of independent components in our study to ten components. This number is consistent with previous studies of brain networks, in which eight to ten components are most often applied.^{18,34} A standard threshold level of 0.5 was used to describe significance of individual voxels within a spatial map. This indicates that the probability of a voxel being a signal component is greater than the probability of a voxel being noise.

To investigate voxel-wise group differences in grey matter volume, VBM analysis was performed. Here, the modulated grey matter images were analyzed using a general linear model in FSL for statistical inference.

Voxel-wise non-parametric permutation testing with 5000 permutations was performed using FSL randomise.³⁵ Further, the Threshold-Free Cluster Enhancement (TFCE) technique was used,³⁶ to correct for multiple comparisons with a p -value < 0.05 as significant threshold.

Brain structures were identified using the Harvard-Oxford atlas integrated in FSL.

For each participant, the mean voxels' grey matter density value was calculated using the identified anatomical regions that showed significant grey matter volume changes as a mask.

2.4.2. Statistics

Statistical analyses were performed using the Statistical Package for Social Sciences (SPSS for Mac, version 23, SPSS Inc.). Differences in demographic and clinical variables between groups were assessed using analysis of variance (ANOVA), χ^2 and Kruskal-Wallis tests for continuous, categorical and skewed data respectively.

For group comparisons, separate linear regression analysis was performed in each network with correction for age and gender using the network integrity scores as dependent variable. The analysis was performed to compare controls with gene carriers (i.e. pre-HD and HD patients separately). All independent variables were entered in one block. Furthermore, correlations between clinical assessments and genetic markers (i.e. CAG repeat length and disease burden) with the anatomical networks were assessed using linear regression analysis in pre-HD and HD patients.

For the VBM analysis, a design matrix for a general linear model was constructed in FSL to compare grey matter differences between controls and pre-HD and HD patients separately using two-tailed t-statistics, with age and gender as covariates to correct for confounding effects. To correct for multiple comparisons with family wise error, the Threshold-Free Cluster Enhancement (TFCE) technique was used,³⁶ with a p -value < 0.05 as significant threshold.

Linear regression analysis in HD gene carriers was performed to assess the relationship between clinical assessments and genetic markers with grey matter density values based on the mean value of the significant voxels of the VBM analysis.

In this observational study, the identified anatomical networks, grey matter density values, and cognitive tasks that were assessed share a mutual dependency. Considering it is not clear for which dependency to correct, we therefore present our correlational findings with clinical assessments uncorrected for multiple comparisons. As a result, to prevent type 2 errors, the interpretation of slight significant findings will be with caution. The significance threshold was set at a p value < 0.05 .

3. RESULTS

3.1. Demographic characteristics

Demographic and clinical data of all participants are shown in Table 1. There was a significant difference between groups for all clinical measures. Age, gender, handedness and education level did not differ between groups. There was no difference in CAG repeat length in both pre-HD and HD patients.

TABLE 1 Clinical and volumetric group differences between HD patients and controls

	HD (n= 79)	Controls (n=30)	p-value
Clinical characteristics			
Age	46.5 (9.7; 28 – 65)	48.9 (8.4; 35 – 65)	0.229
Gender m/f (%m)	30/49 (38.0%)	14/16 (46.7%)	0.409
CAG	44.1 (2.4; 40 – 51)	NA	NA
Disease duration	3.3 (3.0; 0 – 13)	NA	NA
Disease burden	382.1 (77.8; 234 – 551)	NA	NA
UHDRS-TMS	17.8 (10.8; 6 – 45)	2.6 (2.4; 0 – 7)	<0.001
UHDRS chorea	5.2 (4.8; 0 – 18)	NA	NA
UHDRS hypokinetic-rigid	4.6 (3.2; 0 – 12)	NA	NA
UHDRS dystonia	0.2 (0.6; 0 – 3)	NA	NA
UHDRS eye movements	4.9 (3.2; 0 – 13)	NA	NA
UHDRS gait/balance	1.8 (1.4; 0 – 6)	NA	NA
Subcortical structures			
Accumbens nucleus	732.0 (188.0)	930.5 (207.0)	<0.001
Caudate nucleus	4942.2 (997.5)	6695.4 (839.0)	<0.001
Amygdala	2208.0 (528.5)	2163.4 (379.4)	0.673
Putamen	7093.0 (1229.1)	9280.0 (1289.7)	<0.001
Pallidum	2749.8 (555.8)	3338.5 (471.4)	<0.001
Thalamus	13958.0 (1551.3)	14844.2 (1383.7)	<0.005
Hippocampus	7195.4 (1016.0)	7682.1 (818.3)	0.021

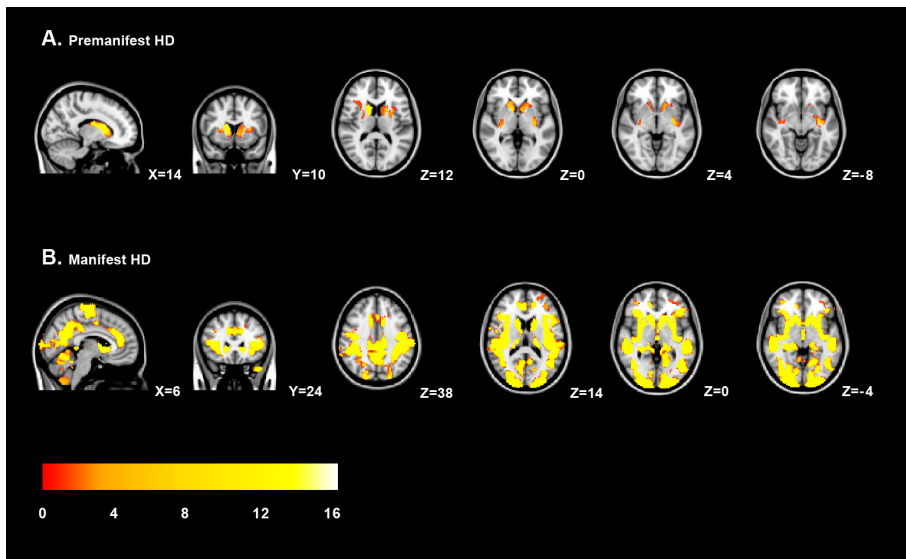
Data are mean (SD; range) or number (%) for gender. Volumes of subcortical structures are expressed in mm³. Mean disease duration is based on a smaller sample size (n=65) due to missing data. Independent sample t-test was used to compare groups, except for gender (χ^2 -test). Statistically significant p-values are highlighted in bold (p<0.05). NA = Not applicable; CAG = Cytosine-Adenine-Guanine; HD = Huntington's Disease; UHDRS = Unified Huntington's Disease Rating Scale; TMS = Total Motor Score.

3.2. Voxel-based morphometry analysis

Regional volumetric voxel-based analysis was performed to assess voxel-wise differences between HD gene carriers and controls. In pre-HD, significant local grey matter volume reductions in the basal ganglia, mainly in the putamen, nucleus accumbens and caudate nucleus (Figure 1A and Table 2) was found compared to controls. Cortical volume changes in pre-HD were limited to the insular cortex ($p = 0.018$) and a small region containing the planum temporale, parietal operculum cortex and posterior supramarginal gyrus ($p = 0.045$).

In HD patients, grey matter volume reductions were more distributed across the brain (Figure 1B and Table 2). VBM analysis showed subcortical volume loss in the caudate nucleus, putamen and pallidum. Significant cortical grey matter changes were primarily located in the pre- and postcentral gyrus, the supplementary motor cortex and the lateral occipital cortex.

FIGURE 1 Regional grey matter volume changes in HD



Voxel-based morphometric analysis showed regional grey matter volume changes in premanifest gene carriers (A) and Huntington's disease patients (B) compared to controls. The grey matter changes are overlaid on sagittal, transversal and coronal slices of MNI-152 standard T1-weighted images. Corresponding MNI x-, y- and z- coordinates are displayed. The threshold for display is $p < 0.05$ (corrected using familywise error). The color scale bar represents T-scores.

TABLE 2 Results of voxel-based morphometry analysis

Cluster size	Anatomical region	MNI coordinates			T-score	p-value
		x	y	z		
Premanifest gene carriers						
1126	Left putamen	-32	-16	-6	5.39	0.005
	Left caudate nucleus	-20	14	8	4.25	0.013
	Left accumbens	-6	12	2	4.14	0.015
	Insular cortex	-28	6	10	4.49	0.018
1018	Right caudate nucleus	14	8	6	5.78	0.001
	Right thalamus	14	-8	18	4.92	0.003
	Right putamen, right pallidum	28	-16	8	3.99	0.025
10	Planum temporale					
	Parietal operculum cortex	-46	-36	16	4.47	0.045
	Posterior supramarginal gyrus					
HD patients						
61398	Caudate nucleus	16	10	8	12.29	0.001
	Putamen, pallidum	24	-4	8	5.17	0.001
	Postcentral gyrus	-18	-36	70	3.28	0.001
	Precentral gyrus	-14	-22	60	2.98	0.001
	Supplementary motor cortex	10	-22	58	3.22	0.001
	Lateral occipital cortex	-46	-72	4	3.96	0.001
11	Frontal pole	22	44	18	4.24	0.041

Anatomical regions that showed significant grey matter volume changes in Huntington's disease compared to controls using voxel-based morphometry analysis. Regions were identified using the cluster tool and the Harvard-Oxford Subcortical and Cortical Structural Atlases in FSL. The most significant local maxima are presented with T-statistics and a Threshold-Free Cluster Enhancement (TFCE) family-wise error corrected *p*-value.

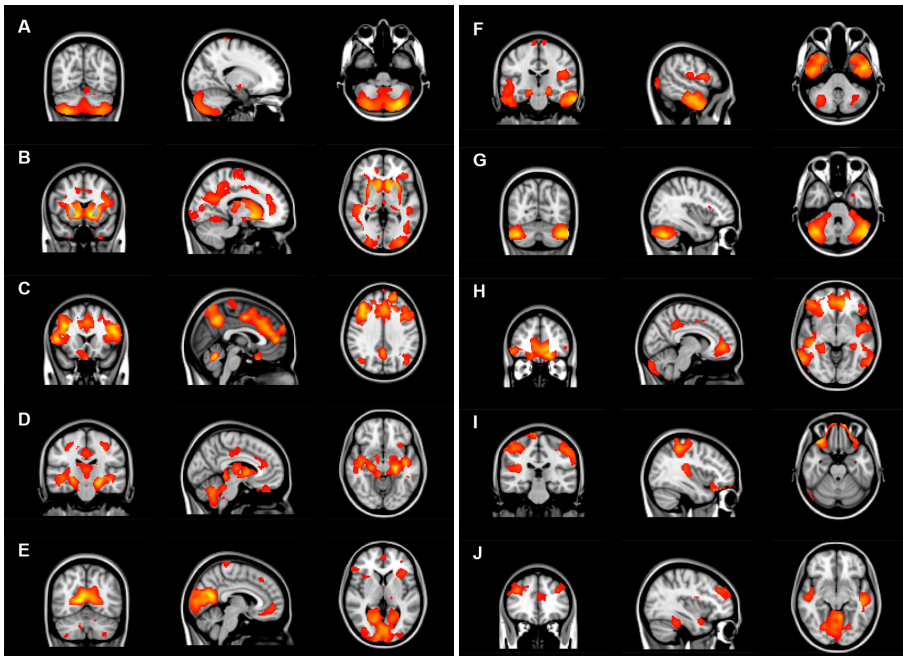
3.3. Anatomical networks and group comparisons

Ten grey matter anatomical networks were identified in all participants (Figure 2 and Table 3). Two structural covariance networks, the caudate nucleus network (network B) and the hippocampal network (network D), revealed a significant association in both pre-HD and HD patients compared to controls, meaning network integrity is reduced in both gene carrier groups compared to controls (Figure 2B, 2D and Table 4). The

caudate nucleus network includes the nucleus accumbens, pallidum, putamen, and precuneus. The hippocampal network is further comprised of the parahippocampal gyrus, cerebellum, pallidum, and planum polare. One other network, the intracalcarine network (network E), showed only a significant change in network integrity in HD patients compared to controls, but not in pre-HD (Figure 2E and Table 4).

This network includes the precuneus, cuneal and lateral occipital cortices and lingual gyrus. There were no significant group differences in network integrity in the 7 other identified networks (Figure 2A,C, F-J and Table 4). These networks include: anterior cingulate gyrus (network C), temporal gyrus (network F), lateral occipital cortex (network H), precuneus (network I), lingual gyrus (network J) and two cerebellar networks (networks A and G).

FIGURE 2 Overview of structural covariance networks



The ten identified anatomical networks are based on the structural covariance of grey matter among all participants. The networks are overlaid on sagittal, transversal and coronal slices of MNI-152 standard T1-weighted images.

TABLE 3 Identified anatomical brain networks

Brain cluster	Voxel size	Max T	MNI coordinates
			x y z
Network A			
Cerebellum	12110	16	-28 -76 -46
Right putamen, right pallidum, right hippocampus and right amygdala	233	4.66	28 -24 -4
Postcentral gyrus and precentral gyrus	50	4.08	16 -32 80
Network B			
Caudate nucleus , nucleus accumbens, pallidum, putamen and Precuneous	37999	7.55	-10 10 -4
Anterior cingulate cortex	349	3.4	16 44 4
Cerebellum	189	2.25	22 -56 -60
Network C			
Anterior cingulate cortex , supplementary motor cortex and middle and inferior frontal gyrus	19616	4.24	10 -4 44
Precuneous, superior parietal lobule, lateral occipital cortex, posterior cingulate cortex, postcentral gyrus	4747	4.06	-10 -62 48
Cerebellum	2156	3.97	2 -58 -22
Superior and middle temporal gyrus	649	2.93	42 -28 0
Network D			
Hippocampus , parahippocampal gyrus, cerebellum, pallidum and planum polare	16112	6.66	-22 -24 -14
Postcentral gyrus and precentral gyrus, superior parietal lobule, angular gyrus and supramarginal gyrus	1012	3.91	-30 -28 50
Posterior and anterior cingulate gyrus, supplementary motor cortex	881	3.46	4 -26 38
Insular cortex, caudate nucleus, frontal orbital cortex	504	3.88	32 24 -4
Network E			
Intracalcarine cortex , precuneous, cuneal cortex, lateral occipital cortex and lingual gyrus	11288	6.76	12 -64 8
Frontal medial cortex, paracingulate cortex and subcallosal cortex	833	3.26	10 52 -6
Frontal operculum cortex	595	3.34	-38 26 8
Postcentral gyrus and precentral gyrus	439	3.42	-10 -34 80
Cerebellum	438	3.37	26 -48 -42
Thalamus	196	3.2	-14 -28 -4
Network F			
Middle and inferior temporal gyrus , temporal fusiform cortex	7272	5.48	54 -10 -22
Lingual gyrus, posterior cingulate gyrus, intracalcarine cortex and occipital fusiform gyrus	3391	4.4	-14 -50 0
Frontal operculum cortex, precentral gyrus, parietal operculum cortex and frontal orbital cortex	2432	3.86	-30 22 14

Brain cluster	Voxel size	Max T	MNI coordinates		
			x	y	z
Superior frontal gyrus and paracingulate gyrus	662	4.08	16	32	62
Cerebellum	145	2.54	36	-62	-38
Network G	Cerebellum	4555	9.34	-40	-36
	Postcentral gyrus	182	3.33	70	-4
Network H	Lateral occipital cortex , central opercular cortex, planum polare, inferior frontal gyrus, and supramarginal gyrus	10329	4.18	-54	-66
	Superior and middle temporal gyrus and angular gyrus	8011	4.57	44	-26
	Frontal medial cortex, paracingulate gyrus, frontal operculum cortex and insular cortex	7214	5.32	-14	48
	Precuneous and cingulate cortex	1721	3.62	-10	-40
	Cerebellum	885	2.91	4	-90
Network I	Precuneous	3337	3.58	-10	-52
	Precentral gyrus, Hirschl's gyrus and central opercular cortex	2608	3.87	52	0
	Frontal orbital cortex	2593	5.87	32	28
	Postcentral gyrus	2518	3.99	-46	-34
	Superior parietal lobule	2289	4.65	40	-38
	Cerebellum	620	3.59	-26	-54
Network J	Lingual gyrus , cerebellum, parahippocampal gyrus, and occipital fusiform gyrus	5661	5.88	2	-78
	Supramarginal gyrus, opercular cortex and postcentral gyrus	4074	4.13	68	-36
	Middle and inferior temporal gyrus	2459	4.28	-48	-20
	Superior and middle frontal gyrus	1629	4.29	44	38
	Paracingulate gyrus	591	3.59	-14	42

Each anatomical network is divided into brain clusters, using a cluster tool integrated in FSL. Voxel size and MNI (Montreal Neurological Institute)-152 standard space image x-, y- and z-coordinates of each cluster are presented. Max T is the maximum T statistic of each local maximum. Structures displayed in bold are the largest structures identified in each anatomical network. Anatomical brain structures were identified using the Harvard-Oxford Atlas implemented in FSL.



TABLE 4 Differences per anatomical network between controls compared to premanifest gene carriers and HD patients

Network		Unstandardized B (95% CI)	Standardized β	R ²	p-value
A – Cerebellum	Premanifest	-0.003 (-0.010 to 0.003)	-0.148	0.141	0.269
	Manifest	-0.005 (-0.011 to 0.001)	-0.227	0.153	0.079
B – Caudate nucleus	Premanifest	-0.009 (-0.015 to -0.003)	-0.402	0.174	0.003
	Manifest	-0.023 (-0.029 to -0.018)	-0.718	0.551	< 0.001
C – Anterior cingulate cortex	Premanifest	-0.001 (-0.009 to 0.007)	-0.028	0.274	0.816
	Manifest	-0.001 (-0.008 to 0.006)	-0.035	0.185	0.778
D – Hippocampus	Premanifest	-0.008 (-0.014 to -0.001)	-0.300	0.168	0.023
	Manifest	-0.009 (-0.014 to -0.004)	-0.376	0.330	0.001
E – Intracalcarine cortex	Premanifest	-0.004 (-0.011 to 0.002)	-0.177	0.143	0.180
	Manifest	-0.007 (-0.013 to -0.001)	-0.281	0.118	0.032
F – Temporal gyrus	Premanifest	-0.001 (-0.007 to 0.004)	-0.066	0.130	0.616
	Manifest	-0.002 (-0.008 to 0.005)	-0.068	0.077	0.604
G – Cerebellum	Premanifest	0.002 (-0.004 to 0.009)	0.094	0.072	0.492
	Manifest	0.003 (-0.003 to 0.009)	0.121	0.085	0.357
H – Lateral occipital cortex	Premanifest	0.000 (-0.007 to 0.007)	-0.017	0.034	0.902
	Manifest	-0.001 (-0.008 to 0.006)	-0.044	0.015	0.745
I – Precuneous	Premanifest	0.003 (-0.004 to 0.010)	0.127	0.033	0.361
	Manifest	-0.005 (-0.011 to 0.001)	-0.216	0.057	0.110
J – Lingual gyrus	Premanifest	-0.003 (-0.010 to 0.005)	-0.105	0.078	0.446
	Manifest	-0.004 (-0.010 to 0.002)	-0.181	0.145	0.155

β = standardized Beta coefficient. Controls were compared to pre-HD and HD patients with adjustment for age and gender influences. Significant p-values (uncorrected $p < 0.05$) are displayed in bold.

3.4. Correlations of structural changes with clinical assessments

The caudate nucleus network, hippocampal network and intracalcarine network were selected to further assess the relationship with clinical scores, as these anatomical networks showed significant differences between controls and HD gene carriers. Six clinical assessments were analyzed in the HD gene carrier group and consisted of motor, functional and cognitive scores. CAG repeat length and disease burden score were used as a measurement of genetic burden in HD gene carriers. The caudate nucleus network showed a significant correlation with the TFC score and the UHDRS total motor score (Table 5). This means that a higher motor score is associated with a reduction in network integrity for this specific network. Significant correlations were also found with the caudate nucleus network and both CAG repeat length and disease burden score, meaning that a larger CAG repeat length and higher disease burden score are associated with a reduction in network integrity scores. Furthermore, all cognitive assessments showed a significant correlation with this network, i.e. the SDMT score, Stroop word reading test, TMT score and MMSE. The hippocampal network revealed no significant correlations with any of the clinical assessments or the measures of genetic burden. Two clinical assessments showed significant correlations with the intracalcarine network, the TFC score and the TMT score (Table 5). Furthermore, the disease burden score also showed a significant correlation with this network. The identified voxel-based anatomical regions of grey matter volume changes in HD were additionally used to assess relationships with clinical assessments in HD gene carriers. Overall, grey matter density values were significantly lower in manifest HD compared to controls and pre-HD ($F(2,87) = 24.1, p < 0.001$). For all clinical motor, functional and cognitive assessments, there was a significant correlation with grey matter density values in HD gene carriers (Table 5).

TABLE 5 Correlations between changes in structural covariance networks and clinical assessments

	Network B		Network D		Network E		Voxel-based grey matter volume changes	
	Caudate nucleus network		Hippocampus network		Visuomotor network			
	β	<i>p</i> -value	β	<i>p</i> -value	β	<i>p</i> -value	β	<i>p</i> -value
UHDRS-TMS	-0.519	< 0.001	0.057	ns	-0.160	ns	-0.525	< 0.001
TFC	0.329	0.002	0.019	ns	0.272	0.037	0.437	< 0.001
SDMT	0.544	< 0.001	0.152	ns	0.151	ns	-0.520	< 0.001
Stroop word reading	0.410	0.001	0.171	ns	0.047	ns	0.330	0.003
TMT	-0.420	0.001	-0.109	ns	-0.258	0.049	-0.520	< 0.001
MMSE	0.341	0.008	0.036	ns	-0.025	ns	0.348	0.002
CAG repeat length	-0.578	< 0.001	-0.012	ns	-0.294	ns	-0.564	< 0.001
Disease burden	-0.474	< 0.001	-0.034	ns	-0.263	0.046	-0.452	< 0.001

Significant correlations of motor, functional and cognitive assessments and genetic burden with structural covariance networks and voxel-based grey matter volume changes in HD gene carriers are presented. ns = not significant; β = standardized Beta coefficient; UHDRS-TMS = Unified Huntington's Disease Rating Scale – Total Motor Score; TFC = Total Functional Capacity score; SDMT = Symbol Digit Modality Test; TMT = Trail Making Test; MMSE = Mini Mental State Examination; CAG = cytosine, adenine, guanine; disease burden score = age x (CAG length-35.5) by Penney et al. (1997).

4. DISCUSSION

In this study, we showed that identification of structural covariance networks revealed early grey matter changes in premanifest gene carriers and HD patients. In total, ten anatomical networks were identified in all participants. The regions of grey matter changes were located in two specific structural covariance networks, in which we found network integrity changes in both pre-HD and HD patients. One of these networks contained the basal ganglia, precuneous and anterior cingulate cortex, whereas the other network comprised of the hippocampus, parahippocampal gyrus, cingulate, insular, and sensorimotor cortices, superior parietal lobule, angular gyrus and frontal orbital cortex. One other network, the intracalcarine network, only showed a significant change in network integrity in HD patients, not in pre-HD, compared to controls. The other seven networks involving the cerebellum, temporal and frontal lobes showed no significant differences in network integrity between controls and pre-HD or HD patients.

The mean network integrity score describes the strength of group expression in each network with higher scores indicating strong group expression of the identified network.

Our findings suggest that there is a progressive increasing change of network integrity in grey matter structures from the premanifest phase, when motor symptoms are not yet present, to the manifest stage of the disease.

Network integrity changes found in both pre-HD and HD patients were located in a network containing the precuneous and anterior cingulate cortex. These structures are involved in motor planning, visuospatial processing, and cognitive attention and control.^{37,38} As these motor and cognitive functions are known to be affected in HD,^{20,22} this can explain the strong associations we found in HD gene carriers between this network and performances on motor and cognitive tasks. The identified hippocampal network comprised of cortical structures involved in working memory performance, emotion processing and motor control. Although we showed evidence for change in network integrity in this network in pre-HD and HD patients, there were no significant correlations with clinical assessments. One possible explanation might be that we assessed cognitive tasks that are not designed to measure the domains of working memory and emotion processing. Another possible explanation could be that changes in network integrity precede the clinical decline.

In HD, network-based analysis has been applied in one other recent study that investigated structural covariance networks in brain regions that are functionally related.³⁹ Here, in all pre-specified motor, working memory, cognitive flexibility, and

social-affective networks there were no differences between controls and pre-HD observed.³⁹ In our study, however, we found evidence for early grey matter volume changes in two structural covariance networks in pre-HD compared to controls. This difference might be explained by the fact that we used patterns of co-variation in whole brain grey matter of the participants and were not restricted to pre-defined brain regions.

Further, we assessed correlations with our identified anatomical networks and genetic markers, such as CAG repeat length and disease burden. We found that a larger CAG repeat length and higher disease burden score in HD gene carriers were associated with a reduction in network integrity scores of the caudate nucleus network, suggesting that genetic markers might have an effect on the rate of disease progression. This is consistent with previous studies showing a larger CAG repeat length is associated more widespread atrophy.^{10,12,24}

In general, grey matter structural covariance networks showed to spatially overlap with resting-state functional connectivity networks.^{33,40} It is suggested that the topological organization of anatomical networks reflect the pattern of functional organization of different networks, thus, regions that co-vary in grey matter volume may also be part of the same functional network.^{40,41} The identified anatomical networks in our study also show similarity with resting state functional connectivity networks found in early HD patients in previous studies.⁴²⁻⁴⁴

Visual comparison of our identified networks with results from previous functional neuroimaging studies in HD show spatial overlap between the caudate nucleus network (B) and the functional striatal network, the anterior cingulate cortex network (C) and the executive control network, the hippocampal network (D) and the frontoparietal network, the intracalcarine network (E) and the functional visuomotor network, the temporal gyrus network and the functional medial temporal network, the lateral occipital network (H) and the default mode network, the precuneous network (I) and the sensorimotor network, the lingual gyrus network (J) and the auditory network, and the structural cerebellar networks (A and G) and the functional cerebellar network. Yet, more studies are needed to gain more knowledge about the relationship between structural networks and functional connectivity in HD.

To investigate whether identifying structural covariance networks is an effective approach to examine grey matter changes in HD, regional voxel-based analysis was additionally performed on the same data.

In pre-HD, previous voxel-based analysis studies revealed volume loss in the prefrontal cortex,¹¹ insular cortex and parietal lobe.¹² This is consistent with our regional analysis that showed limited cortical volume loss in pre-HD, located in the insular cortex,

planum temporale, parietal operculum cortex and posterior supramarginal gyrus. However, our network-based analysis revealed that changes were also located in other brain regions like the precuneous, cingulate and sensorimotor cortices, and the parahippocampal gyrus. These results are consistent with previous studies on cortical thinning in early clinical disease stages.^{45,46} For the voxel-based regions that showed volume loss in HD gene carriers, mean grey matter density values were calculated and correlated with scores of clinical assessments. We found significant correlations between grey matter density values and motor, functional and cognitive assessments, as well as CAG repeat length and disease burden. Comparable significant correlations with these clinical assessments were also found in the caudate nucleus network, suggesting that network-based analysis is also sensitive in detecting correlations with clinical measures. Using univariate VBM, however, these correlations are based on voxel-wise differences in grey matter density. Therefore, it is difficult to directly compare the sensitivity of the univariate VBM approach with a multivariate network approach, based on the correlation with clinical assessments.

Nevertheless, based on the current results and previous reports, network-based analyses using structural covariance network with spatially independent regions might be a sensitive method in detecting early grey matter changes in HD as network integrity can change regardless of atrophy. Also, cognitive dysfunctions might not only be caused by localized brain damage, but of a impaired brain network as well.⁴⁷

Still, more studies are needed to determine if structural covariance networks are reliable to be used as a standardized method for grey matter changes in HD.

4.1. Strengths and limitations

The strength of this current study lies in detecting whole brain networks by using the anatomical relationship between spatially distributed brain regions as covariance networks without using pre-defined regions of interest or analyzing voxels separately. However, this study has a cross-sectional design, so a longitudinal follow-up study is preferred to further assess the relationship with disease progression. Additionally, larger sample sizes might provide more information about associations with clinical assessments. Another limitation of this study is the number of components or networks used in our analysis, which was chosen arbitrary.³⁴ When choosing the number of components it is important to take into account that the sensitivity to detect regional effects can be affected and thus might influence outcomes.¹⁸

5. CONCLUSIONS

This study identified spatially independent grey matter regions that form different structural networks based on the co-variance of grey matter in healthy controls, pre-HD and HD patients. Our findings suggest that changes in grey matter volume are widespread, involve several brain regions, and are already detectable in the premanifest stage of the disease. Potentially, structural covariance networks might develop into an early biomarker for identifying grey matter changes in HD that could be used in future clinical trials. Additionally, it is important to understand large-scale anatomical networks in a neurodegenerative disorder like HD, as this might provide new insights into underlying cortical pathophysiological processes, which are still poorly understood.

REFERENCES

1. The Huntington's Disease Collaborative Research Group. A novel gene containing a trinucleotide repeat that is expanded and unstable on Huntington's disease chromosomes. *Cell*. 1993;72(6):971-983.
2. Roos RAC. Huntington's disease: a clinical review. *Orphanet J Rare Dis*. 2010;5(1):40.
3. Aylward EH. Magnetic resonance imaging striatal volumes: A biomarker for clinical trials in Huntington's disease. *Mov Disord*. 2014;29(11):1429-1433.
4. Tabrizi SJ, Langbehn DR, Leavitt BR, et al. Biological and clinical manifestations of Huntington's disease in the longitudinal TRACK-HD study: cross-sectional analysis of baseline data. *Lancet Neurol*. 2009;8(9):791-801.
5. Paulsen JS, Langbehn DR, Stout JC, et al. Detection of Huntington's disease decades before diagnosis: the Predict-HD study. *J Neurol Neurosurg Psychiatry*. 2008;79(8):874-880.
6. van den Bogaard SJA, Dumas EM, Acharya TP, et al. Early atrophy of pallidum and accumbens nucleus in Huntington's disease. *J Neurol*. 2011;258(3):412-420.
7. Kassubek J, Juengling FD, Ecker D, Landwehrmeyer GB. Thalamic atrophy in Huntington's disease co-varies with cognitive performance: A morphometric MRI analysis. *Cereb Cortex*. 2005;15(6):846-853.
8. Douaud G, Gaura V, Ribeiro MJ, et al. Distribution of grey matter atrophy in Huntington's disease patients: A combined ROI-based and voxel-based morphometric study. *Neuroimage*. 2006;32(4):1562-1575.
9. Peinemann A, Schuller S, Pohl C, Jahn T, Weindl A, Kassubek J. Executive dysfunction in early stages of Huntington's disease is associated with striatal and insular atrophy: A neuropsychological and voxel-based morphometric study. *J Neurol Sci*. 2005;239:11-19.
10. Ruocco HH, Bonilha L, Li LM, Lopes-Cendes I, Cendes F. Longitudinal analysis of regional grey matter loss in Huntington disease: effects of the length of the expanded CAG repeat. *J Neurol Neurosurg Psychiatry*. 2008;79(2):130-135.
11. Hobbs NZ, Henley SMD, Ridgway GR, et al. The progression of regional atrophy in premanifest and early Huntington's disease: a longitudinal voxel-based morphometry study. *J Neurol Neurosurg Psychiatry*. 2010;81(7):756-763.
12. Gómez-Ansón B, Alegret M, Muñoz E, et al. Prefrontal cortex volume reduction on MRI in preclinical Huntington's disease relates to visuomotor performance and CAG number. *Park Relat Disord*. 2009;15(3):213-219.
13. Thieben MJ, Duggins AJ, Good CD, et al. The distribution of structural neuropathology in pre-clinical Huntington's disease. *Brain*. 2002;125:1815-1828.

14. de la Monte S, Vonsattel J, Richardson E. Morphometric demonstration of atrophic changes in cerebral cortex, white matter and neostriatum in Huntington's disease. *J Neuropathol Exp Neurol.* 1988;47(5):516-525.
15. Whitwell JL, Josephs KA. Voxel-based morphometry and its application to movement disorders. *Park Relat Disord.* 2007;13:S406-S416.
16. Dogan I, Eickhoff SB, Schulz JB, et al. Consistent neurodegeneration and its association with clinical progression in Huntington's disease: a coordinate-based meta-analysis. *Neurodegener Dis.* 2013;12:23-35.
17. Rombouts SARB, Damoiseaux JS, Goekoop R, et al. Model-free group analysis shows altered BOLD fMRI networks in dementia. *Hum Brain Mapp.* 2009;30(1):256-266.
18. Hafkemeijer A, Altmann-Schneider I, de Craen AJM, Slagboom PE, van der Grond J, Rombouts SARB. Associations between age and gray matter volume in anatomical brain networks in middle-aged to older adults. *Aging Cell.* 2014;13(6):1068-1074.
19. Xu L, Groth KM, Pearlson G, Schretlen DJ, Calhoun VD. Source-based morphometry: The use of independent component analysis to identify gray matter differences with application to schizophrenia. *Hum Brain Mapp.* 2009;30(3):711-724.
20. Lemiere J, Decruyenaere M, Evers-Kiebooms G, Vandenbussche E, Dom R. Cognitive changes in patients with Huntington's disease (HD) and asymptomatic carriers of the HD mutation. *J Neurol.* 2004;251(8):935-942.
21. Aylward E, Sparks B, Field K, et al. Onset and rate of striatal atrophy in preclinical Huntington disease. *Neurology.* 2004;63:66-72.
22. Tabrizi SJ, Scahill RI, Owen G, et al. Predictors of phenotypic progression and disease onset in premanifest and early-stage Huntington's disease in the TRACK-HD study: Analysis of 36-month observational data. *Lancet Neurol.* 2013;12(7):637-649.
23. Huntington Study Group. Unified Huntington's disease rating scale: reliability and consistency. *Mov Disord.* 1996;11(2):136-142.
24. Penney J, Vonsattel JP, MacDonald ME, Gusella JF, Myers RH. CAG repeat number governs the development rate of pathology in Huntington's disease. *Ann Neurol.* 1997;41(5):689-692.
25. Smith SM, Jenkinson M, Woolrich MW, et al. Advances in functional and structural MR image analysis and implementation as FSL. *Neuroimage.* 2004;23:S208-S219.
26. Smith SM. Fast robust automated brain extraction. *Hum Brain Mapp.* 2002;17(3):143-155.
27. Jenkinson M, Bannister P, Brady M, Smith S. Improved optimization for the robust and accurate linear registration and motion correction of brain images. *Neuroimage.* 2002;17(2):825-841.
28. Andersson JLR, Jenkinson M, Smith S. *Non-Linear Registration Aka Spatial Normalisation.* 2007. FMRIB Technical Report TR07Aja2. [<http://fmrib.medsci.ox.ac.uk/analysis/techrep/tr07ja2/tr07ja2.pdf>.]

29. Ashburner J, Friston KJ. Voxel-Based Morphometry—The Methods. *Neuroimage*. 2000;11(6):805-821.
30. Good C, Johnsrude I, Ashburner J, Henson R, Friston K, Frackowiak R. A voxel-based morphometric study of ageing in 465 normal adult human brains. *Neuroimage*. 2001;14(1):21-36.
31. Beckmann CF, Smith SM. Probabilistic independent component analysis for functional magnetic resonance imaging. *IEEE Trans Med Imaging*. 2004;23(2):137-152.
32. Beckmann CF, DeLuca M, Devlin JT, Smith SM. Investigations into resting-state connectivity using independent component analysis. *Philos Trans R Soc*. 2005;360:1001-1013.
33. Segall JM, Allen EA, Jung RE, et al. Correspondence between structure and function in the human brain at rest. *Front Neuroinform*. 2012;6:1-17.
34. Cole DM, Smith SM, Beckmann CF. Advances and pitfalls in the analysis and interpretation of resting-state fMRI data. *Front Syst Neurosci*. 2010;4:1-15.
35. Winkler AM, Ridgway GR, Webster MA, Smith SM, Nichols TE. Permutation inference for the general linear model. *Neuroimage*. 2014;92:381-397.
36. Smith SM, Nichols TE. Threshold-free cluster enhancement: addressing problems of smoothing, threshold dependence and localisation in cluster inference. *Neuroimage*. 2009;44(1):83-98.
37. Cavanna AE, Trimble MR. The precuneus: a review of its functional anatomy and behavioural correlates. *Brain*. 2006;129(3):564-583.
38. Wenderoth N, Debaere F, Sunaert S, Swinnen SP. The role of anterior cingulate cortex and precuneus in the coordination of motor behaviour. *Eur J Neurosci*. 2005;22(1):235-246.
39. Minkova L, Eickhoff SB, Abdulkadir A, et al. Large-scale brain network abnormalities in Huntington's disease revealed by structural covariance. *Hum Brain Mapp*. 2016;37(1):67-80.
40. Seeley WW, Crawford RK, Zhou J, Miller BL, Greicius MD. Neurodegenerative diseases target large-scale human brain networks. *Neuron*. 2009;62(1):42-52.
41. Montembeault M, Joubert S, Doyon J, et al. The impact of aging on gray matter structural covariance networks. *Neuroimage*. 2012;63(2):754-759.
42. Dumas EM, van den Bogaard SJA, Hart EP, et al. Reduced functional brain connectivity prior to and after disease onset in Huntington's disease. *NeuroImage Clin*. 2013;2(1):377-384.
43. Poudel GR, Egan GF, Churchyard A, Chua P, Stout JC, Georgiou-Karistianis N. Abnormal synchrony of resting state networks in premanifest and symptomatic Huntington disease: the IMAGE-HD study. *J Psychiatry Neurosci*. 2014;39(2):87-96.
44. Wolf RC, Sambataro F, Vasic N, et al. Abnormal resting-state connectivity of motor and cognitive networks in early manifest Huntington's disease. *Psychol Med*. 2014;44:3341-3356.
45. Rosas HD, Hevelone ND, Zaleta AK, Greve DN, Salat DH, Fischl B. Regional cortical thinning in preclinical Huntington disease and its relationship to cognition. *Neurology*. 2005;65(5):745-747.

46. Rosas HD, Salat DH, Lee SY, et al. Cerebral cortex and the clinical expression of Huntington's disease: complexity and heterogeneity. *Brain*. 2008;131(4):1057-1068.
47. Hafkemeijer A, Möller C, Dopfer EGP, et al. Differences in structural covariance brain networks between behavioral variant frontotemporal dementia and Alzheimer's disease. *Hum Brain Mapp*. 2016;988:978-988.

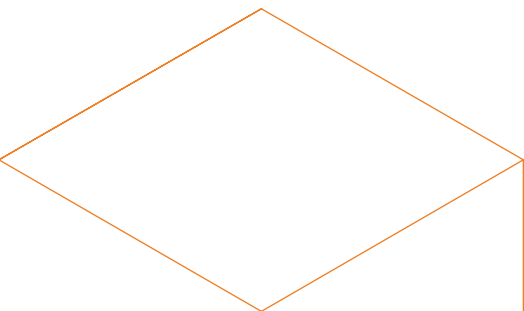
4



Patterns of corticostriatal degeneration in early Huntington's disease patients

Emma M. Coppen, Anne Hafkemeijer,
Jeroen van der Grond, Jurriaan J.H. Barkey Wolf,
Raymund A.C. Roos

Submitted



ABSTRACT

Background: Progressive striatal atrophy is the neuropathological hallmark of Huntington's disease (HD), a hereditary neurodegenerative disorder. Cortical atrophy is additionally present in HD, but it is unknown if striatal degeneration is related with cortical atrophy or if these are independent neurodegenerative processes.

Objective: To investigate the extent of corticostriatal degeneration in early manifest disease stages and examine the relationship between cortical thinning and striatal volume loss.

Methods: Ninety-two participants (18 healthy controls, 31 HD stage 1, and 43 HD stage 2) underwent structural MRI scanning. Thickness and surface area of cortical brain regions and striatal volumes were calculated using FreeSurfer. Based on independent corticostriatal circuits (motor, oculomotor, prefrontal, limbic, and visual loops), associations between cortical thickness and striatal volumes (caudate nucleus, putamen, and accumbens nucleus) in HD gene carriers were assessed using multiple linear regression analyses adjusted for age and gender, and corrected for multiple comparisons ($p < 0.003$).

Results: Atrophy of the striatum, especially the caudate nucleus, was more extensive than thinning of the cerebral cortex in HD gene carriers. In HD stage 2, cortical thinning was mainly located in parietal and occipital cortices. Although both striatal volume loss and cortical thinning was observed, no significant associations were found between cortical thickness and striatal volumes.

Conclusion: In early stage HD, cortical atrophy is mainly located in parietal and occipital brain regions. Since no relationship was observed in the degree of atrophy within corticostriatal circuits, our findings imply that cortical degeneration might be independent from striatal atrophy.

1. INTRODUCTION

Progressive striatal degeneration is the neuropathological hallmark of Huntington's disease (HD), an autosomal dominant inherited neurodegenerative disorder caused by an elongated cytosine-adenosine-guanine (CAG) repeat length on chromosome four.^{1,2} The gradual loss of medium spiny projection neurons in the striatum are thought to explain the clinical signs of HD, such as choreiform movements, oculomotor dysfunction, and even cognitive and psychiatric symptoms.³⁻⁵ Early microscopic changes in the striatum usually begins in the body and tail of the caudate nucleus, and further deterioration occurs in a dorsal to ventral direction.⁴ In addition to striatal atrophy, widespread neuronal cell loss in different regions of the cerebral cortex have been found in advanced HD patients, resulting in an overall brain weight loss of more than 40%.⁶⁻⁸ Regional cortical atrophy can also be detected in early disease stages, although to a lesser extent than striatal atrophy.⁹⁻¹⁴

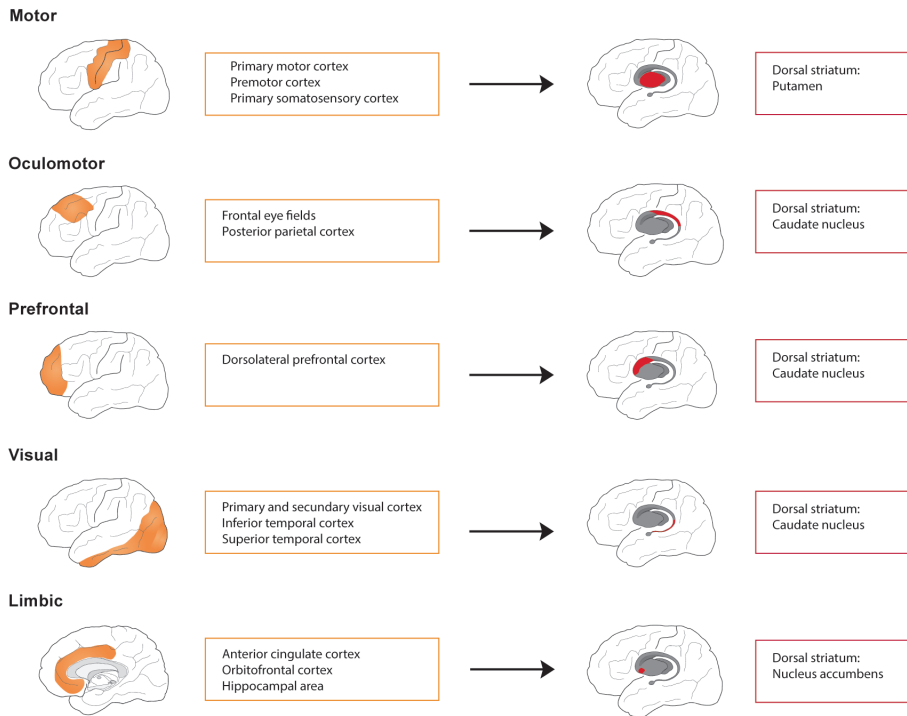
Currently, it is suggested that cortical atrophy in HD originates in posterior brain regions and progresses to the anterior cerebral cortex,¹⁵ but it is unknown if the degree of regional cortical degeneration is related to striatal volume loss. It is hypothesized that either the striatum is the primary site of degeneration in HD and other subcortical and cortical brain regions are subsequently affected, or that striatal atrophy is secondary to degeneration in the cerebral cortex.¹ However, it is also possible that striatal and cortical degeneration occur relatively independent of each other.¹⁶

In general, different cortical regions have projections to different striatal regions (i.e., the putamen, caudate nucleus, or accumbens nucleus) that subsequently project to the pallidum, thalamus, and finally back to the cortex. Five major independent corticostriatal circuits have been identified: the motor, oculomotor, prefrontal, limbic, and visual loops (Figure 1).^{5,17-19} Dysfunction of the corticostriatal pathways may lead to neurodegeneration of both cortical and striatal neurons.⁶

Identifying the pathways of corticostriatal neurodegeneration in HD is important because this can provide more insight into the debate to which extent the striatum plays a causal or modulatory role in the onset of clinical signs. To date, striatal atrophy is often used as a marker to track disease progression or to measure the effect of a pharmacological treatment in clinical trials. When cortical degeneration indeed occurs independent from striatal atrophy, this could have consequences for future clinical trial designs and therapeutic interventions, especially since cognitive, affective and behavioral disturbances in HD patients have been linked to cortical atrophy.^{9,13}

Therefore, with this study, we aimed to identify the degree of corticostriatal degeneration in early manifest HD disease stages and examine the relationship between cortical thinning and striatal volume loss.

FIGURE 1 Corticostriatal circuits



Schematic overview of the main corticostriatal circuits in the human brain, adapted from Alexander et al.¹⁷ and Lawrence et al.¹⁸ Each circuit is a closed loop projecting from the cerebral cortex to specific regions of the striatum, pallidum, and thalamus, which project back to the cerebral cortex. The sensorimotor cortex mainly connects to the putamen, the orbitofrontal, parietal, and occipital cortices with the caudate nucleus, whereas the limbic structures and prefrontal cortex are involved with the nucleus accumbens. Note that the connections between striatal regions (i.e., the indirect and direct pathways), and to the pallidum and thalamus are not displayed in this figure.

2. METHODS

2.1. Participants

A total of 92 individuals (18 healthy controls and 31 manifest HD gene carriers stage 1 (HD1) and 43 manifest HD gene carriers stage 2 (HD2)) were included in this study. Participants were recruited from the outpatient clinic of our Neurology department. Spouses and gene-negative relatives without neurological or psychiatric disorders were included as healthy controls. All HD gene carriers had a genetically confirmed CAG repeat length of ≥ 36 and scored above 5 points on the Total Motor Score of

the Unified Huntington's Disease Rating Scale (UHDRS), a scale to evaluate motor functioning in HD, ranging from 0 to 124.²⁰ Usually, a score above 5 points on the UHDRS-TMS refers to clinical presence of typical HD-related motor signs.¹⁰ Based on the UHDRS Total Functional Capacity (TFC) score, which assesses global daily functioning, manifest HD gene carriers were divided into disease stages²¹ The TFC score ranges from 0 to 13, with lower scores indicating more impaired function. This resulted in 31 patients in the earliest disease stage (HD1) with TFC score between 11 and 13, and 43 patients in the second disease stage (HD2), with TFC score between 7 and 10. The disease burden score was calculated as indicator of disease pathology, based on the following formula: $\text{age} \times (\text{CAG} - 25.5)$.²²

The local medical ethical committee approved this study and written informed consent was obtained from all participants.

2.2. MRI acquisition

All participants underwent structural Magnetic Resonance Imaging (MRI) scanning between January 2016 and December 2017 on a 3 Tesla MRI scanner (Philips Achieva, Best, the Netherlands). Anatomical T1-weighted images were acquired using a standard 32-channel whole head coil. The following image parameters were used: TE = 3.3, TR = 7.2 ms, flip angle = 9°, FOV = 256 x 240 x 176 mm and 176 slices with a slice thickness of 1 mm and no gap between slices, resulting in a voxel size of 1.00 x 1.00 x 1.00 mm, and scan duration of approximately 9 minutes.

2.3. Image processing

FreeSurfer (version 5.3.0) was used to calculate the cortical thickness and surface area of the cortical brain regions.²³ Automated parcellation and segmentation was performed by the FreeSurfer algorithm, which assigns a neuroanatomical label to each location on a cortical surface model, based on probabilistic information. Frontal, medial and lateral temporal, parietal, occipital and cingulate regions in each hemisphere were identified based on the Desikan-Killiany atlas, resulting in 34 cortical regions.²⁴ Thickness and surface area measures were averaged across the two hemispheres. Then, average thickness values per region (comprising of the frontal, parietal, temporal, and occipital lobes and the cingulate cortex) were calculated based on a weighted sum of mean thickness which accounted for surface area that has been described previously.^{13,25} In addition, volumetric measures of striatal structures, i.e., caudate nucleus, putamen, and nucleus accumbens were obtained automatically using FreeSurfer's subcortical segmentation pipeline.²⁶

2.4. Statistical analysis

Group differences in demographic variables were analyzed using analysis of variance (ANOVA) or χ^2 for continuous and categorical data respectively. Differences between HD1 and HD2 for clinical outcome measures (CAG, disease burden score, disease duration and UHDRS-TMS) were analyzed using independent samples t-tests.

Differences between HD1, HD2, and controls in striatal volumes and average cortical thickness for each lobe were analyzed using ANOVA, with Bonferroni correction.

Based on the corticostriatal circuits presented in Figure 1, we used multiple linear regression analyses in all HD gene carriers (i.e., HD1 and HD2 combined) to assess associations between cortical thickness of specific brain regions within each circuit and the corresponding striatal volumes (i.e., caudate nucleus, putamen, and accumbens nucleus). Each specific cortical region's thickness was entered as dependent variable with the corresponding striatal volume as independent variable, adjusted for age and gender. All independent variables were entered in one block.

An alpha-level of $p < 0.05$ was used as significant threshold and, if applicable, an adjusted p -value was set to account for multiple comparisons. Statistical analyses were performed using the Statistical Package for Social Sciences (SPSS for Mac, version 23, SPSS Inc.).

3. RESULTS

3.1. Demographic characteristics

Demographic data are presented in Table 1. There were no significant group differences in age and gender. CAG repeat length and disease burden score were not different between the HD disease stages. The HD2 group had a significant longer disease duration and higher score on the UHDRS-TMS compared to HD1.

3.2. Striatal volume and cortical thickness

Significant reduced volumes of all striatal structures were found for both HD1 and HD2 compared to controls (Table 2 and Figure 2).

The caudate nucleus showed the largest volume loss in HD gene carriers compared to controls with 31.1% and 31.4% volume loss in HD1 and HD2 respectively. There were no significant differences in striatal volumes between HD1 and HD2. After correction for multiple comparisons, each lobe showed reduced average cortical thickness in HD2 compared to controls, with largest volume reductions in the parietal and occipital brain regions, while no significant reductions in HD1 compared to controls were found.

TABLE 1 Demographic characteristics of study population

	Controls	HD1	HD2	<i>p</i> -value
N	18	31	43	
Age (years)	46.2 ± 10.7 (24.1 – 61.3)	50.1 ± 9.1 (30.5 – 64.8)	51.2 ± 10.1 (28.4 – 65.7)	0.198
Gender (M/F)	7/11	17/14	22/21	0.548
Disease burden score	NA	375 ± 86 (246 – 562)	382 ± 87 (185 – 544)	0.741
Disease duration (years)	NA	3.5 ± 2.6	5.3 ± 2.9	0.005
CAG	NA	43.3 ± 2.4 (40-49)	43.2 ± 1.9 (40-48)	0.973
UHDRS – Total motor score	NA	17.1 ± 8.1 (6 – 40)	24.4 ± 12.3 (8 – 52)	0.007

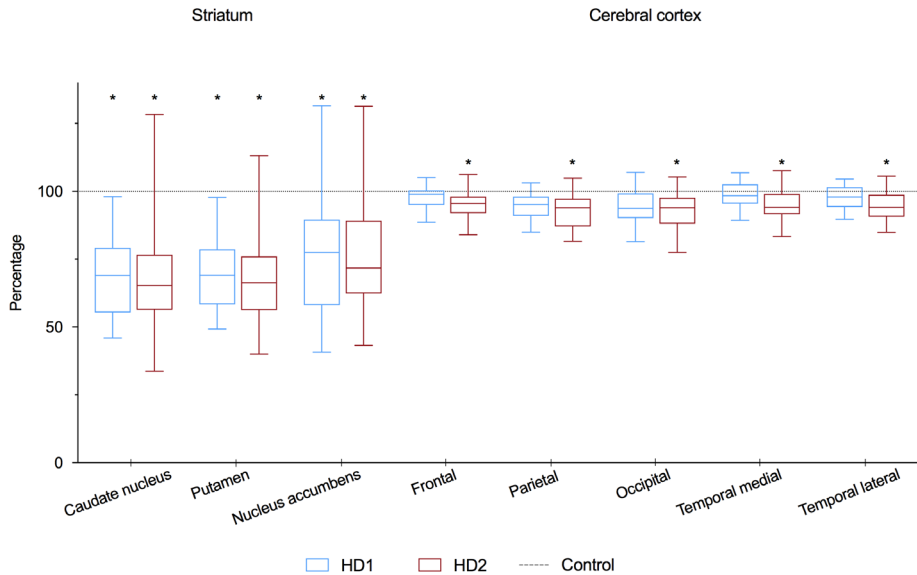
Data are presented with mean ± SD (range), except for gender (male/female) in numbers. UHDRS: Unified Huntington’s Disease Rating Scale – Total Motor score. NA: not applicable. Significant group differences are displayed in bold.

TABLE 2 Structural brain data

	Controls	HD1	HD2	Controls vs. HD1 <i>p</i> -value	Controls vs. HD2 <i>p</i> -value
Average subcortical volumes (mm³)					
Caudate	3580 ± 426	2467 ± 584	2449 ± 662	< 0.001	< 0.001
Putamen	4863 ± 586	3392 ± 644	3333 ± 643	< 0.001	< 0.001
Accumbens	472 ± 112	378 ± 115	362 ± 102	0.014	0.002
Average cortical thickness per brain region (mm)					
Frontal cortex	2.55 ± 0.11	2.49 ± 0.09	2.43 ± 0.12	0.227	< 0.001
Medial temporal cortex	2.86 ± 0.17	2.81 ± 0.14	2.71 ± 0.16	0.997	0.003
Lateral temporal cortex	2.75 ± 0.12	2.68 ± 0.12	2.60 ± 0.14	0.262	< 0.001
Parietal cortex	2.34 ± 0.11	2.22 ± 0.11	2.17 ± 0.14	0.006	< 0.001
Occipital cortex	2.03 ± 0.12	1.92 ± 0.13	1.88 ± 0.14	0.016	< 0.001
Cingulate cortex	2.56 ± 0.14	2.50 ± 0.09	2.43 ± 0.11	0.209	< 0.001

Mean ± SD of subcortical volumes (mm³) and cortical thickness per brain region (mm) are presented. The average cortical thickness for each brain region was calculated using a weighted sum of thickness values accounted for surface area using the following formula described previously by Johnson et al., 2015¹³, and Segura et al., 2014²⁵: Average thickness of region A and B = ((Thickness region A * Surface area region A) + (Thickness region B * Surface area region B)) / (Surface area region A + Surface area region B). One-way ANOVA was used to analyze group differences, with post-hoc comparisons using Bonferonni correction. Significant differences compared to controls after correction for multiple comparisons (*p* < 0.006) are displayed in bold.

FIGURE 2 Striatal volume and cortical thickness in HD gene carriers



Boxplots of striatal volumes and cortical thickness per region in HD gene carriers compared to controls (100%). Using analysis of variance (ANVOA), significant reductions in caudate nucleus and putamen volumes were observed for both HD1 and HD2 patients compared to controls. Furthermore, significant cortical thinning for all brain regions was present in HD2 patients compared to controls.

* Significant different compared to controls, $p < 0.006$ (corrected for multiple comparisons, 0.05/8)

3.3. Relationship between cortical and striatal atrophy

In the whole HD gene carriers group (HD1 and HD2 combined), the relationship between striatal volume and cortical thickness was examined adjusted for age and gender for each corticostriatal loop described in Figure 1. Multiple linear regression analyses after correction for multiple comparisons showed no significant associations between any cortical region and corresponding striatal volume within a corticostriatal loop (Table 3 and Figure 3).

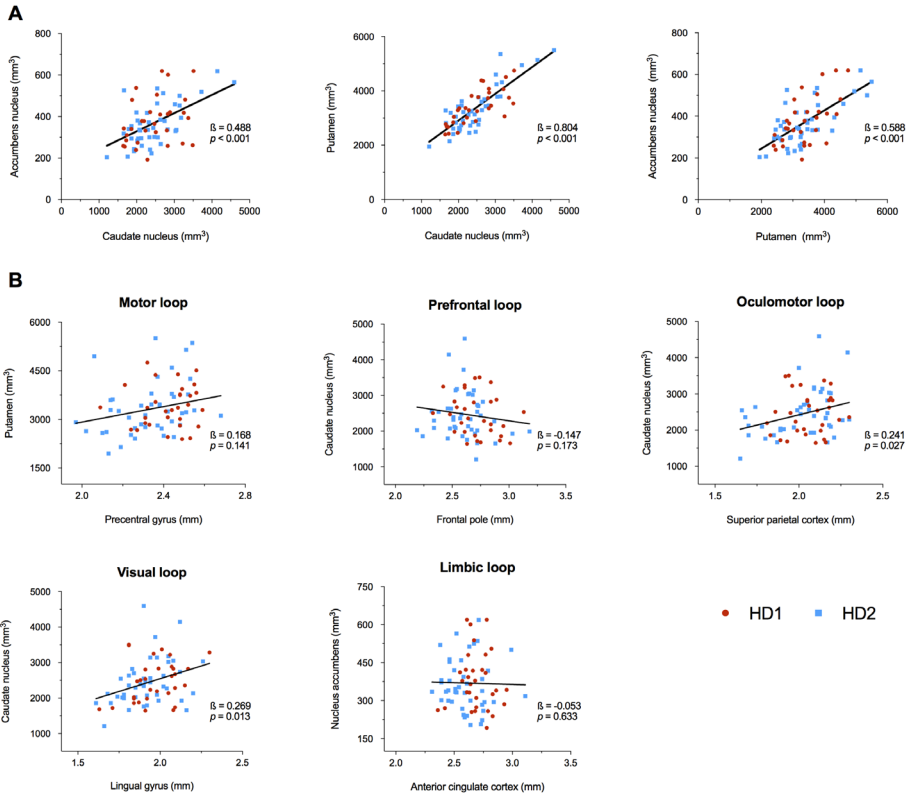
TABLE 3 Associations between regional cortical thickness and striatal volumes

	Cortical region	Lobe	Caudate nucleus		Putamen		Nucleus accumbens	
			Standardized β	<i>p</i> -value	Standardized β	<i>p</i> -value	Standardized β	<i>p</i> -value
Motor loop	Precentral gyrus (BA4)	Frontal			0.168	0.141		
	Paracentral lobule (BA6)	Frontal			0.020	0.410		
	Postcentral gyrus (BA1, 2,3)	Parietal			0.151	0.170		
Prefrontal loop	Middle frontal gyrus (BA9, 46)	Frontal	0.074	0.513				
	Frontal pole (BA10)	Frontal	-0.147	0.173				
Oculomotor loop	Superior frontal gyrus (BA8)	Frontal	0.077	0.504				
	Precuneus (BA7)	Parietal	0.237	0.022				
	Superior parietal cortex (BA5, 7)	Parietal	0.241	0.027				
Visual loop	Inferior frontal gyrus (BA44, 45)	Frontal	-0.033	0.776				
	Inferior temporal cortex (BA20)	Lateral temporal	0.019	0.863				
	Superior temporal (BA22)	Lateral temporal	-0.008	0.945				
	Pericalcarine cortex (BA17)	Occipital	0.091	0.408				
	Cuneus (BA18)	Occipital	0.239	0.028				
	Lingual gyrus (BA18)	Occipital	0.269	0.013				
	Lateral occipital cortex (BA19)	Occipital	0.265	0.014				
	Fusiform (BA19, 37)	Medial temporal	0.191	0.084				
Limbic loop	Orbitofrontal cortex (BA47)	Frontal					0.022	0.836
	Entorhinal cortex (BA28, 34)	Medial temporal					-0.010	0.925
	Parahippocampal gyrus (BA27, 28)	Medial temporal					0.077	0.471
	Anterior cingulate cortex (BA24)	Cingulate					-0.053	0.633

Data are standardized Beta coefficients using linear regression corrected for age and gender. Unadjusted significant *p*-values (*p* < 0.05) are displayed in bold. After correction for multiple comparisons (*p* < 0.003), no significant associations were observed between regional cortical thickness and striatal regions.



FIGURE 3 Relationship within striatum and in corticostriatal circuits



A: Scatter plots of relationships between striatal structures (i.e., caudate nucleus, putamen, and accumbens nucleus). The most pronounced association was present between the putamen and caudate nucleus.

B: Scatter plots of relationships between cortical thickness and striatal volume in HD gene carriers. For each corticostriatal circuit, an example is presented. However, after correction for multiple comparisons, there were no significant associations between cortical thickness and striatal volumes for all corticostriatal loops.

4. DISCUSSION

This study showed striatal atrophy and cortical thinning, primarily in parietal and occipital regions in the earliest manifest HD disease stage, but we found no association between cortical thinning and striatal volume loss. This suggests that striatal degeneration in early HD gene carriers might be independent of cortical degeneration and can therefore be seen as two separate neurodegenerative processes that occur simultaneously.

Furthermore, it is surprising that the frontal lobe is relatively unaffected in early disease stages, since the striatum predominantly projects to frontal cortical regions, such as the primary motor cortex and dorsolateral prefrontal cortex.^{17,18} Still, the parietal and occipital cortices, brain regions that seem to be mainly affected in HD, are also connected to the striatum.¹⁹ More specifically, orbitofrontal, parietal, and occipital brain regions are connected to the caudate nucleus, whereas the sensorimotor cortex in the fronto-parietal cortices are mainly connected with the putamen.¹⁷⁻¹⁹ The limbic structures and the prefrontal cortex have projections to the nucleus accumbens, the ventral part of the striatum.¹⁷⁻¹⁹ Our findings showed a trend towards a possible association between the volume of the caudate nucleus and the thickness of cortical regions of the oculomotor loop and visual loop. However, these associations were not significant after correction for multiple comparisons.

Early manifest HD gene carriers can be divided in disease stage 1 (HD1) and stage 2 (HD2) based on the patients' capacity of daily functioning.²¹ In our study, extensive atrophy of the caudate nucleus, putamen, and nucleus accumbens was present in similar degrees in both disease stages. Cortical thinning, however, was found throughout the entire brain in HD2 patients. In HD1 patients, our data showed a trend towards thinning of parietal and occipital cortices compared to controls, however, this was not significant due to correction for multiple comparisons. These results suggest that the degree of striatal atrophy seems to stabilize after disease onset whereas the degree of cortical atrophy increases, beginning in the posterior brain regions with relative sparing of the frontal, parietal, and cingulate cortices. Our findings are consistent with previous studies in manifest HD that showed thinning of the superior and posterior cortical brain regions with minimal involvement of the anterior frontal and lateral temporal lobes.^{9,10} Other studies additionally showed that cortical involvement contributes to behavioral, cognitive and motor symptoms in HD patients.^{6,9,13,14} For instance, worse performance on attentional and executive tasks was correlated with thinning in the primary motor cortex, and parietal and occipital regions.^{9,13} In addition, cell loss in the

anterior cingulate cortex was found in HD patients with prominent mood symptoms,⁶ whereas oculomotor abnormalities have been related with volume reductions in occipital regions.¹⁴

Our findings support the hypothesis that cortical and striatal degeneration might be independent neurodegenerative processes in HD. This could explain the fact that affective, behavioral and cognitive symptoms of HD have been linked to cortical atrophy instead of striatal atrophy.^{6,9,13}

Only few studies have previously assessed cortical thinning in early manifest HD gene carriers and most studies consisted of small sample sizes without subdividing manifest HD gene carriers in different disease stages.^{9,27-30} The strength of our study lies in the fact that we can confirm a distinct pattern of cortical thinning in a relatively large sample of early manifest HD gene carriers, considering HD is a rare neurodegenerative disorder.

A limitation of this study is that we used automated global volumetric segmentations of striatal structures using relatively large structural models. In the early disease stages of HD, striatal atrophy mainly involves the body and tail of the caudate nucleus.⁴ However, our structural models did not allow us to subdivide the caudate nucleus. Furthermore, although we assessed patterns of neurodegeneration in different disease stages to better understand the structural changes during disease progression, longitudinal studies are still necessary to validate our findings.

Many longitudinal studies have previously focused on evaluating the rate of decline in striatal volume in different disease stages, even in HD gene carriers close to disease onset but without motor symptoms.^{10,31,32} Striatal atrophy has also been linked to clinical signs in HD, such as motor symptoms,^{11,14} and executive dysfunction,^{33,34} thus making striatal volume an interesting outcome measure in clinical intervention trials.

Nevertheless, given the relationship of cortical atrophy with other specific HD related signs and our suggestion that cortical degeneration occurs independent from striatal atrophy, cortical thickness measurements might also be valuable for future clinical trial designs.

In conclusion, cortical degeneration in the earliest manifest HD disease stage primarily begins in parietal and occipital brain regions, while the frontal lobe remains less affected in this stage. This is interesting, since the striatum mainly projects to the frontal lobe. Still, thinning of parietal and occipital cortices is not related with striatal atrophy, suggesting that cortical and striatal degeneration are independent neurodegenerative processes in HD. This is important for future clinical trial designs that target cognitive, affective or behavioral symptoms in HD patients, as these symptoms have been linked to cortical atrophy.

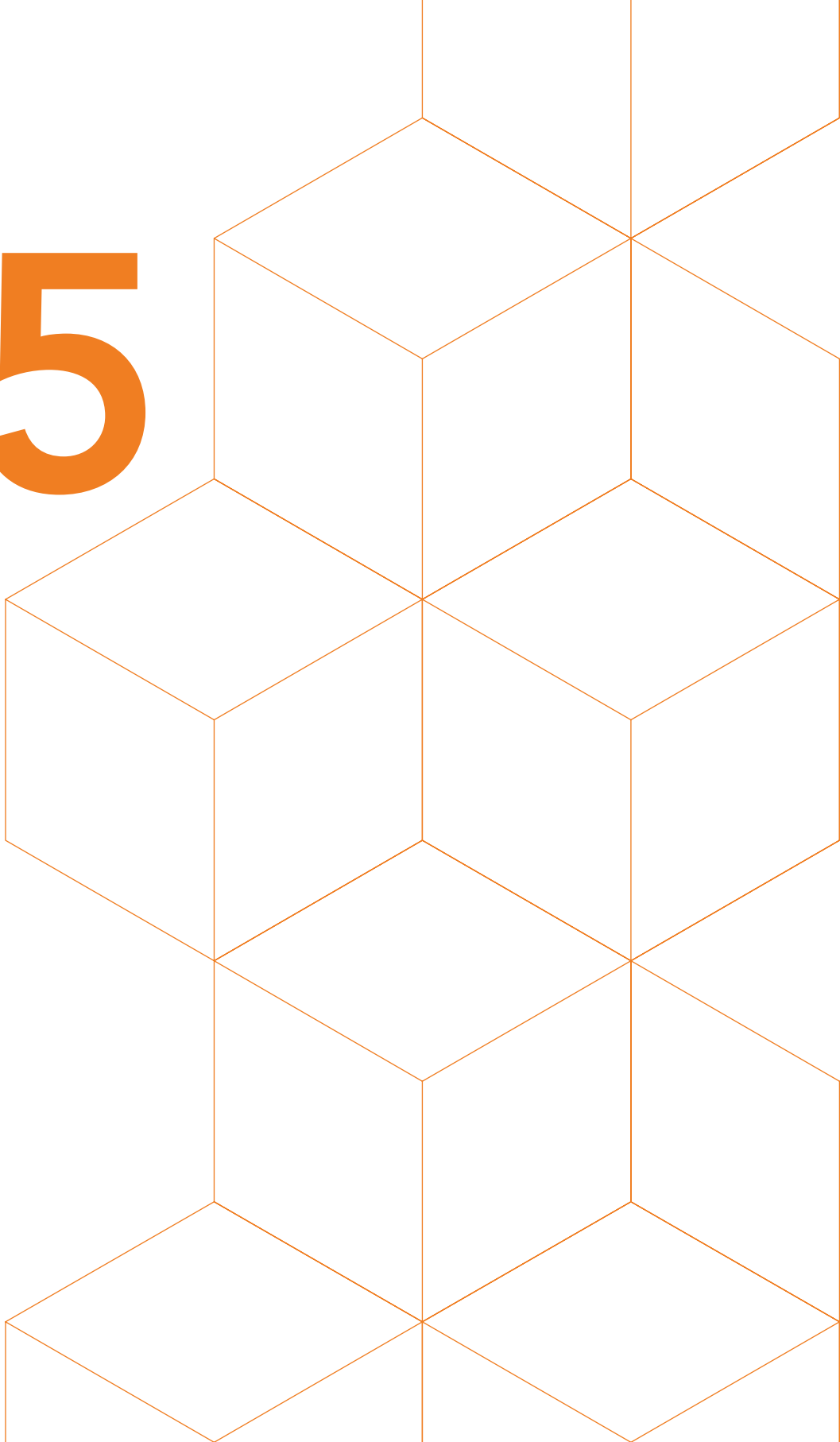
REFERENCES

1. Rüb U, Seidel K, Heinsen H, Vonsattel JP, den Dunnen WF, Korf HW. Huntington's disease (HD): the neuropathology of a multisystem neurodegenerative disorder of the human brain. *Brain Pathol.* 2016;26:726-740.
2. The Huntington's Disease Collaborative Research Group. A novel gene containing a trinucleotide repeat that is expanded and unstable on Huntington's disease chromosomes. *Cell.* 1993;72(6):971-983.
3. Reiner A, Albin RL, Anderson KD, D'Amato CJ, Penney JB, Young AB. Differential loss of striatal projection neurons in Huntington disease. *Proc Natl Acad Sci U S A.* 1988;85(15):5733-5737.
4. Vonsattel JP, Myers RH, Stevens TJ, Ferrante RJ, Bird ED, Richardson EP. Neuropathological classification of Huntington's disease. *J Neuropathol Exp Neurol.* 1985;44(6):559-577.
5. O'Callaghan C, Bertoux M, Hornberger M. Beyond and below the cortex: the contribution of striatal dysfunction to cognition and behaviour in neurodegeneration. *J Neurol Neurosurg Psychiatry.* 2014;85(4):371-378.
6. Thu DCV, Oorschot DE, Tippett LJ, et al. Cell loss in the motor and cingulate cortex correlates with symptomatology in Huntington's disease. *Brain.* 2010;133(4):1094-1110.
7. Nana AL, Kim EH, Thu DCV, et al. Widespread heterogeneous neuronal loss across the cerebral cortex in Huntington's disease. *J Huntingtons Dis.* 2014;3:45-64.
8. Waldvogel HJ, Kim EH, Thu DCV, Tippett LJ, Faull RLM. New perspectives on the neuropathology in Huntington's disease in the human brain and its relation to symptom variation. *J Huntingtons Dis.* 2012;1:143-153.
9. Rosas HD, Salat DH, Lee SY, et al. Cerebral cortex and the clinical expression of Huntington's disease: complexity and heterogeneity. *Brain.* 2008;131(4):1057-1068.
10. Tabrizi SJ, Langbehn DR, Leavitt BR, et al. Biological and clinical manifestations of Huntington's disease in the longitudinal TRACK-HD study: cross-sectional analysis of baseline data. *Lancet Neurol.* 2009;8(9):791-801.
11. Scahill RI, Hobbs NZ, Say MJ, et al. Clinical impairment in premanifest and early Huntington's disease is associated with regionally specific atrophy. *Hum Brain Mapp.* 2013;34(3):519-529.
12. Harrington DL, Liu D, Smith MM, et al. Neuroanatomical correlates of cognitive functioning in prodromal Huntington disease. *Brain Behav.* 2014;4(1):29-40.
13. Johnson EB, Rees EM, Labuschagne I, et al. The impact of occipital lobe cortical thickness on cognitive task performance: An investigation in Huntington's Disease. *Neuropsychologia.* 2015;79:138-146.

14. Coppens EM, Jacobs M, van den Berg-huysmans AA, van der Grond J, Roos RAC. Grey matter volume loss is associated with specific clinical motor signs in Huntington's disease. *Park Relat Disord.* 2018;46:56-61.
15. Coppens EM, van der Grond J, Hart EP, Lakke EAJF, Roos RAC. The visual cortex and visual cognition in Huntington's disease: An overview of current literature. *Behav Brain Res.* 2018;351:63-74.
16. Younes L, Ratnanather JT, Brown T, et al. Regionally selective atrophy of subcortical structures in prodromal HD as revealed by statistical shape analysis. *Hum Brain Mapp.* 2014;35(3):792-809.
17. Alexander GE, DeLong MR, Strick PL. Parallel organization of functionally segregated circuits linking basal ganglia and cortex. *Annu Rev Neurosci.* 1986;9:357-381.
18. Lawrence AD, Sahakian BJ, Robbins TW. Cognitive functions and corticostriatal circuits: Insights from Huntington's disease. *Trends Cogn Sci.* 1998;2(10):379-388.
19. Seger CA. The visual corticostriatal loop through the tail of the caudate: circuitry and function. *Front Syst Neurosci.* 2013;7:1-15.
20. Huntington Study Group. Unified Huntington's disease rating scale: reliability and consistency. *Mov Disord.* 1996;11(2):136-142.
21. Shoulson I, Fahn S. Huntington disease: Clinical care and evaluation. *Neurology.* 1979;(29):1-3.
22. Penney J, Vonsattel JP, MacDonald ME, Gusella JF, Myers RH. CAG repeat number governs the development rate of pathology in Huntington's disease. *Ann Neurol.* 1997;41(5):689-692.
23. Fischl B, Dale AM. Measuring the thickness of the human cerebral cortex from magnetic resonance images. *Proc Natl Acad Sci U S A.* 2000;97(20):11050-11055.
24. Desikan RS, Segonne F, Fischl B, et al. An automated labeling system for subdividing the human cerebral cortex on MRI scans into gyral based regions of interest. *Neuroimage.* 2006;31:968-980.
25. Segura B, Baggio HC, Marti MJ, et al. Cortical thinning associated with mild cognitive impairment in Parkinson's disease. *Mov Disord.* 2014;29(12):1495-1503.
26. Fischl B, Salat DH, Busa E, et al. Whole brain segmentation: Automated labeling of neuroanatomical structures in the human brain. *Neuron.* 2002;33:341-355.
27. Rosas HD, Liu AK, Hersch S, et al. Regional and progressive thinning of the cortical ribbon in Huntington's disease. *Neurology.* 2002;58(5):695-701.
28. Nopoulos PC, Aylward EH, Ross CA, et al. Cerebral cortex structure in prodromal Huntington disease. *Neurobiol Dis.* 2010;40(3):544-554.
29. Rupp J, Dziedzic M, Bleker T, et al. Comparison of vertical and horizontal saccade measures and their relation to gray matter changes in premanifest and manifest Huntington disease. *J Neurol.* 2012;259(2):267-276.

30. Nanetti L, Contarino VE, Castaldo A, et al. Cortical thickness, stance control, and arithmetic skill: An exploratory study in premanifest Huntington disease. *Park Relat Disord.* 2018;51:17-23.
31. Aylward EH, Liu D, Nopoulos PC, et al. Striatal volume contributes to the prediction of onset of Huntington disease in incident cases. *Biol Psychiatry.* 2012;71(9):822-828.
32. Paulsen JS, Long JD, Ross CA, et al. Prediction of manifest Huntington's disease with clinical and imaging measures: A prospective observational study. *Lancet Neurol.* 2014;13(12):1193-1201.
33. Peinemann A, Schuller S, Pohl C, Jahn T, Weindl A, Kassubek J. Executive dysfunction in early stages of Huntington's disease is associated with striatal and insular atrophy: A neuropsychological and voxel-based morphometric study. *J Neurol Sci.* 2005;239:11-19.
34. Wolf RC, Thomann PA, Thomann AK, et al. Brain structure in preclinical huntington's disease: A multi-method approach. *Neurodegener Dis.* 2013;12(1):13-22.

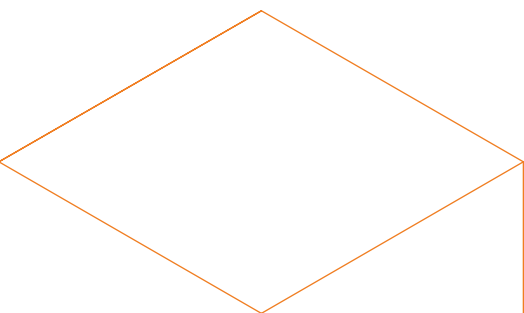
5



The visual cortex and visual cognition in Huntington's disease: an overview of current literature

Emma M. Coppen, Jeroen van der Grond, Ellen P. Hart,
Egbert A.J.F. Lakke, Raymund A.C. Roos

Behavioural Brain Research. 2018 May;351:63-74



ABSTRACT

The processing of visual stimuli from retina to higher cortical areas has been extensively studied in the human brain. In Huntington's disease (HD), an inherited neurodegenerative disorder, it is suggested that visual processing deficits are present in addition to more characteristic signs such as motor disturbances, cognitive dysfunction, and behavioral changes. Visual deficits are clinically important because they influence overall cognitive performance and have implications for daily functioning.

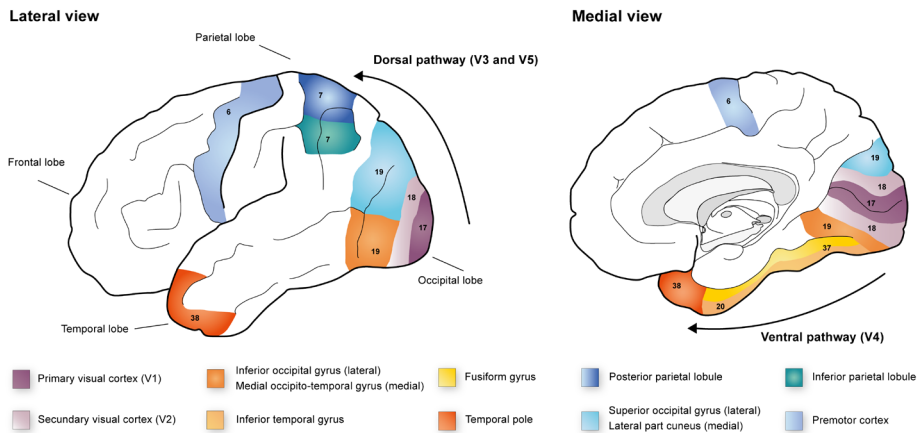
The aim of this review is to summarize current literature on clinical visual deficits, visual cognitive impairment, and underlying visual cortical changes in HD patients. A literature search was conducted using the electronic database of PubMed/Medline.

This review shows that changes of the visual system in patients with HD were not the primary focus of currently published studies. Still, early atrophy and alterations of the posterior cerebral cortex was frequently observed, primarily in the associative visual cortical areas such as the lingual and fusiform gyri, and lateral occipital cortex. Changes were even present in the premanifest phase, before clinical onset of motor symptoms, suggesting a primary region for cortical degeneration in HD. Although impairments in visuospatial processing and visual perception were reported in early disease stages, heterogeneous cognitive batteries were used, making a direct comparison between studies difficult. The use of a standardized battery of visual cognitive tasks might therefore provide more detailed information regarding the extent of impairments in specific visual domains. Further research could provide more insight into clinical, functional, and pathophysiological changes of the visual pathway in HD.

1. INTRODUCTION

Many regions of the human brain are involved in processing visual stimuli, from the retina to cortical brain areas. The organization and function of the visual cortex has been extensively studied in primates, both in macaques and healthy human adults.^{1,2} Visual field mapping using functional Magnetic Resonance Imaging (fMRI) showed that approximately 20-30% of the human brain is directly or indirectly involved in visual processing.^{3,4} Incoming visual stimuli are transmitted from the retina through the afferent visual pathway via the optic nerve and optic tract, to the lateral geniculate nucleus in the thalamus.⁵ Then, via the optic radiation, signals reach the primary visual cortex in the occipital lobe and eventually the associative (secondary and tertiary) visual cortices for further processing.⁵

FIGURE 1 Visual cortex in human brain



Schematic lateral and medial overview of cortical regions involved in the processing of visual stimuli in the human brain. Stimuli pass the retina via the optic tract to the primary visual cortex (V1) and secondary visual cortex (V2) for basic processing (i.e. shape and contrast). Although there are no clear demarcations among the regions of the posterior cortex, it is clear that higher-level visual processing occurs in the regions surrounding the primary visual cortex, which are divided into visual areas V3, V4 and V5. The ventral pathway runs through the medial part of Brodmann area 19, located in the anterior medial occipito-temporal gyrus, towards Brodmann area 37 (or V4) which is located in the caudal two-thirds of the lateral occipito-temporal gyrus (e.g. fusiform gyrus). V4 projects to Brodmann area 20, located in the inferior temporal gyrus, to Brodmann area 38, located in the anterior temporal pole, and to the limbic system. The dorsal pathway (V3 and V5) conveys visual information to the posterior parietal cortex (Brodmann area 7) and the premotor cortex (Brodmann area 6). In general, the ventral pathway in the temporal-occipital region is involved in object recognition and color processing, whereas the dorsal pathway processes depth and movement perception. Numbers in each cortical region depict corresponding Brodmann areas.

The primary visual cortex (also known as V1, striate cortex or Brodmann area 17) is located around the edges of the calcarine fissures on the medial and dorsolateral surface of the occipital lobe.^{3,6} The visual association areas (also known as the extra-striate cortices) are responsible for the interpretation of the visual input, such as color discrimination, motion perception, depth, and contrast.³ The secondary visual cortex (V2 or Brodmann area 18) processes basic visual characteristics such as color perception and orientation.^{2,7} On the medial occipital lobe surface, V2 is located in the cuneus above V1 and in the medial occipito-temporal gyrus (e.g. lingual gyrus) below V1, whereas on the lateral surface, V2 is located in the occipital gyrus anterior to V1.² From V2 onwards, visual processing proceeds along two parallel pathways, the ventral (occipito-temporal) pathway, and the dorsal (occipito-parietal) pathway.⁸ The ventral stream is also known as the 'what' visual pathway, and is involved in the recognition of objects, faces and shapes and color processing.^{2,7} The dorsal stream is known as the 'where' visual pathway and it is suggested that this area is necessary for depth (three-dimensional vision) and movement perception in relation to objects in space in the frontal eye fields.^{1,2,9,10} A summary of the visual cortical areas and their function is presented in Table 1 and Figure 1.

TABLE 1 Visual cortex and higher visual function

Visual area	Brodmann area	Cortex	Function
V1	17	Calcarine fissure Occipital pole	Mapping and processing visual stimuli
V2	18	Cuneus Lingual gyrus	Color discrimination
V4	19 (medial) / 37 20	Fusiform gyrus Inferior temporal gyrus	<i>Ventral 'what' pathway:</i> Object recognition
V3	19	Lateral part of cuneus	<i>Dorsal 'where' pathway:</i>
V5	19 (lateral) / 7	Superior occipital gyrus Posterior parietal cortex	Movement and spatial perception

Any alteration in the visual pathway may result in clinical visual deficits and changes in cognitive performance. In Huntington's disease (HD), a hereditary neurodegenerative disorder, cortical degeneration of visual brain regions is suggested to be present in early disease stages, in addition to striatal atrophy.¹¹⁻¹³ HD is autosomal dominantly inherited and caused by a cytosine-adenine-guanine (CAG) repeat mutation of the Huntingtin (HTT) gene on chromosome 4.¹⁴ The estimated prevalence of the disease is 5-10 per 100.000 in the Caucasian population.¹⁵ The manifest phase of the disease is generally characterized by progressive motor disturbances, cognitive decline, and behavioral changes.¹⁵ However, clinical signs can vary considerably among patients during the course of the disease as well as time of disease onset. Typically, the mean age of disease onset is between 30 and 50 years (range from 2 to 85 years) and the mean disease duration is between 17 to 20 years.¹⁵

Most reported behavioral and psychiatric symptoms in HD include apathy, depression, irritability, and obsessive-compulsive behavior.¹⁶ Visual hallucinations or other psychotic symptoms are rarely seen in HD patients. In a study of 1,993 HD gene mutation carriers, mild psychosis was only observed in 2.9% of the study population and only 1.2% scored moderate to severe psychosis, but no visual hallucinations were reported.¹⁶

Early cognitive deficits in HD mainly involve impairments in executive functioning, such as attention and planning difficulties, and cognitive inflexibility, which gradually progresses over time and eventually results in dementia.^{15,17} Executive dysfunction can already be present in the premanifest phase, before motor symptoms occur.^{17,18} Although deficits in visual acuity or visual dysfunction are not typical clinical features of HD, visuospatial deficits are reported in HD patients. Such visuospatial deficits are of clinical importance because they can influence overall cognitive performance and may have major functional implications, for example the impact on driving a car or using electronic devices such as mobile phones and computers. Also, visual deficits should be taken into account when conceptualizing cognitive assessments for measuring drug efficacy in clinical trials. By providing an overview regarding the brain structure and function of the visual cortex in patients with HD, we propose to provide novel information on disease progression and cortical degeneration. Therefore, the aim of this review is to summarize the current literature regarding visual cognitive impairment and identify the posterior cortical changes that occur in HD patients.

2. METHODS

A review of the existing literature on visual impairment in HD was conducted using the electronic database of PubMed/Medline. All literature published before August 2017 was critically reviewed. The following search terms were used in several combinations to identify the available literature: "Huntington", "Huntington's disease", "visual", "visual cognition", "visual processing", "visuospatial", "atrophy", "occipital cortex", "cerebral blood flow", "visual pathway", and "visual system". In addition, potential eligible studies were also screened using the reference lists of the studies found. Only original research papers and review articles written in English were considered for further review. Animal model studies, letters to editors and editorial comments were excluded. Articles that examined the visual cortex and/or assessed visual cognition in manifest and premanifest HD gene carriers were included for further evaluation.

3. RESULTS

3.1. Search results

Of the 1,406 articles that were identified by the initial database search, 85 articles were selected for further review based on the abstract. Twenty-two studies were included for this review as these studies specifically investigated visual function in HD. Of these 22 studies, one post-mortem brain study and six neuroimaging studies addressed changes of the visual cortex in HD gene carriers, and 15 neuropsychological studies assessed visual cognitive functioning in HD. We will first focus on the structural and functional changes of the visual cortex reported in manifest and premanifest HD gene carriers in paragraphs 3.2.1 and 3.2.2. An overview of the literature regarding changes of the visual cortex is also provided in Table 2. In paragraph 3.2.3, we will discuss the findings of studies investigating visual cognition in HD using the following cognitive domains: visual perception, visuospatial processing, visual working memory, visuconstruction and visuomotor function. These visual cognitive domains and their associated neuropsychological tasks are summarized in Table 3. Furthermore, a summary of the current literature on visual cognition in HD is given in Table 4. Besides the 22 studies that investigated visual function in HD, another 26 articles were additionally reviewed, of which 24 articles assessing whole brain changes in HD, and two articles examining an extensive neuropsychological assessment battery in HD. These studies did not specifically aim to focus on the visual system, but did report relevant findings on the visual pathway in HD and will therefore be discussed in the corresponding paragraphs.

3.2. The visual cortex in Huntington's disease

Neuropathological alterations in HD are primarily found in the striatum, especially in the caudate nucleus and putamen, due to loss of striatal medium-sized spiny neurons.¹⁹ Although striatal atrophy is considered to be the origin of choreiform movements seen in HD patients, it is suggested that other symptoms of HD are related to cortical degeneration, as extensive neuronal loss is seen throughout the cerebral cortex when the disease progresses.²⁰⁻²²

3.2.1. Structure of the cerebral cortex

A post-mortem brain study showed a 32% reduction of nerve cells in the primary visual area (Brodmann area 17) in brains of 7 HD patients in advanced disease stages compared to 7 controls.²³ The authors conclude that damage to the primary visual area contributes to the pathogenesis of visual dysfunction.²³ This study, however, only examined nerve cells in Brodmann area 17 in the occipital lobe and did not assess other brain regions, which is contrary to another study that examined the patterns of neuronal cell loss in the frontal, parietal, temporal, and occipital lobes in post-mortem brains of 14 end stage HD patients.²¹ Compared to controls, HD patients showed the highest difference in pyramidal neuron cells in the secondary visual cortex (42% decrease), whereas no significant pyramidal cell differences was observed in the primary visual cortex (3% decrease).²¹ In comparison, a 27-34% reduction in pyramidal cell number was found in HD patients compared to controls for the superior frontal, middle temporal, superior parietal, and primary sensory cortices.²¹ Between HD patients, there was additionally more neuronal loss in the secondary visual cortex (36% loss) than in the primary visual cortex (12% loss), suggesting that mainly associative visual regions are impaired in HD.²¹ These latter findings were confirmed by a MRI study that observed reduced cortical thickness of the lingual gyrus and lateral occipital cortex in premanifest gene carriers close to disease onset (n=58) and early stage HD patients (n=40) that was associated with worse visuospatial task and visual working memory performance measured with the Map Search task, Spot the change task and the Trail Making Test part A.¹³ No associations were found between cognitive performance and thickness of the cuneus. This implies a distinct association between higher-level cognitive performance and cortical occipital degeneration.¹³ An additional MRI study examined structural posterior brain changes in relation to visuospatial attention in premanifest (n=119) and early stage manifest HD (n=104), and found associations between poorer visuospatial performance (measured using the Map Search and mental rotation tasks) and volume loss in the cuneus, lingual, fusiform gyri, and motor regions in manifest HD compared to controls.²⁴ Another study focused on the link between visuomotor

performance and prefrontal cortex atrophy, but additionally found focal volume loss in the occipital cortex and associations between this volume loss and poorer visuomotor performance (measured using the 15-Object test, a visuomotor integration task).²⁵ Yet, another study examining visuomotor function using the Circle Tracing task and cortical volume loss did not find any significant association between visuomotor task performance and the visual and motor cortices,²⁶ but this might be explained by the fact that in these studies different cognitive assessments were used to evaluate visuomotor function.

In studies focusing on whole brain cortical changes and associations with clinical impairments, reduced cortical thickness of the cuneus,^{12,27} and volume loss of the occipital lobe,^{11,28-31} and parietal lobe¹² were observed in both premanifest and early manifest disease stages compared to controls.

In conclusion, volumetric changes of posterior cortical regions can already be detected in early stages of the disease, even in the premanifest phase, while frontal and temporal regions remain largely unaffected.

3.2.2. Cortical brain function

It is thought that clinical manifestations of HD not only depend on brain atrophy, but are also influenced by neuronal dysfunction and loss in neuronal network structure.³²

Functional MRI (fMRI) can be used to study neural function. Several fMRI studies in HD gene carriers showed changes in multiple functional brain networks before brain atrophy or clinical symptoms were present.^{32,33}

Only one functional imaging study focused on the visual system in 20 early HD patients using resting-state fMRI.³⁴ Resting-state fMRI assesses overall brain connectivity that is not related to task performance. Reduced fusiform cortex activity in HD patients was found after correcting for whole brain atrophy compared to controls.³⁴ The authors therefore conclude that activation differences in the occipital cortex could not sufficiently be explained by regional brain volume loss alone. Another study reported reduced brain connectivity using whole brain resting-state fMRI in the occipital cortices in both premanifest and manifest HD gene carriers compared to controls.³⁵ However, decline in brain connectivity over time in the occipital region was not confirmed in longitudinal resting-state fMRI studies.^{36,37}

It is suggested that visual stimulation results in an increase in glucose uptake in the brain and cerebral blood flow.³⁸ Therefore, a ³¹phosphorus nuclear magnetic resonance (NMR) spectroscopy study used a basic visual stimulation task to activate the occipital cortex and measure metabolite concentrations for the assessment of brain energy deficits in manifest HD (n=15) compared to controls (n=15).³⁹ An increase in metabolite

concentrations was observed in controls, whereas HD patients did not show any response to brain activation, indicating impaired mitochondrial function in the visual cortex.³⁹ In addition, two small task-based fMRI studies demonstrated reduced neural activity of the occipital cortex, during a Porteus Maze task in 3 premanifest individuals,⁴⁰ and during a serial reaction time task in early and premanifest HD patients (n=8).⁴¹ These studies also showed reduced activation in the caudate, parietal and sensorimotor cortices,⁴⁰ and in the middle frontal gyri and precuneus.⁴¹ As these tasks were examined in small patient groups and involve a combination of basic and higher visual processing, motor speed, and spatial functioning, a direct conclusion cannot be drawn regarding neural dysfunction of the occipital cortex alone.

3.2.3. Cerebral metabolism

With positron emission tomography (PET) imaging, functional or metabolic changes in HD can be studied using a radioactive labeled tracer that binds to specific structures within the brain. Several reviews have recently discussed the developments of PET imaging in HD.⁴²⁻⁴⁴ Overall, there is increasing evidence of reduced glucose metabolism in the striatum, and frontal and temporal cortices, which seem to be reliable predictors of disease progression in HD.⁴²⁻⁴⁴ There have been no PET studies performed to date that specifically focused on the glucose metabolism of the visual cortex in HD patients. However, an interesting finding was observed by a study group that examined spatial covariance patterns between different networks of regions with altered glucose metabolism using PET imaging.^{45,46} A relative increase in glucose metabolism was found in thalamic, motor, occipital and cerebellar regions, in association with a decrease in striatal metabolism in HD patients compared to healthy controls.^{45,46} A recent study reports similar findings of striatal hypometabolism in combination with hypermetabolism in the cerebellum, thalamus, and occipital cortex.⁴⁷ Here, hypermetabolism in the cuneus and lingual gyrus was negatively correlated with hypokinetic motor scores. These findings suggest that a decrease in glucose metabolism might be linked to clinical disease onset, whereas an increase in glucose metabolism indicates a compensatory mechanism for neuronal loss and/or motor disturbances.^{46,47} As neuronal loss is indirectly measured using functional MRI, the reduced brain activity in the occipital cortex of HD patients found in previous fMRI studies might indeed explain the hypermetabolism found in these PET studies.

Another approach to assess alterations in metabolism is by measuring cerebral blood flow (CBF) or cerebral blood volume (CBV) using transcranial Doppler (TCD) ultrasonography, PET imaging or arterial spin labeling MRI.⁴⁸

Reductions in cerebral blood flow and elevations in cerebral blood volume were primarily observed in frontal cortical regions in premanifest HD gene carriers.^{49,50} In manifest HD, hypoperfusion was additionally observed in the fronto-parietal regions and anterior cingulate cortex during a word generation task,⁵¹ motor task,⁵² and executive functioning tasks,^{53,54} but no alterations in cerebral perfusion were detected in the posterior cortex during task performance. One study reported heterogeneous regional CBF reductions in rest in 17 early manifest HD extending to the sensorimotor, paracentral, inferior temporal and lateral occipital regions, with normal CBF in the thalamus, postcentral gyrus, insula, and medial occipital areas.⁵⁵ However, the degree of cortical thinning exceeded CBF reductions in the temporal and occipital cortices, and in the striatum, suggesting that structural and vascular alterations might originate from different underlying pathologic mechanisms.⁵⁵ More studies are necessary to evaluate the manner of perfusion changes over the course of the disease but hypoperfusion seems to play a role in the pathophysiology of neuronal dysfunction in HD.

In conclusion, although the visual system has not been the main focus in many imaging studies in HD to date, atrophy (i.e. volume loss and cortical thinning), reduced neural activity and functional connectivity, and changes in glucose metabolism of the posterior cerebral cortex have been reported in both early stage HD patients and premanifest gene carriers. This suggests that the posterior cerebral cortex might be one of the first cortical regions to undergo pathological and functional changes.

3.3. Visual cognition in Huntington's disease

Many studies investigated the progression of cognitive impairment in different HD disease stages.¹⁷ Here, we will focus on studies assessing cognitive deficits in HD that involve a visual component. Visual cognitive functioning can be divided into different domains of visual processing, however, the terminology that is used to define visual cognition widely differs among the current literature. Also, many neuropsychological assessments that are used to evaluate visual cognitive function often require a combination of several domains, such as visual attention, spatial orientation and working memory. Additionally, in HD patients, possible influence of a motor component on cognitive performances should also be considered. Below, we will discuss the reviewed studies using the following domains: visual perception, visuospatial processing, visual working memory, visuoconstruction and visuomotor function (Table 3).

In general, color, patterns, depth, motion perception, and the recognition of facial expressions of emotions are usually classified as visual perceptual skills. Visuospatial processing or visual scanning and attention are needed to visually perceive objects and assess the spatial distance and relationship among items or objects. Visual working

TABLE 2 Overview of current literature on the visual cortex in HD

	Study population	Clinical HD disease stage	Study design	Assessments	Main significant finding
Gomez-Anson et al., 2009 ²⁵	Controls n = 21 PreHD n = 20	YTO: not available PreHD1: n = 12 (UHDRS-TMS = 0) PreHD2: n = 8 (UHDRS-TMS = 8)	Structural MRI	15-Objects test	Volume loss in cerebellum, prefrontal and posterior temporal cortices. Correlation with visuomotor task performance and prefrontal and occipital cortices.
Say et al., 2011 ²⁶	Controls n = 122 PreHD n = 119 HD n = 120	PreHD-A n = 62, YTO: 14.1 years PreHD-B n = 57, YTO: 8.7 years HD1 n = 75 HD2 n = 45 Disease duration: not available	Structural MRI (TRACK-HD)	Circle tracing task (direct and indirect)	No associations of task performance and loss of volume in visual and motor cortices. Only slower performance of indirect task was associated with lower grey matter volume in somatosensory cortex.
Mochel et al., 2012 ³⁹	Controls n = 15 HD n = 15	HD1 n = 15 Disease duration: not available	³¹ phosphorus NMR spectroscopy	Visual stimulation checkerboard	Unchanged metabolic concentrations during and after visual stimulation in HD.
Wolf et al., 2014 ³⁴	Controls n = 20 HD n = 20	HD1/2 n = 20 Disease duration: 3.2 years	Resting-state fMRI	SDMT VOSP	Decreased activity of left fusiform cortex, associated with lower scores on SDMT and higher disease burden in HD.
Johnson et al., 2015 ¹³	Controls n = 97 PreHD n = 109 HD n = 69	PreHD-A n = 51, YTO > 10.8 years PreHD-B n = 58, YTO < 10.8 years HD1 n = 40 HD2 n = 29 Disease duration: not available	Structural MRI (TRACK-HD)	SDMT Stroop Word Reading TMT A Map Search Mental Rotation Spot the change	Reduced occipital cortical thickness in preHD and HD patients. Except for mental rotation, poor performance on all cognitive tests was associated with thinner cortex for lingual and lateral occipital cortices in HD.
Rüb et al., 2015 ²³	Controls n = 7 HD n = 7	Age at death: 52.43 years Age at disease onset: 40.57 years Disease duration: 11.86 years	Post-mortem neuropathological study	N/A	A 32% reduction of estimated absolute nerve cell number in Brodmann area 17 in HD patients compared to controls.
Labuschagne et al., 2016 ²⁴	Controls n = 110 PreHD n = 119 HD n = 104	PreHD-A n = 55, YTO > 10.8 years PreHD-B n = 64, YTO < 10.8 years HD1 n = 59 HD2 n = 45 Disease duration: not available	Structural MRI (TRACK-HD)	Map Search Mental Rotation	Cognitive performance was associated with parieto-occipital (cuneus, calcarine, lingual) and temporal (posterior fusiform) volume and thickness in HD gene carriers.

Clinical stages of the study population are provided in the table, if information was available in the original papers. PreHD-A and PreHD-B indicate premanifest HD gene carriers classified based on the estimated time to disease onset (far or close respectively). Manifest HD gene carriers can be divided into HD stages based on their functional capacity, in which HD1 and HD2 represent early disease stages, and HD3 the most advanced stage.

Abbreviations: PreHD = premanifest HD gene carriers, HD = manifest Huntington's Disease, YTO = estimated years to disease onset, MRI = Magnetic Resonance Imaging, NMR = nuclear magnetic spectroscopy, UHDRS-TMS = Unified Huntington's Disease Rating Scale – Total Motor Score, SDMT = Symbol Digit Modality Test, VOSP = Visual Object and Space Perception, TMT = Trail Making Test, N/A = Not Applicable

TABLE 3 Visual cognitive domains and associated neuropsychological assessments

Domain	Definition	Assessments
Visual perception		
Color perception	Perception of colors and ability to distinguish contrast	Ishihara Color Test, Contrast Sensitivity Test
Visual recognition	Recognition of faces and facial expression of emotions	Emotion Recognition Tasks
Visual organization	Perceptual reorganizing to distinguish incomplete fragmented visual stimuli	Closure Speed, Visual Object and Space Perception battery, Hooper Visual Organization Test
Visuospatial function		
Visual attention	Awareness of visual stimuli	Line Bisection Test, Cancellation Task, Visual Search and Attention Test, Embedded Figures, Map Search, Trail Making Test A
Visual scanning	Ability to acquire information regarding environment and spatial distance (e.g. for reading, writing, telling time)	Counting dots, Visual Scanning Test, Mental Rotation, Street Map Task, Symbol Digit Modalities Test, Digit Symbol Task
Visual working memory		
Visual recognition memory	Ability to retrieve visuospatial information from memory	Recurring Figures Test, Family Pictures (subtest of Wechsler Memory Scale-III), Trail Making Test B
Visual Recall	Reproduction of a design or object	Visual Reproduction Task (immediate and delayed recall), Spot the change Task
Visuospatial Learning	Learning and recall memory of visuospatial stimuli	Visuospatial Learning Test, Trail Learning Test
Visuoconstruction		
Visuoconstructive ability	Spatial ability to reproduce complex geometric designs	Rey-Osterrieth Complex Figure Test
Visuomotor function		
Visuomotor	Ability to maintain gaze on a moving target	Circle-Tracing Task (direct and indirect feedback), 15-Objects task

Based on Lezak et al., 2004 ⁵⁶

memory accounts for the recall of visuospatial stimuli. Visuoconstruction is defined as the ability to organize and manually manipulate spatial information to make a design, i.e. copying a complex figure or constructing three-dimensional figures from two-dimensional units.⁵⁶ Last, visuomotor function involves visual scanning and tracking of movement and the ability to maintain gaze on a moving target.⁵⁷ A summary of the reviewed literature regarding visual cognition is presented in Table 4.

3.3.1. Visual perception

The perception of colors, contrast, and motion, the recognition of objects, facial expression, and emotions, and conceptual organizing skills are all classified as visual perception. The lateral geniculate nucleus is involved in the processing of colors and contrast resolution before further functional differentiation occurs in the striate cortex.⁵⁸ Limited studies have been performed that address basic visual processing of contrast and motion in HD. Patients with HD showed impaired contrast sensitivity for moving stimuli,⁵⁹ while contrast sensitivity for static stimuli seems unaffected in HD patients.^{59,60} This might indicate involvement of the (pre)-striate visual cortex early in the disease process.⁵⁹ Still, no structural or functional neuroimaging studies have been performed that confirm this hypothesis.

Conceptual organization or visual object perception has been examined in several studies in patients with HD, but methods differ and findings are inconsistent. One study assessed visuo-perceptive function using the Hooper Visual Organization test in premanifest and manifest HD gene carriers, for which participants needed to recognize and name the object that is displayed on a card in fragmented form.⁶¹ Both early and more advanced HD patients scored significantly lower on this task compared to premanifest and control individuals. No differences in scores were observed between premanifest HD and controls. Remarkably, 70% of the premanifest individuals scored above 25 points (maximum of 30 points), while only 20% of the early manifest individuals reached this score, which illustrates the impaired task performance in manifest HD.⁶¹ Three other studies assessed visuo-perceptual skills in HD patients using the Visual Object and Space Perception (VOSP) battery, which measures object recognition and space perception separately in eight subtests with minimal involvement of motor skills and executive functioning.^{34,62,63} A cross-sectional study showed that out of all the subtests of the VOSP, only the performance on the object decision task was impaired in HD patients (39% of the HD patients performed below the fifth percentile of the control norm),⁶³ while another cross-sectional study found an overall worse performance on the silhouettes and object decision subtasks in early HD patients compared to

controls.³⁴ Brain activity of the fusiform gyrus did not predict the performance on visual object perceptual tests,³⁴ which is unexpected since the fusiform gyrus is thought to be involved in object and facial recognition.⁶⁴ A longitudinal study that assessed in addition to visual cognition also executive function, language, learning, and intelligence, reported a decline in performance for object recognition and space perception in HD patients after a follow-up period of 2.5 years, measured using sum scores for all object recognition tasks and space perception tasks.⁶²

In contrast, a small study in 10 HD patients reported that the identification of individual objects and objects adjacent to each other remained unaffected, while deficits were found in the simultaneous perception of multiple objects that were presented in an overlapping manner.⁶⁵

The perception of motion can be measured using a motion discrimination task, in which participants need to decide whether dots moved to the right or left in a field of noise. Here, findings are also inconsistent, when assessing a motion discrimination task in HD patients.^{59,60} In a pilot study of 8 HD patients and 9 premanifest HD gene carriers, the discrimination of motion trajectories in noise was impaired in the manifest HD group, but not in premanifest HD gene carriers.⁶⁰ In a subsequent study with a larger sample (201 controls, 52 premanifest and 36 manifest HD gene carriers), no differences were observed in the performance on this task among different HD gene carrier groups and controls.⁵⁹ The authors explained these different findings because of possible differences in the severity of HD participants that were included in the two studies.⁵⁹ Therefore, no conclusions can be drawn from this limited evidence on the motion perception performance in HD patients.

In contrast, visuo-perceptual recognition of facial expressions and emotions has been extensively studied in HD patients. Several reviews have recently evaluated the current literature on emotion recognition in HD.⁶⁶⁻⁶⁸ Briefly, the ability to recognize basic emotions from facial expressions has consistently been found to be impaired in both manifest and premanifest HD, especially for negative emotions such as anger, disgust, and fear.^{67,68} Impairments in facial emotion recognition in HD seem to be associated with regional loss of brain tissue, altered brain activation, and changes in brain connectivity.⁶⁸ A large study by the Predict-HD study group found that, in premanifest HD gene carriers, deficits in negative emotion recognition were associated with atrophy of the fronto-striatal network, the precuneus and occipital regions, such as the lingual gyrus, cuneus, lateral occipital cortex, and middle-temporal cortex.⁶⁹

3.3.2. Visuospatial function

The dorsal temporo-occipital pathway is suggested to be involved in visuospatial cognition.¹ Visuospatial attention involves the awareness of visual stimuli to perceive objects, while visuospatial scanning is necessary to acquire information regarding the environment, spatial distance and relationship among objects. Therefore, visuospatial processing is important for daily functioning, such as walking, driving, reading, and writing, and is often essential when measuring other cognitive domains.

Eight studies specifically investigated visuospatial function, visual attention or visual scanning in HD patients.^{13,24,34,61,70-73} One study assessed a wide range of visuospatial tasks in HD patients and controls.⁷⁰ Factor analyses showed that overall visuospatial processing capacity (measured using the performance subscales of the WAIS-R, Embedded Figures Test, and Mental Reorientation Test) and spatial manipulation (involving performance on the Mental Rotation and Street Map task) were impaired in HD, whereas spatial judgment (comprising of scores of the Rod-And-Frame Test and In-Front-Of Test) appeared unaffected.⁷⁰

Another study also examined the ability to spatially rotate a mental image (i.e. a mental rotation task) in patients with HD and patients with Alzheimer's disease (AD).⁷¹ HD patients were able to mentally rotate a figure through space, but showed slowing in information processing speed (i.e. bradyphrenia) resulting in a worse performance, whereas in AD patients the accuracy, not the speed, was impaired compared to their respective age-matched controls.⁷¹ Other more recent studies, however, reported worse performance on the Mental Rotation task in both premanifest and manifest HD gene carriers compared to controls, with poorer performance in the more advanced disease stages that was not influenced by bradyphrenia.^{13,24}

Different neuropsychological assessments were used to measure visual scanning and attentional deficits in HD patients in several studies.^{24,34,61,72,73} The Cancellation Task and Line Bisection Test did not show any differences in visual attentional function between healthy controls, premanifest, and manifest HD gene carriers.⁶¹ In a longitudinal study, decline in performance on the Map Search attentional task was only observed in more advanced HD patients after a 12 months follow-up period.²⁴

The Symbol Digit Modalities Test (SDMT) and the Trail Making Test (TMT) are widely used assessments to measure cognitive function in HD patients.^{62,74,75} The SDMT is found to be the most sensitive cognitive task in large longitudinal studies to detect progressive change in HD gene carriers.^{62,74,75} An explanation for this might be that the SDMT is a demanding task that requires a high degree of visual scanning and memory, processing speed, object recognition, oculomotor function and motor speed. One study assessed the association between cognitive task performance and visual brain

activity changes.³⁴ Here, early HD patients' lower fusiform activity was associated with worse performance on the SDMT, which is not surprising as the SDMT also involves the recognition of symbols and shapes.³⁴

Among a large group of 767 premanifest HD gene carriers, the TMT part A was associated with visual search and sustained attention, whereas TMT part B was associated with executive functioning, processing speed and working memory.⁷² Premanifest HD gene carriers close to disease onset performed worse on both TMT part A and part B. Interestingly, only part A scores seemed to be mildly affected by motor disturbances.⁷²

Only one study specifically assessed visual scanning in premanifest and manifest HD gene carriers using the Digit Symbol Subtest, a subscale of the Wechsler Adult Intelligence Scale - Revised (WAIS-R), and quantitative eye movements.⁷³ While all participants used a similar visual scanning strategy, slowing and irregular visual scanning in both premanifest and manifest HD was related to worse performance on the Digit Symbol task compared to controls.⁷³ Although this might suggest deficits in visual scanning in early disease stages, the influence of motor impairment on cognitive performance was not taken into account.

Overall, visuospatial function in HD patients has been examined using various cognitive batteries, making it difficult to directly compare study findings. Some visual attentional tasks (such as the Mental Rotation, TMT part A and the SDMT) revealed impaired performance in both premanifest and manifest HD, while other tasks (such as the Line Bisection Test and Cancellation Task) showed no differences in task performance.

3.3.3. Visual working memory

Visual working memory accounts for the ability to retrieve visuospatial information from memory, and involves learning and recall of visuospatial stimuli. Six studies assessed visuospatial memory function in HD patients.^{13,63,76-79}

Compared with other neurodegenerative disorders, such as Alzheimer's' disease (AD) and Parkinson's disease (PD), patients with HD showed impairments in spatial working memory and visuospatial learning.^{76,77} In these studies, visuospatial working memory was determined as the ability to recall a sequence of squares at the right location on a screen⁷⁶, the recognition of abstract visual stimuli⁷⁶, and the recall of the right naming and location of sketched objects on cards.⁷⁷ Patients with HD were better at correctly naming the objects than recalling their spatial location, whereas the opposite was true for the AD and PD patients.⁷⁷ This was confirmed by a study in early stage HD patients that measured visual object and visuospatial working memory using an extensive battery of cognitive visual assessments.⁶³ Here, deficits in pattern and spatial

recognition memory, decreased reaction times in visual search, and an impaired spatial working memory were found in HD patients, while visual object working memory showed no changes compared with healthy controls.

To evaluate the influence of slowness of execution (bradykinesia), thinking (bradyphrenia) or motor speed on visual memory task performance, one study assessed accuracy and reaction times between different disease stages on a visual comparison task to spot the change of randomly selected colors between images.⁷⁸ Premanifest HD gene carriers close to disease onset and early stage HD patients showed lower working memory accuracy and slower response times compared to controls. As premanifest individuals without motor signs also showed impairments in task performance, the findings of this study imply that results are influenced by a decrease in cognitive performance and impaired information processing, rather than reduced motor speed.⁷⁸

A more recent study also reported poorer performance on the 'Spot the change' task in more advanced disease stages.¹³ In addition, task performance was associated with thickness of the lateral occipital cortex and lingual gyrus, while a non-visual motor task showed no associations with the visual cortex.¹³ This implies that the changes in occipital thickness are specific to visual cognition rather than general disease progression.¹³ In another study, visuospatial memory function was evaluated in HD patients and healthy controls using the Visual Spatial Learning Test (VSLT), which is a nonverbal memory test that measures immediate and delayed memory for designs and locations without requiring motor or language skills.⁷⁹ Compared to controls, premanifest HD gene carriers showed, besides an impaired recall for associations between object and spatial location, no deficits in the memory for objects, while HD patients showed impairments on all measures.⁷⁹

Generally, retrieving visuospatial information from memory seems to be inaccurate in early manifest stages and even in premanifest HD gene carriers close to disease onset, whereas the recognition and recall of naming objects from memory appears to be less affected.

3.3.4. Visuoconstructive abilities

Visuoconstruction involves the spatial ability to reproduce complex geometric designs. Interpretation of visuoconstructive deficits can be difficult because tests that are used to measure visuoconstruction often involve other domains, such as visuospatial, executive and motor functioning. Only two studies investigated visuoconstructive skills in HD patients by assessing the ability to copy a complex figure using the Rey-Osterrieth Complex Figure Test.^{61,80} The first study explored these visuoconstructive abilities of HD patients with age-matched controls for HD by recording the accuracy and time

to copy the design.⁸⁰ Here, patients with HD showed no differences in accuracy but needed more time to complete the test compared to their matched control group, which may have been due to the presence of motor disturbances.⁸⁰ A second study examined the same part of the Rey-Osterrieth Complex Figure test, in premanifest and manifest HD gene carriers but measured the correct elements that were copied instead of evaluating the accuracy of the lines to minimize motor interference.⁶¹ In HD patients, total correct scores declined in more advanced disease stages. Furthermore, early HD patients showed mild deficits in visuoconstruction but this was not significant compared with premanifest HD gene carriers.

Based on this literature, visuoconstructive skills become impaired in the more advanced disease stages. Still, more studies are necessary to fully determine the extent of these impairments and the possible influence of motor signs and bradyphrenia.

3.3.5. *Visuomotor function*

Visuomotor deficits in the tracking of movements and the ability to maintain gaze on a moving target have been reported in HD patients.^{25,26,81,82}

In two studies using a circle-tracing task to measure indirect and direct visual feedback, early HD patients were slower, less accurate and needed more time to detect errors.^{26,82}

This is consistent with another study using a visual tracking task that showed a higher error rate and longer time scores in HD patients, especially in the non-dominant hand, compared to controls.⁸¹ Premanifest HD gene carriers also showed less accuracy in completing the task compared to controls, however, no associations were found between visuomotor integration deficits in HD gene carriers and volumes of visual and motor cortices.²⁶ This might be explained by the multifactorial demands of the circle-tracing task that was used as an outcome measure.

To the contrary, another study found correlations between impaired visuomotor performance in premanifest HD gene carriers and decreased volumes of the prefrontal and occipital cortices.²⁵ In this study, visuomotor integration performance was measured using the time to complete the 15-objects test that contains 2 figures, each with overlapping drawings of 15 different items.²⁵ This task, however, can also be used to assess visual perception and in addition, it remains uncertain if other signs of HD, such as bradyphrenia, motor and eye movement disturbances, or visuoperceptual deficits rather than visuomotor dysfunction may have influenced the results of these studies.

TABLE 4 Overview of current literature on visual cognition in HD

	Study population	Clinical HD disease stage	Domain	Assessments	Main significant finding
Brouwer et al., 1984 ⁶⁰	Controls n = 25 * HD n = 10 AD n = 14	Disease duration: 3.4 years	Visuoperceptual, memory and constructive function	Road Map Test Rey-Osterrieth Complex Figures Mosaic Comparisons Test Stylus Maze Test	Impairments in visual discrimination, no difference in visuoconstructive ability and route learning in HD compared to controls
Oepen et al., 1985 ⁸¹	Controls n = 63 HD n = 15 HD at risk n = 17	YTO: not available (before genetic testing) Disease duration: not available	Visuomotor function	Continuous and discontinuous drawing/tracking task	Significant higher error rate (less accuracy) and longer time scores in HD compared to controls, especially in non-dominant hand
Mohr et al., 1991 ⁷⁰	Controls n = 19 HD n = 20	Disease duration: 6 years	Visuospatial function	Performance subtests of WAIS-R Embedded Figures Test Rod-and-Frame Test Mental Rotation Test Street Map Test Mental Reorientation Test In-Front-Of Test	Impaired visuospatial processing capacity and spatial manipulation in HD, no impairments in spatial judgment (Rod-and-Frame test and In-Front-Of Test) in HD compared to controls
Lange et al., 1995 ⁷⁶	Controls n = 85 * AD n = 13 HD n = 10	Disease duration: not available	Visuospatial learning and memory	Pattern and Spatial Recognition Test Matching-to-Sample test	Worse performance on spatial pattern recognition task and Spatial recognition of abstract stimuli
Gomez-Tortosa et al., 1996 ⁶¹	Controls n = 11 PreHD n = 15 HD n = 35	YTO: not available Disease duration: not available HD1 n = 13 HD2 n = 9 HD3 n = 13	Visual attention, visuoconstruction, and visuoperception	Cancellation task Line Bisection Rey-Osterrieth Complex Figures Hooper Visual Organization Test	Impaired visuoperception in HD patients, no significant differences between preHD and controls
Lawrence et al., 2000 ⁶³	HD-a n = 19 vs. Controls-a n = 20 HD-b n = 19 vs. Controls-b n = 20 HD-c n = 21 vs. Controls-c n = 17	Age at onset: 42.5 years Disease duration: 5 years	Visual object and visuospatial memory	HD-a: DMTS, VSMTS, VOSP HD-b: PAL HD-c: Pattern and Spatial recognition test, spatial working memory task	Deficits in pattern and spatial recognition memory, reaction times in visual search, and spatial working memory

TABLE 4 Continued

	Study population	Clinical HD disease stage	Domain	Assessments	Main significant finding
O'Donnell et al., 2003 ⁶⁰	Controls n = 20 PreHD n = 9 HD n = 8	YTO: not available Disease duration: 1 – 2 years	Early stage visual processing	Digit Symbol test Contrast sensitivity Motion discrimination	Impaired motion discrimination in HD, not in preHD
Brandt et al., 2005 ⁷¹	Controls n = 147 AD n = 143 PD n = 77 HD n = 110	Disease duration: 7.7 years	Visuospatial object and location memory	'Hopkins Board' (object identity and recall of spatial locations)	Impaired delayed recall of spatial location of items in HD compared to AD and PD
Lemay et al., 2005 ⁸²	Controls n = 13 HD n = 13	Disease duration: 0.5 – 6 years	Visuomotor function	Circle tracing task (direct and indirect)	Early HD patients were slower and deviated more than controls for the indirect visual feedback task. No differences in direct visual feedback
Lineweaver et al., 2005 ⁷¹	Controls n = 40 * AD n = 18 HD n = 18	Disease duration: not available	Visuospatial function	Mental Rotation task	Decreased speed in mental rotation task in HD and reduced accuracy in AD, compared to controls
Finke et al., 2007 ⁶⁵	Controls n = 15 HD n = 10	Age at onset: 37.4 years Disease duration: 4.6 years	Visual attention Object recognition	Simultaneous perception task	Simultaneous perception of multiple object in overlapping manner was impaired in HD, identification of single objects or objects adjacent to each other was unaffected in HD
Blekher et al., 2009 ⁷³	Controls n = 23 PreHD n = 21 HD n = 19	YTO: not available Disease duration: not available	Visual scanning	Digit Symbol test Visual scanning using eye movements	Slow and irregular visual scanning related to worse cognitive performance in preHD and HD
Gomez-Anson et al., 2009 ²⁵	Controls n = 21 PreHD n = 22	YTO: not available PreHD1: n = 12 (UHDRS-TMS = 0) PreHD2: n = 8 (UHDRS-TMS = 8)	Visuomotor function	15-Objects test Stroop TMT A and B Digit Symbol test Rey's Complex Figure Benton's Line Orientation test	PreHD performed slower on the 15-Objects test than controls. In total, 13 preHD (59%) had impaired performance in at least one of the other assessments
O'Rourke et al., 2011 ⁷²	Controls = 217 PreHD = 767	PreHD Far n = 297, YTO > 15 years PreHD Mid n = 287, YTO: 9 – 15 years PreHD Near n = 183, YTO: < 9 years	Perceptual processing, visual scanning and attention	TMT part A TMT part B	In preHD, TMT part A measures visual search and sustained attention, TMT part B measures cognitive flexibility and working memory
Say et al., 2011 ²⁶	Controls n = 122 PreHD-A n = 62 PreHD-B n = 57	PreHD-A n = 62, YTO: 14.1 years PreHD-B n = 57, YTO: 8.7 years HD1 n = 75	Visuomotor function	Circle tracing task (direct and indirect)	Less accuracy and slower task performance in both circle-tracing conditions for early and

TABLE 4 Continued

	Study population	Clinical HD disease stage	Domain	Assessments	Main significant finding
	HD1 n = 75 HD2 n = 45	HD2 n = 45 Disease duration: not available			preHD. With indirect condition, early and preHD required longer to detect and correct errors compared to controls
Dumas et al., 2012 ⁷⁸	Controls n = 122 PreHD n = 120 HD n = 121	PreHD-A n = 62, YTO: 14 years PreHD-B n = 58, YTO 9 years HD1 n = 77, disease duration: 5 years HD2 n = 44, disease duration: 8 years	Visuospatial working memory	Spot the change	Slow response times in preHD close to disease onset and early manifest HD
Wolf et al., 2014 ³⁴	Controls n = 20 HD n = 20	HD1/2 n = 20 Disease duration: 3.2 years	Visual scanning and visual object function	SDMT VOSP - subtests for object function	Decreased performance on all tasks in HD, lower fusiform activity only associated with worse performance on SDMT in HD
Johnson et al., 2015 ¹³	Controls n = 97 PreHD n = 109 HD n = 69	PreHD-A n = 51, YTO > 10.8 years PreHD-B n = 58, YTO < 10.8 years HD1 n = 40 HD2 n = 29 Disease duration: not available	Visual scanning, visuospatial processing and attention, visual working memory	SDMT Stroop Word Reading Trail Making Task part A Map Search Mental Rotation Spot the Change VLST	Worse performance on all tasks in advanced HD. Except for Mental Rotation, relation between task performance and occipital thickness in HD, see also Table 2
Pirogovsky et al., 2015 ⁷⁹	Controls n = 31 PreHD n = 30 HD n = 19	YTO: not available Age at onset HD: 44.7 years Disease duration: not available	Visuospatial memory	VLST	Impaired recall and recognition of designs in HD, object-place association memory impaired in preHD
Labuschagne et al., 2016 ²⁴	Controls n = 110 PreHD n = 119 HD n = 104	PreHD-A n = 55, YTO > 10.8 years PreHD-B n = 64, YTO < 10.8 years HD1 n = 59 HD2 n = 45 Disease duration: not available	Visuospatial attention / processing	Map Search Mental rotation	Lower scores on Map Search and Mental rotation task in all groups compared to controls. At follow-up, only declined performance in HD

* Controls were age-matched for AD and HD separately

Clinical stages of the study population are provided in the table, if information was available in the original papers. PreHD-A and PreHD-B indicate premanifest HD gene carriers classified based on the estimated time to disease onset (far or close respectively). Manifest HD gene carriers can be divided into HD stages based on their functional capacity, in which HD1 and HD2 represent early disease stages, and HD3 the most advanced stage.

Abbreviations: PreHD = premanifest HD gene carriers, HD = Huntington's Disease patients, YTO = estimated years to disease onset, Digit: Symbol test is a subscale of the Wechsler Adult Intelligence Scale - Revised (WAIS-R), SDMT = Symbol Digit Modality Test, VOSP = Visual Object and Space Perception, VLST = Visual Spatial Learning Test, TMT = Trail Making Test, PAL = Paired-Associate Learning, DMTS = Delayed Matching-To-Sample, VSMTS = Visual Search Matching-To-Sample



4. DISCUSSION

This review presents an overview regarding changes of the visual system in premanifest and manifest HD gene carriers. Although the visual cortex was not the main focus of many neuroimaging studies, there is increasing evidence of early neurodegeneration of the posterior cerebral cortex. Based on the current literature, alterations were primarily found in the associative visual areas, such as the lingual and fusiform gyri, and the lateral occipital cortex. The cuneus and primary visual cortex appear to be affected in more advanced disease stages. As changes of the visual association cortex were already detectable in the pre-symptomatic and early disease stages, this implies that the visual cortex might be an early marker of disease progression that can be used as an outcome measure in disease-modifying intervention trials.

Clinical visual deficits or visual hallucinations are not commonly reported as typical features of HD. Still, studies assessing visual cognitive function in HD report impairments in several domains, specifically tasks involving visual object perception, facial emotion recognition and visuospatial processing and working memory.

Studies assessing driving competence in HD patients also showed that visual processing speed, visual scanning, and visual attention are more sensitive predictors of performance on on-road driving assessments, compared to motor functioning.^{83,84}

The assessment of visual cognitive impairment is therefore of clinical importance as it can have implications in daily functioning, such as the impact on driving performance, the use of electronic devices and subsequently affects participating in social activities. For example, the impairment to recognize negative facial emotions, such as anger, disgust and fear, could affect communication and social relationships.⁶⁸ Also, patients with HD might have a higher risk of falling or experience difficulty with walking because of visual perceptual and visuomotor deficits. In addition, visual cognitive impairment can influence overall cognitive performance.

Visual cognitive impairments have primarily been found in the manifest disease stage, although visuospatial working memory deficits and changes in facial emotion recognition are also reported in HD gene carriers prior to clinical motor onset. Neuropsychological studies in HD patients, however, have used heterogeneous cognitive batteries to examine visual cognition involving various visual skills, making a direct comparison between studies difficult. This was particularly found in studies assessing visual attention in HD, where the Map Search, TMT part A, SDMT, Stroop, Digit Symbol task, Line Bisection test and Cancellation task were all used to measure visual attention. A standardized battery of cognitive tasks focusing on visual processing skills might provide more information regarding the specific underlying deficits. Using

cognitive tasks with minimal motor involvement is recommended to reduce the possible influence of other HD related signs, such as the Visual Object and Space Perception battery, the Visual Spatial Learning test and the Stroop tasks.

Visual cognitive impairment in HD gene carriers has previously been interpreted as a result of disturbances in the fronto-striatal network.^{57,63,80} However, more recent studies suggest that degeneration of cortical-striatal circuits that are linked to the associative cortical regions in the parietal lobe contribute to visual memory and visuospatial impairments associated with HD.^{77,79}

We believe that the posterior cerebral cortex is one of the first cortical areas that undergoes changes in early stages of HD. Therefore, systematic and preferably longitudinal assessment of the visual cortex in HD is warranted, to improve the understanding of structural and functional alterations in the visual pathway in patients with HD.

Linking structural changes of the visual cortex with functional cognitive decline over time can provide valuable information on disease progression and cortical degeneration. The use of a standardized battery of visual cognitive tasks might additionally provide more detailed information regarding impairments in specific visual domains. To reduce interference on task performance, we are of the opinion that visual neuropsychological tasks should be selected that are not influenced by motor speed, bradyphrenia or language skills.

To summarize, based on the current literature, early involvement of the visual cortex in the neurodegenerative process in HD has been reported. Structural, metabolic, and functional changes are primarily found in the associative cortices, such as the cuneus, lingual gyrus, and fusiform gyrus. Further research is nevertheless required to provide more insight into the pathophysiological changes of the posterior cerebral cortex in HD. Clinical visual deficits or visual hallucinations are not commonly reported as typical features of HD. However, visual cognitive impairments are seen in several domains, specifically tasks involving visual object perception, facial emotion recognition and visuospatial processing and working memory were impaired in pre-symptomatic and early disease stages. Because heterogeneous cognitive batteries were used, a direct comparison between studies was difficult. We are of the opinion that tasks with minimal motor involvement are most recommended for the assessment of visual cognitive function in future clinical trials, such as the Visual Object and Space Perception battery, the Visual Spatial Learning test, and the Stroop tasks. In addition, a motor task without a visual component, such as the Paced Tapping task, can be included in the test battery as a general proxy for disease progression.⁷⁵ In this way, the relationship between visual task performance and visual cortical changes can be measured exclusively.^{13,75}

Investigating the association of brain structure and function with visual cognition in HD using a standardized visual cognitive battery and different imaging modalities can quantify alterations and hopefully link structural posterior brain changes to functional impairments.

REFERENCES

1. Kravitz DJ, Saleem KS, Baker CI, Mishkin M. A new neural framework for visuospatial processing. *Nat Rev Neurosci.* 2011;12:217-230.
2. Tootell RBH, Tsao D, Vanduffel W. Neuroimaging weighs in: Humans meet macaques in "primate" visual cortex. *J Neurosci.* 2003;23(10):3981-3989.
3. Gustavo De Moraes C. Anatomy of the Visual Pathways. *J Glaucoma.* 2013;22(5):2-7.
4. Wandell BA, Dumoulin SO, Brewer AA. Visual field maps in human cortex. *Neuron.* 2007;56:366-383.
5. Prasad S, Galetta SL. Anatomy and physiology of the afferent visual system. In: *Handbook of Clinical Neurology.* Volume 102.; 2011:3-19.
6. Wichmann W, Müller-forell W. Anatomy of the visual system. *Eur J Radiol.* 2004;49:8-30.
7. Tobimatsu S, Celesia GG. Studies of human visual pathophysiology with visual evoked potentials. *Clin Neurophysiol.* 2006;117(7):1414-1433.
8. Ungerleider LG, Haxby J V. "What" and "where" in the human brain. *Curr Opin Neurobiol.* 1994;4:157-165.
9. Barton JJ. Higher cortical visual function. *Curr Opin Ophthalmol.* 1998;9(VI):40-45.
10. Braddick O, Atkinson J. Development of human visual function. *Vision Res.* 2011;51(13):1588-1609.
11. Tabrizi SJ, Langbehn DR, Leavitt BR, et al. Biological and clinical manifestations of Huntington's disease in the longitudinal TRACK-HD study: cross-sectional analysis of baseline data. *Lancet Neurol.* 2009;8(9):791-801.
12. Nopoulos PC, Aylward EH, Ross CA, et al. Cerebral cortex structure in prodromal Huntington disease. *Neurobiol Dis.* 2010;40(3):544-554.
13. Johnson EB, Rees EM, Labuschagne I, et al. The impact of occipital lobe cortical thickness on cognitive task performance: An investigation in Huntington's Disease. *Neuropsychologia.* 2015;79:138-146.
14. The Huntington's Disease Collaborative Research Group. A novel gene containing a trinucleotide repeat that is expanded and unstable on Huntington's disease chromosomes. *Cell.* 1993;72(6):971-983.
15. Roos RAC. Huntington's disease: a clinical review. *Orphanet J Rare Dis.* 2010;5(1):40.
16. van Duijn E, Craufurd D, Hubers AAM, et al. Neuropsychiatric symptoms in a European Huntington's disease cohort (REGISTRY). *J Neurol Neurosurg Psychiatry.* 2014;85(12):1411-1418.
17. Dumas EM, van den Bogaard SJA, Middelkoop HAM, Roos RAC. A review of cognition in Huntington's disease. *Front Biosci.* 2013;S5:1-18.
18. Bates GP, Dorsey R, Gusella JF, et al. Huntington disease. *Nat Rev Dis Prim.* 2015;1:1-21.

19. Vonsattel JP, Myers RH, Stevens TJ, Ferrante RJ, Bird ED, Richardson EP. Neuropathological classification of Huntington's disease. *J Neuropathol Exp Neurol*. 1985;44(6):559-577.
20. Thu DCV, Oorschot DE, Tippett LJ, et al. Cell loss in the motor and cingulate cortex correlates with symptomatology in Huntington's disease. *Brain*. 2010;133(4):1094-1110.
21. Nana AL, Kim EH, Thu DCV, et al. Widespread heterogeneous neuronal loss across the cerebral cortex in Huntington's disease. *J Huntingtons Dis*. 2014;3:45-64.
22. Waldvogel HJ, Kim EH, Thu DCV, Tippett LJ, Faull RLM. New perspectives on the neuropathology in Huntington's disease in the human brain and its relation to symptom variation. *J Huntingtons Dis*. 2012;1:143-153.
23. Rüb U, Seidel K, Vonsattel JP, et al. Huntington's disease (HD): Neurodegeneration of Brodmann's primary visual area 17 (BA17). *Brain Pathol*. 2015;25(6):701-711.
24. Labuschagne I, Cassidy AM, Scahill RI, et al. Visuospatial processing deficits linked to posterior brain regions in premanifest and early stage Huntington's disease. *J Int Neuropsychol Soc*. 2016;22:595-608.
25. Gómez-Ansón B, Alegret M, Muñoz E, et al. Prefrontal cortex volume reduction on MRI in preclinical Huntington's disease relates to visuomotor performance and CAG number. *Park Relat Disord*. 2009;15(3):213-219.
26. Say MJ, Jones R, Scahill RI, et al. Visuomotor integration deficits precede clinical onset in Huntington's disease. *Neuropsychologia*. 2011;49(2):264-270.
27. Rosas HD, Salat DH, Lee SY, et al. Cerebral cortex and the clinical expression of Huntington's disease: complexity and heterogeneity. *Brain*. 2008;131(4):1057-1068.
28. Scahill RI, Hobbs NZ, Say MJ, et al. Clinical impairment in premanifest and early Huntington's disease is associated with regionally specific atrophy. *Hum Brain Mapp*. 2013;34(3):519-529.
29. Aylward EH, Nopoulos PC, Ross CA, et al. Longitudinal change in regional brain volumes in prodromal Huntington disease. *J Neurol Neurosurg Psychiatry*. 2011;82(4):405-410.
30. Hobbs NZ, Henley SMD, Ridgway GR, et al. The progression of regional atrophy in premanifest and early Huntington's disease: a longitudinal voxel-based morphometry study. *J Neurol Neurosurg Psychiatry*. 2010;81(7):756-763.
31. Klöppel S, Draganski B, Golding CV, et al. White matter connections reflect changes in voluntary-guided saccades in pre-symptomatic Huntington's disease. *Brain*. 2008;131:196-204.
32. Paulsen JS. Functional imaging in Huntington's disease. *Exp Neurol*. 2009;216(2):272-277.
33. Rees EM, Scahill RI, Hobbs NZ. Longitudinal neuroimaging biomarkers in Huntington's disease. *J Huntingtons Dis*. 2013;2:21-39.
34. Wolf RC, Sambataro F, Vasic N, et al. Visual system integrity and cognition in early Huntington's disease. *Eur J Neurosci*. 2014;40(2):2417-2426.
35. Dumas EM, van den Bogaard SJA, Hart EP, et al. Reduced functional brain connectivity prior to and after disease onset in Huntington's disease. *NeuroImage Clin*. 2013;2(1):377-384.

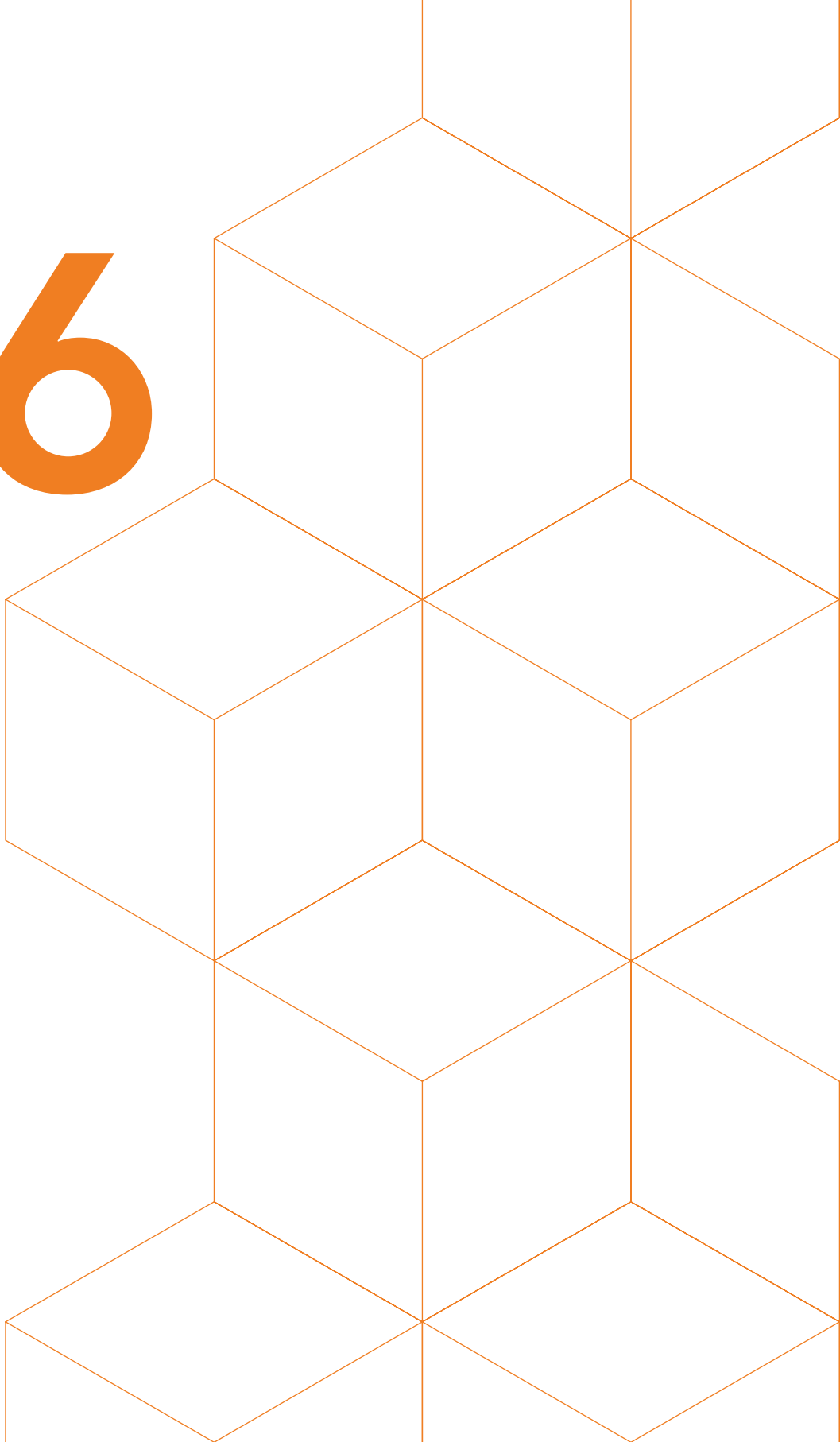
36. Seibert TM, Majid DSA, Aron AR, Corey-Bloom J, Brewer JB. Stability of resting fMRI interregional correlations analyzed in subject-native space: a one-year longitudinal study in healthy adults and premanifest Huntington's disease. *Neuroimage*. 2012;59(3):2452-2463.
37. Odish OFF, van den Berg-Huysmans AA, van den Bogaard SJA, et al. Longitudinal resting state fMRI analysis in healthy controls and premanifest Huntington's disease gene carriers: A three-year follow-up study. *Hum Brain Mapp*. 2014;119:110-119.
38. Sappey-Marinier D, Calabrese G, Fein G, Hugg JW, Biggins C, Weiner MW. Effect of photic stimulation on human visual cortex lactate and phosphates using ¹H and ³¹P Magnetic Resonance Spectroscopy. *J Cereb Blood Flow Metab*. 1992;12:584-592.
39. Mochel F, N'Guyen TM, Deelchand D, et al. Abnormal response to cortical activation in early stages of Huntington disease. *Mov Disord*. 2012;27(7):907-910.
40. Clark VP, Lai S, Deckel AW. Altered functional MRI responses in Huntington's disease. *Neuroreport*. 2002;13(5):40-43.
41. Kim JS, Reading SAJ, Brashers-Krug T, Calhoun VD, Ross CA, Pearlson GD. Functional MRI study of a serial reaction time task in Huntington's disease. *Psychiatry Res - Neuroimaging*. 2004;131:23-30.
42. Pagano G, Niccolini F, Politis M. Current status of PET imaging in Huntington's disease. *Eur J Nucl Med Mol Imaging*. 2016;43:1171-1182.
43. Ciarmiello A, Giovacchini G, Giovannini E, et al. Molecular imaging of Huntington's disease. *J Cell Physiol*. 2017;(232):1988-1993.
44. Roussakis AA, Piccini P. PET imaging in Huntington's disease. *J Huntingtons Dis*. 2015;4:287-296.
45. Feigin A, Leenders KL, Moeller JR, et al. Metabolic network abnormalities in early Huntington's disease: An [¹⁸F]FDG PET study. *J Nucl Med*. 2001;42:1591-1596.
46. Feigin A, Tang C, Mattis P, et al. Thalamic metabolism and symptom onset in preclinical Huntington's disease. *Brain*. 2007;(130):2858-2867.
47. Gaura V, Lavisse S, Payoux P, et al. Association between motor symptoms and brain metabolism in early Huntington disease. *JAMA Neurol*. 2017;74(9):1088-1096.
48. Ma Y, Eidelberg D. Functional imaging of cerebral blood flow and glucose metabolism in Parkinson's disease and Huntington's disease. *Mol Imaging Biol*. 2007;9(4):223-233.
49. Wolf RC, Grön G, Sambataro F, et al. Magnetic resonance perfusion imaging of resting-state cerebral blood flow in preclinical Huntington's disease. *J Cereb Blood Flow Metab*. 2011;31(9):1908-1918.
50. Hua J, Unschuld PG, Margolis RL, van Zijl PCM, Ross CA. Elevated arteriolar cerebral blood volume in prodromal Huntington's disease. *Mov Disord*. 2014;29(3):396-401.
51. Lepron E, Péran P, Cardebat D, Démonet JF. A PET study of word generation in Huntington's disease: Effects of lexical competition and verb/noun category. *Brain Lang*. 2009;110:49-60.

52. Weeks RA, Ceballos-Baumann A, Piccini P, Boecker H, Harding AE, Brooks DJ. Cortical control of movement in Huntington's disease. A PET activation study. *Brain*. 1997;120:1569-1578.
53. Deckel AW, Cohen D, Duckrow R. Cerebral blood flow velocity decreases during cognitive stimulation in Huntington's disease. *Neurology*. 1998;51(6):1576-1583.
54. Hasselbalch SG, Oberg G, Sorensen SA, et al. Reduced regional cerebral blood flow in Huntington's disease studied by SPECT. *J Neurol Neurosurg Psychiatry*. 1992;55:1018-1023.
55. Chen JJ, Salat DH, Rosas HD. Complex relationships between cerebral blood flow and brain atrophy in early Huntington's disease. *Neuroimage*. 2012;59(2):1043-1051.
56. Lezak M, Howieson D, Loring D. *Neuropsychological Assessment*. 4th ed. Oxford University Press; 2004.
57. Lasker AG, Zee DS. Ocular motor abnormalities in Huntington's disease. *Vision Res*. 1997;37(24):3639-3645.
58. Wandell BA. Computational neuroimaging of human visual cortex. *Annu Rev Neurosci*. 1999;22:145-173.
59. O'Donnell BF, Blekher TM, Weaver M, et al. Visual perception in prediagnostic and early stage Huntington's disease. *J Int Neuropsychol Soc*. 2008;14:446-453.
60. O'Donnell BF, Wilt MA, Hake AM, Stout JC, Kirkwood SC, Foroud T. Visual function in Huntington's disease patients and presymptomatic gene carriers. *Mov Disord*. 2003;18(9):1027-1034.
61. Gómez-Tortosa E, del Barrio A, Barroso T, García Ruiz PJ. Visual processing disorders in patients with Huntington's disease and asymptomatic carriers. *J Neurol*. 1996;243(3):286-292.
62. Lemiere J, Decruyenaere M, Evers-Kiebooms G, Vandenbussche E, Dom R. Cognitive changes in patients with Huntington's disease (HD) and asymptomatic carriers of the HD mutation. *J Neurol*. 2004;251(8):935-942.
63. Lawrence AD, Watkins LH, Sahakian BJ, Hodges JR, Robbins TW. Visual object and visuospatial cognition in Huntington's disease: implications for information processing in corticostriatal circuits. *Brain*. 2000;123:1349-1364.
64. Kanwisher N, McDermott J, Chun MM. The fusiform face area: A module in human extrastriate cortex specialized for face perception. *J Neurosci*. 1997;17(11):4302-4311.
65. Finke K, Schneider WX, Redel P, et al. The capacity of attention and simultaneous perception of objects: A group study of Huntington's disease patients. *Neuropsychologia*. 2007;45:3272-3284.
66. Henley SMD, Novak MJU, Frost C, King J, Tabrizi SJ, Warren JD. Emotion recognition in Huntington's disease: A systematic review. *Neurosci Biobehav Rev*. 2012;36:237-253.
67. Bora E, Velakoulis D, Walterfang M. Social cognition in Huntington's disease: A meta-analysis. *Behav Brain Res*. 2016;297:131-140.

68. Kordsachia CC, Labuschagne I, Stout JC. Beyond emotion recognition deficits: A theory guided analysis of emotion processing in Huntington's disease. *Neurosci Biobehav Rev.* 2017;73:276-292.
69. Harrington DL, Liu D, Smith MM, et al. Neuroanatomical correlates of cognitive functioning in prodromal Huntington disease. *Brain Behav.* 2014;4(1):29-40.
70. Mohr E, Brouwers P, Claus JJ, Mann UM, Fedio P, Chase TN. Visuospatial cognition in Huntington's disease. *Mov Disord.* 1991;6(2):127-132.
71. Lineweaver TT, Salmon DP, Bondi MW, Corey-Bloom J. Differential effects of Alzheimer's disease and Huntington's disease on the performance of mental rotation. *J Int Neuropsychol Soc.* 2005;(11):30-39.
72. O'Rourke JF, Beglinger LJ, Smith MM, et al. The Trail Making Test in prodromal Huntington disease: contributions of disease progression to test performance. *J Clin Exp Neuropsychol.* 2011;33(5):567-579.
73. Blekher T, Weaver MR, Marshall J, et al. Visual Scanning and Cognitive Performance in Prediagnostic and Early-Stage Huntington's Disease. *Mov Disord.* 2009;24(4):533-540.
74. Stout J, Jones R, Labuschagne I, et al. Evaluation of longitudinal 12 and 24 month cognitive outcomes in premanifest and early Huntington's disease. *J Neurol Neurosurg Psychiatry.* 2012;83:687-694.
75. Tabrizi SJ, Scahill RI, Owen G, et al. Predictors of phenotypic progression and disease onset in premanifest and early-stage Huntington's disease in the TRACK-HD study: Analysis of 36-month observational data. *Lancet Neurol.* 2013;12(7):637-649.
76. Lange KW, Sahakian BJ, Quinn NP, Marsden CD, Robbins TW. Comparison of executive and visuospatial memory function in Huntington's disease and dementia of Alzheimer type matched for degree of dementia. *J Neurol Neurosurg Psychiatry.* 1995;58:598-606.
77. Brandt J, Shpritz B, Munro C, Marsh L, Rosenblatt A. Differential impairment of spatial location memory in Huntington's disease. *J Neurol Neurosurg Psychiatry.* 2005;76:1516-1519.
78. Dumas E, Say M, Jones R, et al. Visual working memory impairment in premanifest gene-carriers and early Huntington's disease. *J Huntingtons Dis.* 2012;1:97-106.
79. Pirogovsky E, Nicoll DR, Challener DM, et al. The Visual Spatial Learning Test: Differential impairment during the premanifest and manifest stages of Huntington's disease. *J Neuropsychol.* 2015;(9):77-86.
80. Brouwers P, Cox C, Martin A, Chase T, Fedio P. Differential Perceptual-Spatial Impairment in Huntington's and Alzheimer's Dementias. *Arch Neurol.* 1984;41:1073-1076.
81. Oepen G, Mohr U, Willmes K, Thoden U. Huntington's disease: visuomotor disturbance in patients and offspring. *J Neurol Neurosurg Psychiatry.* 1985;48:426-433.
82. Lemay M, Fimbel E, Beuter A, Chouinard S, Richer F. Sensorimotor mapping affects movement correction deficits in early Huntington's disease. *Exp Brain Res.* 2005;165:454-460.

83. Devos H, Nieuwboer A, Tant M, De Weerd W, Vandenberghe W. Determinants of fitness to drive in Huntington disease. *Neurology*. 2012;79:1975-1982.
84. Jacobs M, Hart EP, Roos RAC. Driving with a neurodegenerative disorder: an overview of the current literature. *J Neurol*. 2017;264(8):1678-1696.

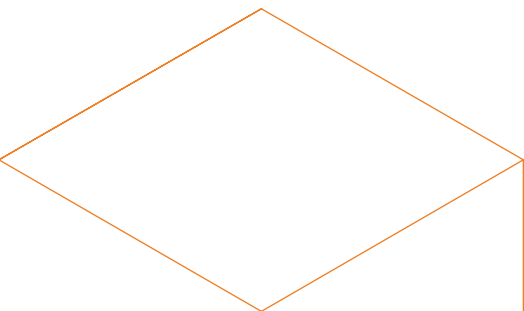
6



Structural and functional changes of the visual cortex in early Huntington's disease

Emma M. Coppen, Jeroen van der Grond, Anne Hafkemeijer, Jurriaan J.H. Barkey Wolf, Raymund A.C. Roos

Human Brain Mapping. 2018 Dec; 39(12):4776-4786



ABSTRACT

Huntington's disease (HD) is an autosomal-dominant inherited neurodegenerative disorder characterized by motor disturbances, psychiatric disturbances, and cognitive impairment. Visual cognitive deficits and atrophy of the posterior cerebral cortex are additionally present in early disease stages. This study aimed to assess the extent of structural and functional brain alterations of the visual cortex in HD gene carriers using different neuroimaging modalities.

Structural and functional magnetic resonance imaging (MRI) data were acquired from 18 healthy controls, 21 premanifest, and 20 manifest HD gene carriers. Voxel-based morphometry (VBM) analysis and cortical thickness measurements were performed to assess structural changes in the visual cortex. Brain function was measured by assessing neuronal connectivity changes in response to visual stimulation and at rest in visual resting-state networks. Multiple linear regression analyses were performed to examine the relationship between visual cognitive function and structural imaging measures.

Compared to controls, pronounced atrophy and decreased neuronal function at rest were present in associative visual cortices in manifest HD. The primary visual cortex did not show group differences in cortical thickness and in vascular activity after visual stimulation. Thinning of the associative visual cortex was related to worse visual perceptual function. Premanifest HD gene carriers did not show any differences in brain structure or function compared to controls.

This study improves the knowledge on posterior brain changes in HD, as our findings suggest that the primary visual cortex remains preserved, both structurally and functionally, while atrophy of associative visual cortices is present in early HD and linked to clinical visual deficits.

1. INTRODUCTION

Visual processing is involved in routine daily functioning, such as walking, driving a car, and in social communication. In the human brain, transmission of incoming stimuli from the retina pass the afferent visual pathway via the optic nerve, optic tract, lateral geniculate nucleus in the thalamus, and optic radiation to the primary visual (striate) cortex in the occipital lobe and higher posterior cortical areas.¹ Higher-level visual processing occurs in the associative extra-striate regions surrounding the primary visual cortex, from the secondary visual cortex to the ventral occipital-temporal pathway and dorsal occipital-parietal pathway.² In Huntington's disease (HD), an autosomal dominant inherited neurodegenerative disorder, progressive structural changes in the posterior cerebral cortex can be detected in early stages of the disease, while frontal and temporal regions remain less affected.³⁻⁸ The manifest stage of HD is clinically characterized by progressive motor disturbances such as chorea and dystonia, cognitive decline and psychiatric symptoms.^{9,10} Cognitive decline mainly involves progressive impairment in executive function.¹¹ Nonetheless, neuropsychological studies assessing visual cognitive function in HD reported impairments in several visual domains, specifically tasks involving visual object perception,^{12,13} facial emotion recognition,^{14,15} visuospatial processing and visual working memory.^{7,16,17}

Striatal atrophy is considered to be the origin of the characteristic choreatic motor signs, but it is suggested that other symptoms of HD might be related to cortical degeneration.^{4,18,19} Thinning of regions in the occipital lobe has been linked to worse performance on cognitive visuospatial tasks, which implies a distinct association between higher-level cognitive performance and occipital degeneration in HD gene carriers.^{6,7}

In contrast to many structural magnetic resonance imaging (MRI) studies that showed neurodegenerative changes of the posterior cerebral cortex, only one study has assessed the functional aspects of visual brain function in HD using resting-state functional MRI.²⁰ Here, functional connectivity changes were limited to the fusiform cortex in patients with HD, despite the presence of widespread posterior cortical atrophy. Still, little is known about brain function in patients with HD, and the link between structural cortical brain changes and functional impairments has not yet been fully investigated. Using different neuroimaging modalities and a visual cognitive test battery, this study aimed to improve the understanding of functional and structural alterations in the visual cortex in premanifest individuals (i.e., before the presence of motor symptoms) and in patients with early stage HD and investigate if there is an association between brain changes and visual cognitive task performance.

2. METHODS

2.1. Participants

A total of 59 participants (18 healthy controls, 20 premanifest HD gene carriers, and 20 premanifest HD gene carriers) were included in this cross-sectional, observational study (Table 1).

Individuals were recruited from the outpatient clinic of the Neurology department at the Leiden University Medical Center between January 2017 and September 2017. HD gene carriers required a positive genetic test with a cytosine, adenine, guanine (CAG) repeat expansion of 36 or more on the Huntingtin gene. Partners and HD gene-negative relatives were recruited as healthy controls. All participants were between 18 and 65 years of age at the time of visit. To ensure an optimal primary visual acuity, individuals with an impaired primary visual ability (measured as below 0.5; i.e., 20/40 vision) on the visual acuity test or ophthalmic disorders were excluded from the study. Other exclusion criteria were additional major co-morbidities not related to HD (including cardiovascular diseases, hypertension, diabetes mellitus and other neurological disorders), the inability to undergo MRI scanning (due to metallic implants, claustrophobia or pregnancy), or the participation in intervention trials. The Medical Ethical Committee of the Leiden University Medical Center approved this study and written informed consent according to the Declaration of Helsinki was obtained from all participants.

2.2. Clinical assessments

Demographic information, CAG repeat length (for HD gene carriers only), and medical history was collected. Primary visual ability was measured with a visual acuity test. To assess the ability to perceive color differences the Ishihara Color Test was performed. Trained investigators assessed the degree of motor disturbances using the Unified Huntington's Disease Rating Scale - Total Motor Score (UHDRS-TMS), a scale that measures different domains that are characteristically impaired in HD, including the oculomotor function, the tongue protrusion, the gait and postural stability, and the presence of choreatic or dystonic movements.²¹ Higher scores indicate increased motor impairment. Based on the UHDRS-TMS, HD gene carriers were divided into 21 premanifest individuals, with a score of 5 or less, and 20 manifest individuals, with a score of more than 5.²¹ The UHDRS Total Functional Capacity (TFC) score was administered to assess five components of global daily functioning, including capacity to work, management of finances, ability to perform domestic chores, independency in activities of daily living (such as eating, bathing, and dressing), and care environment. Here, lower TFC scores indicate more impaired function. In manifest HD, the TFC score

is used to divide participants into disease stages, in which Stages 1 and 2 represent an early disease stage and Stage 5 the most advanced stage.²²

The cognitive battery used in this study consisted of specific neuropsychological assessments with a large visual component. All cognitive tasks were administered by certified neuropsychological investigators and lasted approximately 30 minutes.

The selection of cognitive assessments was based on findings from previous studies that focused on cognitive dysfunction in premanifest and manifest HD gene carriers.^{13,23–25}

The Symbol Digit Modalities Test (SDMT), Stroop Word Reading Test (SWRT), and Trail Making Test (TMT) were administered to assess visuospatial function, such as visual scanning and visual attention.^{24,26,27} Visual object perception was measured using subtests from the Visual Object and Space Perception (VOSP) battery and the Groningen Intelligence Test (GIT).^{28,29} Individual scores on each cognitive assessment were converted to standardized Z-scores. These Z-scores were summed and averaged resulting in cognitive domain scores to assess overall visuospatial and visual perceptual function.

2.3. Image acquisition

All participants underwent structural and functional MRI scanning on a 3.0 Tesla MRI scanner (Philips Achieva, Best, the Netherlands). Both structural and functional MRI data were acquired using a standard 32-channel whole head coil. MRI proof glasses or lenses were used during scanning if participants had a visual acuity below 0.5 (20/40 vision) without correction, to ensure optimal primary visual ability during task performance. Anatomical three-dimensional T1-weighted images were acquired with the following parameters: TE = 3.3 ms, TR = 7.2 ms, flip angle = 9°, FOV = 256 x 240 x 176 mm and 176 slices with a slice thickness of 1 mm and no gap between slices, resulting in a voxel size of 1.00 x 1.00 x 1.00 mm, and scan duration of 9 minutes. All functional blood oxygen level-dependent (BOLD)-weighted echo-planar imaging whole brain volumes were obtained with the following parameters: TE = 30 ms, TR = 3000 ms, FOV = 212 x 198 x 158 mm, flip angle = 80° and 48 slices with a slice thickness of 2.81 mm and slice gap of 0.5 mm, resulting in a voxel size of 3.31 x 3.31 x 2.81 mm, and scan duration of 5.42 minutes for the task fMRI, and 8 minutes for the resting state fMRI.

2.4. Image processing

2.4.1. Structural MRI

Cortical morphology was examined using volumetric and thickness outcome measures. Grey matter density alterations of the visual cortex in premanifest and manifest HD

gene carriers compared to controls were examined using voxel-based morphometry (VBM) analysis, which involves a voxel-wise comparison of the local concentration of grey matter between groups, including cortical surface area and cortical folding.³⁰ In addition, to investigate subtle brain changes, the cortical thickness of specific brain regions in the visual cortex were measured.³¹

2.4.2. Voxel-based morphometry

To assess structural voxel-wise grey matter density differences of the visual cortex between groups, we used a standardized VBM analysis protocol,³⁰ using the FMRIB's Software Library (FSL, version 5.0.10, Oxford, United Kingdom) tools.^{32,33} First, non-brain tissue from all T1-weighted images was removed using the semi-automated brain extraction tool.³⁴ Then, these brain-extracted images were segmented into different tissue types (i.e., grey matter, white matter, and cerebrospinal fluid). Quality control was performed on the brain extraction and grey matter segmentation images, and no data was excluded for further analyses. The grey matter images were aligned to the 2 mm Montreal Neurological Institute (MNI)-152 standard space image, using non-linear registration.^{35,36} An averaged study-specific 4D template was subsequently created. Then, all native grey matter images were non-linear registered to this study specific template and modulated to correct for local enlargements and contractions due to the non-linear component of the spatial transformation.³⁰ Finally, the modulated grey matter images were smoothed with an isotropic Gaussian kernel with a sigma of 3 mm, which corresponds to a full width at half maximum (FWHM) smoothing kernel of 7 mm.

2.4.3. Cortical thickness

Cortical thickness of specific regions of interest was measured using cortical parcellation implemented in FreeSurfer version 5.3.0.³⁷ The FreeSurfer algorithm automatically parcellates the cortex and assigns a neuroanatomical label to each location on a cortical surface model, based on probabilistic information. Four occipital regions (lingual gyrus, pericalcarine cortex, cuneus, and lateral occipital cortex), one parietal region (superior parietal cortex), and three temporal regions (temporal pole, fusiform gyrus, inferior temporal gyrus) defined by the Desikan-Killiany atlas were selected for further analyses,³¹ because these regions are all involved in the processing of visual stimuli.¹ As there were no differences in cortical thickness between left and right hemisphere for any cortical region in our cohort, thickness was averaged across the two hemispheres for each region (see supplementary Table S1).

2.4.4. Functional MRI

Alterations in brain function were assessed using task-based and resting-state fMRI. For the task-based fMRI, changes in BOLD signal in response to a visual stimulus were calculated as a proxy for cortical neuronal connectivity.³⁸ In addition, brain function at rest was examined using resting-state functional connectivity analysis with pre-defined visual resting-state networks of interest (NOI).³⁹

2.4.5. Task design

The visual stimulus for the task-based fMRI scan consisted of seven blocks with an 8 Hz flashing black-and-white checkerboard pattern for 20 seconds, followed by 28 seconds of a grey screen with a red dot in the center of the screen. The visual stimuli were projected onto a screen, which the participant observed through a mirror attached to the head coil. To maintain attention and fixation to the checkerboard, each participant was asked to push on a button when the red dot position in the center of the screen changed from lighter to darker red, occurring at random intervals throughout the stimulus run. For the resting-state fMRI measures, participants were asked to close their eyes, not to fall asleep, and not to speak during the complete scanning time.

2.4.6. Pre-processing

All functional images were pre-processed using the FEAT tool implemented in FSL.³² Pre-processing steps included motion correction,³⁵ spatial smoothing using a Gaussian kernel of 8 mm FWHM, high-pass temporal filtering (with a cutoff of 48 seconds for task-fMRI images, and 100 seconds for resting-state fMRI images), and distortion correction of B0 inhomogeneity's. The pre-processed functional images were non-linear registered to individual brain-extracted T1-weighted scans, which were registered to MNI-152 standard space with boundary-based-registration.^{34,35} No scans were excluded after visual quality control to ensure correct registration.

2.4.7. Vascular reactivity

Pre-processed task-based functional MRI scans were further processed to measure cortical vascular reactivity in response to visual stimulation. For this analysis, BOLD timeseries had to be extracted from the preprocessed scans. To this end, a region of interest (ROI) was created for each participant based on the results of an initial subject-level analysis. During this subject-level analysis, brain regions were identified that reacted to the stimulus train using the general linear modeling approach implemented in FSL's FEAT.³² The degree to which each voxel responded to the stimulus train was expressed in a Z-statistic map.

To obtain the functional region of interest for each participant, a binary mask was constructed by taking the top 20% most activated voxels from this Z-statistic activation map. Using this mask, an average BOLD timeseries was calculated for each participant by averaging across all masked voxels. The resulting timeseries was cut up into blocks that each contained stimulus period (20 sec) and a subsequent rest period (28 sec). Then, the timeseries of each block were expressed as percentage BOLD change using the mean value of all blocks. To minimize the effect of non-physiologic noise on the block response, blocks with a percentage BOLD change greater than 3% were discarded.

Based on the method previously described by Dumas et al., 2012,³⁸ a trapezoidal function was fit to the vascular reactivity response (i.e., percentage BOLD signal change) in the average BOLD timeseries, to describe the time-to-peak response, time-to-baseline and amplitude of the response. The time-to-peak was calculated from the beginning of the block at $t = 0$ to onset of the trapezoid ceiling. The time-to-baseline is defined as the duration from the end of the stimulus at $t = 20$ seconds to the baseline. Response amplitude was defined as the distance from baseline to the peak response. The entire algorithm described above was implemented in R (the R foundation for Statistical Computing, Vienna, Austria), version 3.4.2. The full source code, along with additional mathematical details, has been published on GitHub (<https://github.com/jjhbw/TrapFit/>).

2.4.8. Functional connectivity

After pre-processing of the functional resting state images, Independent Component Analysis-based Automated Removal Of Motion Artifacts was used as a data-driven method to identify and remove motion-related independent components from our resting state fMRI data.⁴⁰ Then, functional connectivity analysis was performed using the dual regression method implemented in FSL, previously described by Filippini et al., 2009 and Hafkemeijer et al., 2015.^{41,42}

For the dual regression method, we used standardized resting state NOI to measure functional connectivity as BOLD signal changes in the brain in relation to similar alterations in predefined resting state networks.³⁹ As we focused on the visual cortex, we used two templates of standardized resting state networks, namely the medial visual network (including the calcarine sulcus, precuneus, lateral geniculate nucleus, and primary visual cortex) and the lateral visual network (including the occipital pole, lateral occipital cortex, fusiform areas, and superior parietal regions).³⁹ To account for noise, white matter and cerebrospinal fluid templates were also included in the analyses.⁴³

2.4.9. Statistical analysis

Group differences in demographic and clinical outcome measures were analyzed using ANOVA, χ^2 -test, and Kruskal-Wallis test when applicable for continuous, categorical and skewed data respectively. Analysis of Covariance (ANCOVA), with group as factor and a simple contrast, was used to analyze differences in cortical thickness, task-based fMRI response parameters and cognitive task performance in premanifest and manifest HD compared to controls. Age, gender, and years of education were included as covariates. Multiple linear regression analyses in HD gene carriers (i.e., premanifest and manifest HD) were performed to assess the relationship between neuroimaging (dependent variable) and cognitive outcome measures (independent variable), adjusted for age, gender, years of education, and CAG repeat length. All independent variables were entered in one block. Separate linear regression models were used for each neuroimaging measure. An alpha-level of < 0.05 was used to determine significance. To account for multiple comparisons in this analysis, an adjusted p -value was set based on the number of comparisons made for the analysis. Statistical analyses were performed using the Statistical Package for Social Sciences (SPSS for Mac, version 23, SPSS Inc.).

For the structural VBM and resting state functional connectivity data, statistical analyses to detect group differences between controls, and premanifest and manifest HD were performed using a general linear model in FSL with age and gender as covariates. FSL-randomise was used for voxel-wise non-permutation testing with 5,000 permutations.⁴⁴ For the VBM analysis, a binary mask of the visual cortex extracted from the MNI-152 standard space image was used. For the functional connectivity analysis, analyses of variance F tests were first performed to assess if the group averages accounted for a significant effect in each NOI. Then, two-sample t tests were applied to obtain specific group differences (i.e., an increase or decrease) in functional connectivity. To account for the potential effects of local structural grey matter differences within and between the groups, individual grey matter density maps were used as additional voxel-dependent covariate in the statistical design. The threshold-free cluster enhancement (TFCE) technique was used to correct for multiple comparisons across voxels with family wise error,⁴⁵ with a significant p -value of < 0.05 as significant threshold. Brain structures that showed a significant difference between groups were identified on the TFCE-statistic image using the Harvard-Oxford atlas and the cluster tool integrated in FSL.

3. RESULTS

3.1. Clinical characteristics

Demographic group characteristics are displayed in Table 1. Based on their functional capacity, manifest HD were in an early to moderate disease stage (4 patients in Stage 1, 15 patients in Stage 2, and 1 patient in Stage 3).

There were no significant group differences for gender, handedness, education level, and use of tobacco. CAG repeat length did not differ between premanifest and manifest HD. Premanifest HD were younger ($F[2,56] = 10.90$) compared to controls ($p = 0.028$) and manifest HD ($p < 0.001$). Furthermore, manifest HD had a higher UHDRS-TMS compared to controls and premanifest HD ($F[2,56] = 49.41$, both $p < 0.001$) and a lower UHDRS-TFC score compared to controls and premanifest HD ($H[2] = 41.24$, $p < 0.001$). On all visuospatial and visual perceptual tasks, manifest HD performed worse compared to controls. There were no significant differences in cognitive task performance between controls and premanifest HD.

3.2. Structure of the visual cortex

3.2.1. Voxel-based morphometry

Regional VBM analysis of the visual cortex was used to assess grey matter volume differences between groups. In manifest HD, significant cortical volume loss was identified bilateral in the fusiform gyrus, lingual gyrus, lateral occipital cortex and superior parietal cortex (Figure 1 and Table 2). Furthermore, the left occipital pole and right inferior temporal cortex showed volume loss in manifest HD compared to controls. No significant differences in grey matter volume were found between controls and premanifest HD.

TABEL 1 Demographic and clinical characteristics

	Controls	Premanifest HD	Manifest HD
N	18	21	20
Age, years	46.2 ± 10.7 (24.1 – 61.3)	37.4 ± 9.0* (23.2 – 53.0)	52.1 ± 10.8 (24.1 – 61.3)
Gender (male/female)	7/11	11/10	11/9
Handedness – right (%)	15 (83.3%)	19 (90.5%)	15 (75.0%)
Education, years	17.0 ± 2.2	16.8 ± 3.2	16.4 ± 2.3
Current tobacco use	3 (16.7%)	4 (19.0%)	6 (30.0%)
CAG repeat length	N/A	41.8 ± 2.2 (38 – 45)	42.8 ± 2.4 (40 – 48)
UHDRS – TMS	1.8 ± 1.2 (0 – 5)	2.8 ± 1.0 (1 – 5)	27.2 ± 15.5** (8 – 52)
UHDRS – TFC	13 (11 – 13)	13 (10 – 13)	9 (6 – 13)**
Visual perception (compound Z-score)	0.43 ± 0.43	0.34 ± 0.48	-0.61 ± 0.91**
Visual scanning and attention (compound Z-score)	0.26 ± 0.43	0.13 ± 0.29	-0.26 ± 0.39**

Data are mean ± SD (range) for age, CAG repeat length, years of education, and UHDRS-TMS. Numbers (%) are presented for handedness and tobacco use. Median (range) is given for UHDRS-TFC. Compound standardized Z-scores on visual cognitive tasks were calculated. Scaled Z-scores were summed and averaged resulting in Z-scores per visual cognitive domain. Mean Z-scores ± SD per domain are presented. Analysis of covariance (ANCOVA) with group as simple contrast was used to assess differences in Z-scores compared to controls, with age, gender and years of education as covariates. Abbreviations: N/A = Not applicable; CAG = Cytosine, Adenine, Guanine; UHDRS-TFC = Unified Huntington’s Disease Rating Scale Total Functional Capacity; UHDRS-TMS = Unified Huntington’s Disease Rating Scale Total Motor Score.

* Significant different compared to controls $p < 0.05$

** Significant different compared to controls $p < 0.001$

TABLE 2 Grey matter volume loss in the visual cortex in manifest HD

Cluster voxel size	Anatomical regions	Side	MNI coordinates (mm)			t value	p value
			x	y	z		
870	Fusiform gyrus (BA 19/37)	R	24	-72	-10	4.78	0.003
	Lateral occipital cortex (BA 19)	R	36	-80	-2	3.94	0.004
	Lingual gyrus (BA 18)	R	26	-46	0	4.11	0.014
741	Lateral occipital cortex (BA 19)	L	-46	-64	2	3.87	0.012
	Occipital pole (BA 17)	L	-18	-92	-12	3.75	0.022
	Fusiform gyrus (BA 19/37)	L	-26	-70	-6	3.32	0.038
696	Superior parietal cortex (BA 7)	L	-36	-46	38	4.76	0.012
606	Superior parietal cortex (BA 7)	R	22	-48	56	4.85	0.007
398	Inferior temporal cortex (BA 20)	R	46	-48	-6	4.35	0.019
15	Lingual gyrus (BA 18)	L	-26	-54	0	3.36	0.046

Voxel-wise identified regions of significant cortical volume loss in manifest HD compared to controls. All anatomical regions were identified using the Harvard-Oxford Subcortical and Cortical atlases and the cluster tool implemented in FSL. T-statistics and corresponding *p*-values are presented (with a TFCE-family wise corrected *p*-value of $p < 0.05$).

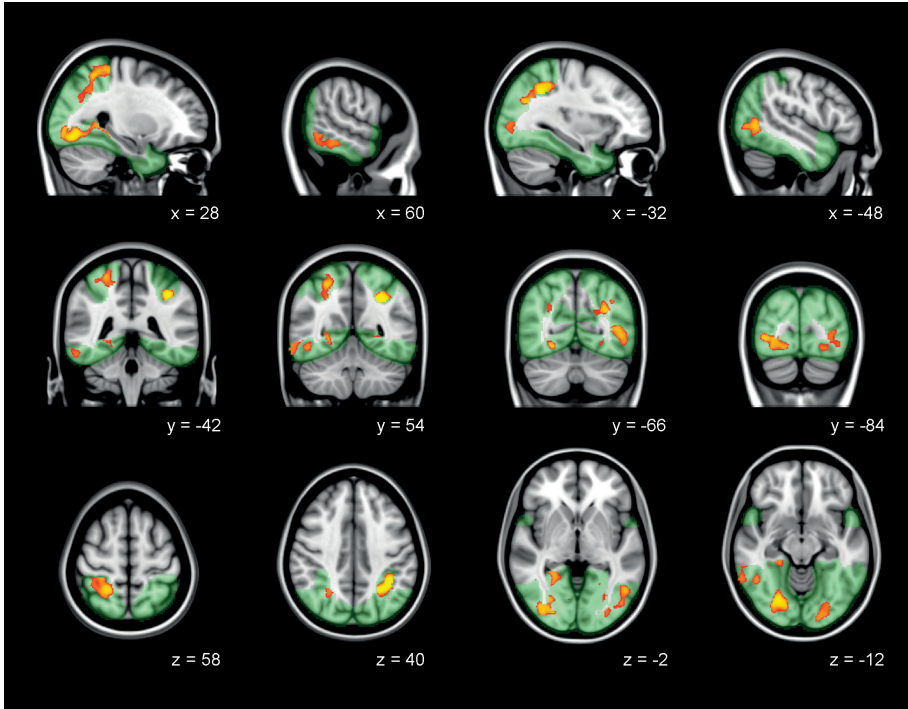
BA: Brodmann area, R: right hemisphere, L: left hemisphere

3.2.2. Cortical thickness

To determine subtle cortical changes in the visual cortex, the cortical thickness of eight regions of interest (cuneus, fusiform gyrus, inferior temporal cortex, lateral occipital cortex, lingual gyrus, pericalcarine cortex, superior parietal cortex, temporal pole) were additionally measured. Except for the pericalcarine cortex and temporal pole, significant cortical thinning was present in manifest HD in the cuneus, fusiform and lingual gyri, and inferior temporal, lateral occipital and superior parietal cortices compared to controls (Table 3). Premanifest HD did not show any significant differences in cortical thickness for all regions of interest compared to controls.

Multiple linear regression analysis was performed to assess the relationship between cortical thickness and cognitive function in HD gene carriers (i.e., both premanifest and manifest HD). Besides the inferior temporal cortex, all regions showed significant associations with visual perceptual function, in which a decrease in cortical thickness

FIGURE 1 Grey matter volume loss in the visual cortex in manifest HD



Voxel-based morphometry analysis. The significant Family-Wise-Error corrected grey matter differences between manifest HD and controls ($p < 0.05$) are presented in red-yellow, overlaid on sagittal, coronal, and transversal slices of Montreal-Neurological-Institute-152 standard T1-weighted images. Green: mask of visual cortex. Corresponding x-, y-, and z-coordinates are given.

TABLE 3 Cortical thickness in visual cortical regions

	Controls	Premanifest HD	Manifest HD	Premanifest HD vs. Controls		Manifest HD vs. Controls	
				Estimated difference [95% CI]	p-value	Estimated difference [95% CI]	p-value
Cuneus	1.95 ± 0.14	1.93 ± 0.13	1.82 ± 0.15	-0.05 [-0.14, 0.05]	0.344	-0.13 [-0.23, -0.04]	0.005
Fusiform gyrus	2.71 ± 0.16	2.72 ± 0.11	2.55 ± 0.21	-0.03 [-0.15, 0.08]	0.539	-0.14 [-0.25, -0.04]	0.010
Inferior temporal cortex	2.70 ± 0.13	2.73 ± 0.13	2.58 ± 0.18	-0.02 [-0.12, 0.09]	0.760	-0.10 [-0.20, -0.01]	0.039
Lateral occipital cortex	2.11 ± 0.13	2.17 ± 0.11	1.99 ± 0.22	0.02 [-0.09, 0.13]	0.750	-0.11 [-0.21, 0.00]	0.048
Lingual gyrus	2.10 ± 0.16	2.08 ± 0.09	1.96 ± 0.18	-0.07 [-0.17, 0.02]	0.143	-0.14 [-0.23, -0.05]	0.004
Pericalcarine cortex	1.74 ± 0.16	1.71 ± 0.13	1.67 ± 0.16	-0.06 [-0.16, 0.05]	0.287	-0.06 [-0.16, 0.04]	0.233
Superior parietal cortex	2.21 ± 0.16	2.19 ± 0.10	2.02 ± 0.19	-0.07 [-0.17, 0.03]	0.178	-0.18 [-0.27, -0.08]	< 0.001
Temporal pole	3.60 ± 0.36	3.77 ± 0.21	3.59 ± 0.40	0.15 [-0.08, 0.38]	0.206	0.02 [-0.21, 0.25]	0.854

Data are mean ± SD (mm). Cortical regions from left and right hemispheres were averaged. Significant group differences are presented in bold. Analysis of covariance (ANCOVA) was used with group as simple contrast to assess group differences with age and gender as covariates.

TABLE 4 Associations between cortical thickness and visual cognitive task performance in HD gene carriers

	Cuneus			Fusiform gyrus			Inferior temporal cortex			Lateral occipital cortex			Lingual gyrus			Superior parietal cortex								
	B	SE	η^2	p	B	SE	η^2	p	B	SE	η^2	p	B	SE	η^2	p	B	SE	η^2	p				
Visual perception (compound Z-score)	0.111	0.027	0.33	<0.001	0.106	0.027	0.28	<0.001	0.075	0.031	0.10	0.020	0.130	0.030	0.39	<0.001	0.097	0.022	0.24	<0.001	0.130	0.027	0.57	<0.001
Visual scanning and attention (compound Z-score)	0.008	0.062	0.05	0.893	0.061	0.060	0.01	0.314	0.082	0.061	0.00	0.185	0.022	0.069	0.04	0.752	0.057	0.051	0.00	0.275	0.008	0.065	0.03	0.908

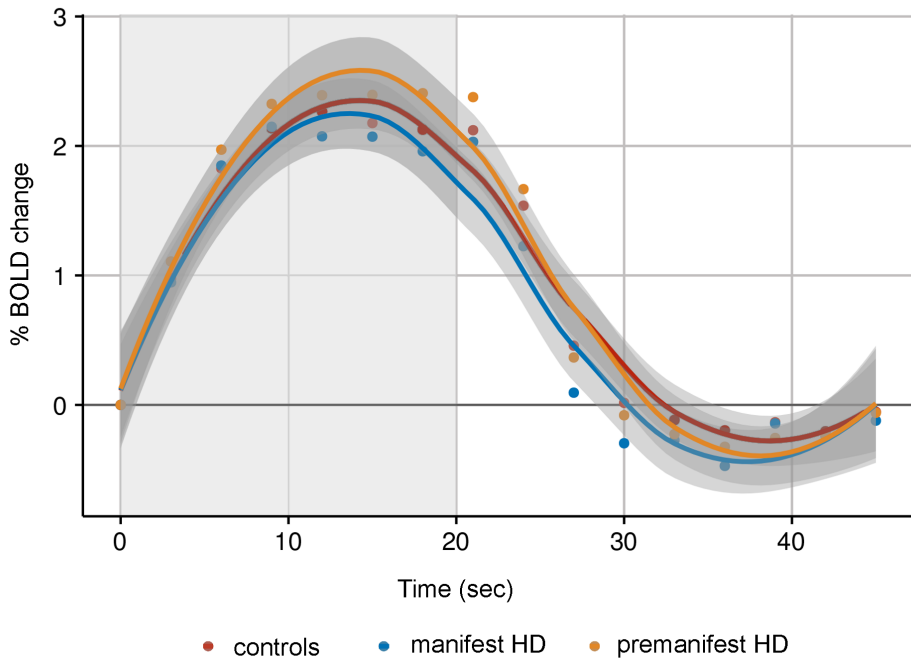
Unstandardized Beta (B), Standard Error (SE), and partial eta squared (η^2) are presented adjusted for age, gender, years of education and CAG. Unstandardized Beta represents change in cortical thickness (mm) for every 1-point change in Z-score for each cognitive domain. Significant p-values ($p < 0.004$) are presented in bold.

3.3. Function of the visual cortex

3.3.1 Vascular reactivity

Vascular brain function of the visual cortex was examined by quantifying alterations in BOLD signal in response to visual stimulation. Relative to baseline (i.e., prior to the start of the stimulus), there were no significant group differences in changes of the average BOLD response for the time to peak, time to baseline and amplitude response (Figure 2).

FIGURE 2 Blood oxygen level-dependent (BOLD) response to visual stimulation

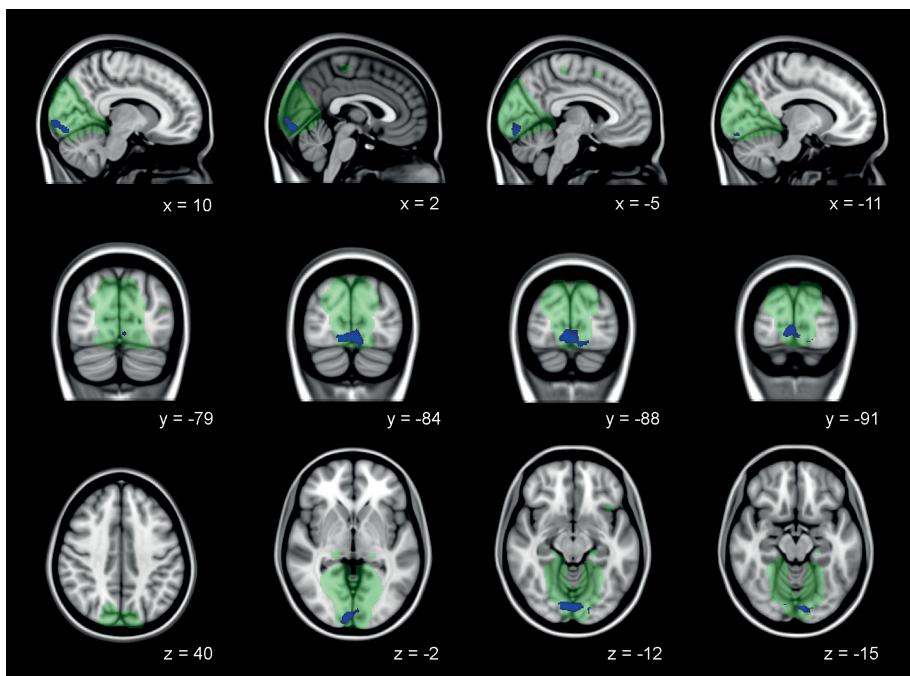


Fitted average BOLD responses per group relative to baseline (0%). The grey area represents the duration of visual stimulation for 20 seconds.

3.3.2. Functional connectivity

Brain function at rest was assessed to detect disease specific functional connectivity network changes within the medial visual network and lateral visual network. Decreased functional connectivity between the bilateral lingual gyrus, occipital pole, and occipital fusiform gyrus and the medial visual network was present in manifest HD compared to controls, independent of local grey matter atrophy (Figure 3 and Table 5). No differences in functional connectivity with the medial visual network were observed between premanifest HD and controls. In addition, there were no group differences in lateral visual network functional connectivity.

FIGURE 3 Decreased functional connectivity in medial visual network in manifest HD



Decreased functional connectivity independent of grey matter atrophy in manifest HD compared to controls in the medial visual network (green). Significant Family-Wise-Error corrected regions are presented in blue overlaid on sagittal, coronal, and transversal slices of Montreal-Neurological-Institute-152 standard T1-weighted images. Corresponding x-, y-, and z-coordinates are given.

TABLE 5 Decreased functional connectivity in medial visual network in manifest HD

Brain structure	Side	MNI coordinates (mm)			t-value	p-value
		x	y	z		
Lingual gyrus (BA 18) Occipital fusiform gyrus (BA 19/37)	R	12	-86	-14	4.65	0.013
Occipital pole (BA 17)	R	12	-98	-6	4.27	0.016
Lingual gyrus (BA 18) Occipital pole (BA 17)	L	0	-88	-14	4.43	0.015
Occipital fusiform gyrus (BA 19/37)	L	-14	-90	-16	3.39	0.035

Brain structures in the medial visual network that showed reduced functional connectivity in manifest HD compared to controls, independent of physiological noise, age, and gender. Structures were identified using the Harvard-Oxford Cortical atlas and cluster tool implemented in FSL. T-statistics and corresponding *p*-values are presented (with a TFCE-family wise corrected *p*-value < 0.05). For each peak voxel *x*-, *y*-, and *z*-coordinates in the MNI-152 standard space image are given. BA: Brodmann area, R: right hemisphere, L: left hemisphere

4. DISCUSSION

This study showed that changes in the visual cortex and visual cognitive deficits are present in early manifest HD gene carriers, but not in premanifest gene carriers.

The most pronounced volume loss and cortical thinning in manifest HD was found in the associative visual cortices, namely the lingual and fusiform gyri, and lateral occipital cortex. Thinning of these cortical regions in the ventral occipital-temporal pathway was associated with impaired visual perceptual function (i.e., object recognition tasks), suggesting that the neurodegenerative processes in the cortex might play a role in the visual deficits found in HD. Interestingly, the primary visual cortex (i.e., pericalcarine region and occipital pole) did not show neurodegenerative alterations and neuronal activity after visual stimulation also did not differ between groups, which suggest that basic visual processing remains preserved in early stages of the disease.

Our findings that cortical morphology of the primary visual cortex in early HD remained unaffected is in line with other studies that did not find atrophy of the primary visual cortex in both early and advanced disease stages.^{4,7,8} Still, our study is the first study that provides evidence of preserved basic visual processing function in early stages of HD using task-based fMRI that involved a black-and-white checkerboard stimulus. The BOLD response to visual stimulation in the primary visual cortex was not different from controls in both manifest and premanifest HD, which suggests that incoming stimuli from the optic radiation and lateral geniculate nucleus in the thalamus are properly received and transmitted by the primary visual cortex to higher visual cortical areas.

In general, visual stimuli that are received by the primary visual cortex (V1) are then projected to the secondary visual cortex (V2), which plays a role in the color perception and orientation.⁴⁶ Then, visual processing proceeds along the associative cortices, which can be divided into the ventral occipito-temporal pathway (V4) involved in color processing and the recognition of objects and shapes, and the dorsal occipito-parietal pathway (V3 and V5), involved in the processing of spatial information and movement perception.^{2,47}

Visual scanning, attention, and visual object and shape recognition was measured using visuospatial and visual perceptual tasks respectively. Manifest HD gene carriers showed impairments in these domains, but only visual perceptual function was associated with cortical thickness. The SDMT and TMT were used to measure visuospatial function, as these tasks require visual scanning and attention skills^{24,26}. However, these tasks also require a high motor demand and processing speed, which are known to be impaired in patients with HD. This might explain that no significant relationship was found between visuospatial task performance and thickness of the visual cortex.

The secondary visual cortex is located in the cuneus and lingual gyrus, which is involved in color discrimination and visual working memory.⁴⁶ From here, stimuli proceed towards the fusiform gyrus and lateral occipital cortex that are known to play a role in object and face recognition.^{48,49} This supports our findings that an impaired visual perceptual function in HD was associated with reduced cortical thickness in these regions.

Other studies reported similar findings in early manifest HD, such as a reduced nerve cell number in the secondary visual cortex,⁴ volume loss of the occipital lobe,^{3,20} and thinning of the cuneus, lingual gyrus and lateral occipital cortex that were associated with worse performance on cognitive tasks involving a visual component.^{6,7} Contrary to our findings, thinning and volume loss of the occipital lobe has also been observed in premanifest HD gene carriers.^{3,7,8,50} This process seems to occur in premanifest HD gene carriers that are within a decade or nearer to disease onset, suggesting a sudden increase in the rate of thinning around disease onset,^{7,8} but there are no longitudinal studies that can confirm this hypothesis. The difference with our findings might be explained by the fact that our cohort consisted of a heterogeneous, relatively young group of premanifest HD gene carriers with a median estimated time to disease onset of 16 years, based on the survival analysis of Langbehn et al., 2004.⁵¹ In contrast, the multicenter TRACK-HD and PREDICT-HD studies included large cohorts of premanifest HD gene carriers which were divided into close (e.g., below 9 or 10 years) and far (above 10 to 15 years) from estimated disease onset.^{3,7,8} Only six premanifest participants in our study were within a decade or nearer to disease onset, which might explain the fact that we found no differences between controls and premanifest HD.

Function of the posterior cerebral cortex has been studied less extensively in HD. Our study examined brain function at rest, in addition to the assessment of brain function during task performance. Resting state fMRI can be used to study functional interactions between brain regions at rest (i.e., connectivity), and as no active input is required during resting state fMRI, the influence of the disease on task performance is not of concern.^{52,53} Despite normal brain function after visual task stimulation, decreased functional connectivity at rest of the lingual and fusiform gyri, and occipital pole was found in manifest HD compared to controls within the medial visual network. One other study specifically focused on the visual cortex at rest using resting state fMRI in manifest HD and found only reduced connectivity in the left fusiform gyrus, despite widespread volume loss in the occipital cortex.²⁰ Our findings of reduced functional connectivity were also independent of grey matter atrophy in these regions, which might suggest that regional atrophy does not cause abnormal neural connectivity at rest.

To improve the understanding of functional alterations in different disease stages, we additionally examined brain function at rest in premanifest individuals. Compared to controls, we found no differences in functional connectivity for both medial and visual networks, which is contrary to a previous study that showed reduced connectivity in the right parietal and bilateral visual cortices of the medial visual network in premanifest HD gene carriers.⁵² Although using several methodological approaches, these reductions in whole brain functional connectivity in premanifest HD were not detectable over time in longitudinal studies.^{54,55} A possible explanation for these discrepancies can be a selection bias, as participants with a faster rate of clinical decline might withdraw earlier from the study, leaving a relatively fitter premanifest group for longitudinal analyses.⁵⁴

Still, our study provides evidence of preserved brain function of the primary visual cortex at rest and after visual stimulation in manifest HD, but reduced function in the ventral occipito-temporal pathway at rest. Structural alterations of the visual cortex seem, nevertheless, to be more pronounced and widespread than functional alterations in early manifest HD, even extending to the inferior temporal and superior parietal cortices. Together with previous studies that additionally found evidence of cortical thinning and volume loss in these regions in premanifest HD gene carriers that are within a decade to disease onset,^{3,7,8,50} this implies that structural alterations might precede functional alterations in HD. Future studies with larger sample sizes are, however, needed to examine brain function using tasks that involve other visual cognitive domains, such as object or facial emotion recognition, or visuomotor function.

A limitation of this study is, that due to the cross-sectional design and our heterogeneous group of premanifest HD gene carriers, it remains uncertain how the posterior cerebral cortex changes over time. It would be interesting to assess the progression of posterior cortical volume loss longitudinally and in addition measure the effect of volume loss on changes in neural connectivity. In this way, potential cortical biomarkers can be identified that can be used in future clinical trials. Another limitation of this study is the relative small sample size of our cohort, which additionally prevents examining the role of gender.

In conclusion, the ventral visual pathway, specifically the lingual and fusiform gyri and the lateral occipital cortex, showed most pronounced structural and functional alterations in early manifest HD. Our study is the first to provide evidence of preserved basic visual function in early disease stages after visual stimulation. Clinically, visual perceptual function was impaired and related to reduced cortical thickness of the

ventral posterior brain regions. Still, changes in the visual cortex were not detectable in our premanifest HD group.

Our findings suggest that clinical visual deficits in HD are linked to atrophy of the posterior cerebral cortex, while basic visual function remains preserved in early disease stages.

REFERENCES

1. Prasad S, Galetta SL. Anatomy and physiology of the afferent visual system. In: *Handbook of Clinical Neurology*. Volume 102.; 2011:3-19.
2. Ungerleider LG, Haxby JV. "What" and "where" in the human brain. *Curr Opin Neurobiol*. 1994;4:157-165.
3. Tabrizi SJ, Langbehn DR, Leavitt BR, et al. Biological and clinical manifestations of Huntington's disease in the longitudinal TRACK-HD study: cross-sectional analysis of baseline data. *Lancet Neurol*. 2009;8(9):791-801.
4. Nana AL, Kim EH, Thu DCV, et al. Widespread heterogeneous neuronal loss across the cerebral cortex in Huntington's disease. *J Huntingtons Dis*. 2014;3:45-64.
5. Rüb U, Seidel K, Vonsattel JP, et al. Huntington's disease (HD): Neurodegeneration of Brodmann's primary visual area 17 (BA17). *Brain Pathol*. 2015;25(6):701-711.
6. Rosas HD, Salat DH, Lee SY, et al. Cerebral cortex and the clinical expression of Huntington's disease: complexity and heterogeneity. *Brain*. 2008;131(4):1057-1068.
7. Johnson EB, Rees EM, Labuschagne I, et al. The impact of occipital lobe cortical thickness on cognitive task performance: An investigation in Huntington's Disease. *Neuropsychologia*. 2015;79:138-146.
8. Nopoulos PC, Aylward EH, Ross CA, et al. Cerebral cortex structure in prodromal Huntington disease. *Neurobiol Dis*. 2010;40(3):544-554.
9. Roos RAC. Huntington's disease: a clinical review. *Orphanet J Rare Dis*. 2010;5(1):40.
10. Bates GP, Dorsey R, Gusella JF, et al. Huntington disease. *Nat Rev Dis Prim*. 2015;1:1-21.
11. Dumas EM, van den Bogaard SJA, Middelkoop HAM, Roos RAC. A review of cognition in Huntington's disease. *Front Biosci*. 2013;S5:1-18.
12. Gómez-Tortosa E, del Barrio A, Barroso T, García Ruiz PJ. Visual processing disorders in patients with Huntington's disease and asymptomatic carriers. *J Neurol*. 1996;243(3):286-292.
13. Lemiere J, Decruyenaere M, Evers-Kiebooms G, Vandenbussche E, Dom R. Cognitive changes in patients with Huntington's disease (HD) and asymptomatic carriers of the HD mutation. *J Neurol*. 2004;251(8):935-942.
14. Kordsachia CC, Labuschagne I, Stout JC. Beyond emotion recognition deficits: A theory guided analysis of emotion processing in Huntington's disease. *Neurosci Biobehav Rev*. 2017;73:276-292.
15. Bora E, Velakoulis D, Walterfang M. Social cognition in Huntington's disease: A meta-analysis. *Behav Brain Res*. 2016;297:131-140.
16. Dumas E, Say M, Jones R, et al. Visual working memory impairment in premanifest gene-carriers and early Huntington's disease. *J Huntingtons Dis*. 2012;1:97-106.

17. Labuschagne I, Cassidy AM, Scahill RI, et al. Visuospatial processing deficits linked to posterior brain regions in premanifest and early stage Huntington's disease. *J Int Neuropsychol Soc.* 2016;22:595-608.
18. Waldvogel HJ, Kim EH, Thu DCV, Tippett LJ, Faull RLM. New perspectives on the neuropathology in Huntington's disease in the human brain and its relation to symptom variation. *J Huntingtons Dis.* 2012;1:143-153.
19. Thu DCV, Oorschot DE, Tippett LJ, et al. Cell loss in the motor and cingulate cortex correlates with symptomatology in Huntington's disease. *Brain.* 2010;133(4):1094-1110.
20. Wolf RC, Sambataro F, Vasic N, et al. Visual system integrity and cognition in early Huntington's disease. *Eur J Neurosci.* 2014;40(2):2417-2426.
21. Huntington Study Group. Unified Huntington's disease rating scale: reliability and consistency. *Mov Disord.* 1996;11(2):136-142.
22. Shoulson I, Fahn S. Huntington disease: Clinical care and evaluation. *Neurology.* 1979;(29):1-3.
23. Stout J, Jones R, Labuschagne I, et al. Evaluation of longitudinal 12 and 24 month cognitive outcomes in premanifest and early Huntington's disease. *J Neurol Neurosurg Psychiatry.* 2012;83:687-694.
24. O'Rourke JJF, Beglinger LJ, Smith MM, et al. The Trail Making Test in prodromal Huntington disease: contributions of disease progression to test performance. *J Clin Exp Neuropsychol.* 2011;33(5):567-579.
25. Lawrence AD, Watkins LH, Sahakian BJ, Hodges JR, Robbins TW. Visual object and visuospatial cognition in Huntington's disease: implications for information processing in corticostriatal circuits. *Brain.* 2000;123:1349-1364.
26. Smith A. *Symbol Digit Modalities Test Manual.* Los Angeles, California; 1973.
27. Stroop J. Studies of interference in serial verbal reactions. *J Exp Psychol.* 1935;18(6):643-662.
28. Warrington E, James M. *Visual Object and Space Perception Battery.* Bury St. Edmunds (UK); 1991.
29. Luteijn F, Barelds DP. Handleiding Groninger Intelligentietest 2 (GIT). [Manual Groningen Intelligence Test]. 2004.
30. Good C, Johnsrude I, Ashburner J, Henson R, Friston K, Frackowiak R. A voxel-based morphometric study of ageing in 465 normal adult human brains. *Neuroimage.* 2001;14(1):21-36.
31. Desikan RS, Segonne F, Fischl B, et al. An automated labeling system for subdividing the human cerebral cortex on MRI scans into gyral based regions of interest. *Neuroimage.* 2006;31:968-980.
32. Smith SM, Jenkinson M, Woolrich MW, et al. Advances in functional and structural MR image analysis and implementation as FSL. *Neuroimage.* 2004;23:S208-S219.

33. Douaud G, Smith S, Jenkinson M, et al. Anatomically related grey and white matter abnormalities in adolescent-onset schizophrenia. *Brain*. 2007;130:2375-2386.
34. Smith SM. Fast robust automated brain extraction. *Hum Brain Mapp*. 2002;17(3):143-155.
35. Jenkinson M, Bannister P, Brady M, Smith S. Improved optimization for the robust and accurate linear registration and motion correction of brain images. *Neuroimage*. 2002;17(2):825-841.
36. Andersson JLR, Jenkinson M, Smith S. *Non-Linear Registration Aka Spatial Normalisation*. 2007. FMRIB Technical Report TR07JA2. [<http://fmrib.medsci.ox.ac.uk/analysis/techrep/tr07ja2/tr07ja2.pdf>].
37. Fischl B, Dale AM. Measuring the thickness of the human cerebral cortex from magnetic resonance images. *Proc Natl Acad Sci U S A*. 2000;97(20):11050-11055.
38. Dumas A, Dierksen GA, Gurol ME, et al. Functional magnetic resonance imaging detection of vascular reactivity in cerebral amyloid angiopathy. *Ann Neurol*. 2012;72(1):76-81.
39. Beckmann CF, DeLuca M, Devlin JT, Smith SM. Investigations into resting-state connectivity using independent component analysis. *Philos Trans R Soc*. 2005;360:1001-1013.
40. Pruim RHR, Mennes M, van Rooij D, Llera A, Buitelaar JK, Beckmann CF. ICA-AROMA : A robust ICA-based strategy for removing motion artifacts from fMRI data. *Neuroimage*. 2015;112:267-277.
41. Filippini N, Macintosh BJ, Hough MG, et al. Distinct patterns of brain activity in young carriers of the APOE-ε4 allele. *Proc Natl Acad Sci U S A*. 2009;106(17):7209-7214.
42. Hafkemeijer A, Möller C, Dopfer EGP, et al. Resting state functional connectivity differences between behavioral variant frontotemporal dementia and Alzheimer's disease. *Front Hum Neurosci*. 2015;9:474.
43. Birn RM. The role of physiological noise in resting-state functional connectivity. *Neuroimage*. 2012;62(2):864-870.
44. Winkler AM, Ridgway GR, Webster MA, Smith SM, Nichols TE. Permutation inference for the general linear model. *Neuroimage*. 2014;92:381-397.
45. Smith SM, Nichols TE. Threshold-free cluster enhancement: addressing problems of smoothing, threshold dependence and localisation in cluster inference. *Neuroimage*. 2009;44(1):83-98.
46. Tootell RBH, Tsao D, Vanduffel W. Neuroimaging weighs in: Humans meet macaques in "primate" visual cortex. *J Neurosci*. 2003;23(10):3981-3989.
47. Kravitz DJ, Saleem KS, Baker CI, Ungerleider LG, Mishkin M. The ventral visual pathway: an expanded neural framework for the processing of object quality. *Trends Cogn Sci*. 2013;17(1):26-49.
48. Kanwisher N, McDermott J, Chun MM. The fusiform face area: A module in human extrastriate cortex specialized for face perception. *J Neurosci*. 1997;17(11):4302-4311.
49. Grill-Spector K, Kourtzi Z, Kanwisher N. The lateral occipital complex and its role in object recognition. *Vision Res*. 2001;41:1409-1422.

50. Rosas HD, Hevelone ND, Zaleta AK, Greve DN, Salat DH, Fischl B. Regional cortical thinning in preclinical Huntington disease and its relationship to cognition. *Neurology*. 2005;65(5):745-747.
51. Langbehn DR, Brinkman RR, Falush D, Paulsen JS, Hayden MR. A new model for prediction of the age of onset and penetrance for Huntington's disease based on CAG length. *Clin Genet*. 2004;65(4):267-277.
52. Dumas EM, van den Bogaard SJA, Hart EP, et al. Reduced functional brain connectivity prior to and after disease onset in Huntington's disease. *NeuroImage Clin*. 2013;2(1):377-384.
53. Biswal BB, Mennes M, Zuo XN, et al. Toward discovery science of human brain function. *Proc Natl Acad Sci U S A*. 2010;107(10):4734-4739.
54. Odish OFF, van den Berg-Huysmans AA, van den Bogaard SJA, et al. Longitudinal resting state fMRI analysis in healthy controls and premanifest Huntington's disease gene carriers: A three-year follow-up study. *Hum Brain Mapp*. 2014;119:110-119.
55. Seibert TM, Majid DSA, Aron AR, Corey-Bloom J, Brewer JB. Stability of resting fMRI interregional correlations analyzed in subject-native space: a one-year longitudinal study in healthy adults and premanifest Huntington's disease. *Neuroimage*. 2012;59(3):2452-2463.

SUPPLEMENTARY MATERIAL

TABLE S1 Cortical thickness per region in left and right hemispheres

	Controls			Premanifest HD			Manifest HD		
	Left	Right	p-value	Left	Right	p-value	Left	Right	p-value
Cuneus	1.96 ± 0.14	1.93 ± 0.15	0.177	1.93 ± 0.13	1.93 ± 0.14	0.734	1.82 ± 0.16	1.81 ± 0.16	0.532
Fusiform gyrus	2.72 ± 0.14	2.70 ± 0.19	0.413	2.74 ± 0.13	2.70 ± 0.12	0.220	2.59 ± 0.19	2.51 ± 0.24	0.312
Inferior temporal	2.69 ± 0.14	2.71 ± 0.15	0.472	2.74 ± 0.14	2.72 ± 0.14	0.400	2.58 ± 0.16	2.58 ± 0.21	0.889
Lateral occipital cortex	2.10 ± 0.13	2.12 ± 0.14	0.421	2.15 ± 0.10	2.18 ± 0.13	0.253	2.00 ± 0.23	1.99 ± 0.23	0.647
Lingual gyrus	2.09 ± 0.17	2.12 ± 0.16	0.213	2.15 ± 0.10	2.18 ± 0.13	0.895	1.97 ± 0.19	1.96 ± 0.17	0.634
Pericalcarine cortex	1.76 ± 0.19	1.72 ± 0.17	0.208	1.72 ± 0.13	1.71 ± 0.17	0.843	1.67 ± 0.17	1.68 ± 0.17	0.810
Superior parietal cortex	2.21 ± 0.15	2.21 ± 0.15	0.968	2.21 ± 0.11	2.17 ± 0.10	0.194	2.05 ± 0.18	2.00 ± 0.20	0.468
Temporal pole	3.56 ± 0.26	3.64 ± 0.52	0.439	3.76 ± 0.22	3.78 ± 0.28	0.763	3.62 ± 0.33	3.56 ± 0.53	0.500

Mean cortical thickness and standard deviation in left and right hemispheres (in mm). Paired t-test was used with significant p-value (two-tailed) < 0.05.

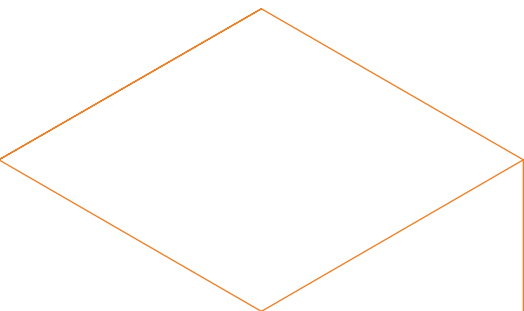
7



The visual pathway in **Huntington's** **disease**; a diffusion tensor imaging and neurophysiological study

Emma M. Coppen, Anne Hafkemeijer,
Jeroen van der Grond, Robert H.A.M. Reijntjes,
Martijn R. Tannemaat, Raymund A.C. Roos

Submitted



ABSTRACT

Objective: To investigate microstructure and function of the visual pathway and determine clinical correlates in Huntington's disease (HD) patients.

Methods: Diffusion tensor-imaging data was acquired of 21 premanifest, 20 manifest HD, and 17 healthy controls. To examine the microstructure of white matter pathways, mean indices of diffusion parameters were measured along the anterior and posterior thalamic radiation tracts using Tract-Based Spatial Statistics (TBSS). Additionally, electrical activity of the brain in response to visual stimuli was measured using pattern-reversal visual-evoked potentials (VEPs). Associations with clinical measures were examined in HD gene carriers using univariate linear regression analyses corrected for age, gender, and HD group.

Results: Microstructural alterations in manifest HD were primarily present in the optic radiations of posterior brain regions and to a lesser extent in the anterior brain regions. Reduced fractional anisotropy, and increased radial and axial diffusivity were associated with higher disease burden scores and increased oculomotor impairment in HD gene carriers. Radial diffusivity showed the strongest associations with oculomotor function and disease burden. Normal latencies of the pattern-reversal VEP were found in HD gene carriers compared to controls. Reduced amplitudes of the early components were present in premanifest HD and manifest HD, but were not associated with clinical measures.

Conclusion: Altered microstructure of the posterior optic radiation is detectable in early manifest HD and is related with disease severity. Our results show that axonal degeneration in the occipital lobe occurs early in the disease process, while functional integrity of the visual pathway remains relatively preserved.

1. INTRODUCTION

Huntington's disease (HD) is a hereditary, neurodegenerative disorder, characterized by a triad of progressive motor disturbances, cognitive decline and behavioral changes.¹ The disease is caused by an abnormal expansion of the CAG (cytosine-adenosine-guanine) repeat length in the Huntingtin gene on chromosome four.² Atrophy of the striatum is the neuropathological hallmark of the disease due to extensive loss of striatal medium-sized spiny neurons.³ As a result, striatal atrophy is thought to be the origin of the typical unwanted choreiform movements that occur in patients with HD.^{3,4} Neuroimaging studies have shown that striatal atrophy can be detected a decade before clinical disease onset in the so-called premanifest phase, and is therefore seen as a robust marker to track disease progression.^{5,6} However, besides the characteristic clinical signs of HD, deficits in visual cognition, such as an impaired visuospatial working memory or changes in facial emotion recognition have been frequently reported,⁷ and are suggested to originate from posterior cortical degeneration, since pronounced reductions in the absolute nerve cell number in the occipital lobe have been found in advanced HD patients.⁸⁻¹⁰

Moreover, in earlier disease stages, volume loss in posterior cortical brain regions is present,¹¹⁻¹⁵ and is even associated with worse visual cognitive task performance and oculomotor dysfunction.^{11,12,15} It has therefore been proposed that besides striatal atrophy, cortical degeneration also contributes to the clinical phenotype of HD.¹⁵

Although there is increasing evidence of the involvement of posterior brain regions in the neurodegenerative process of HD, the extent of structural and functional changes of the *in-vivo* pathways to these regions remains unclear. In our study, we aimed to gain more insight into the neuropathological involvement of posterior brain regions in HD. We therefore assessed white matter diffusion properties and neurophysiological measurement of visual-evoked potentials to investigate structural and functional alterations of the visual pathway in premanifest and manifest HD gene carriers.

2. METHODS

2.1. Participants

Fifty-eight participants (21 premanifest HD gene carriers, 20 manifest HD gene carriers, and 17 healthy controls) were included in this cross-sectional, observational study via the outpatient clinic of the Neurology department at the Leiden University Medical Center (LUMC) in the Netherlands. All HD gene carriers had a genetic test with ≥ 36 CAG repeats. Spouses and HD gene-negative relatives were recruited as

controls. Participants were required to have a normal or corrected-to-normal primary visual ability above 0.5 (20/40) on the visual acuity test and no major ophthalmic or neurologic co-morbidities. Participants were not included if they were unable to undergo MRI scanning (i.e. due to metallic implants, claustrophobia, or pregnancy). Patients that participated in an intervention trial were not included in this study. The Medical Ethical Committee of the LUMC approved this study and written informed consent was obtained from all participants.

Demographic data, including gender, date of birth, age at visit, and years of education, was obtained for all participants. Primary visual acuity and the ability to perceive color differences were assessed using a visual acuity test and the Ishihara Color Test respectively. HD gene carriers were divided into premanifest and manifest HD based on the presence of motor signs using the Unified Huntington's Disease Rating Scale (UHDRS) total motor score.¹⁶ This scale measures the degree of motor disturbances in different domains, such as oculomotor function, gait and postural stability, and the presence of choreiform or dystonic movements. A higher score indicates more motor impairments. The clinically manifest phase of the disease is defined as an UHDRS – total motor score of more than 5, whereas HD gene carriers with a score of 5 or less are defined as premanifest individuals. The ocular and saccadic movement items of the UHDRS were summed to establish a subdomain score (range 0 – 24) of oculomotor function, as described previously.^{12,17} The disease burden score (age x [CAG repeat length – 35.5]) was calculated for all HD gene carriers, in which a higher score reflects an increased disease severity.¹⁸

2.2. DTI acquisition

Diffusion Tensor Imaging (DTI) data was acquired on a 3-Tesla whole body MRI scanning system (Philips Achieva, Best, the Netherlands) using a standard 32-channel head coil. A single shot echo-planar DTI sequence was applied with 32 gradient directions and a total acquisition time of approximately 8 minutes. The follow scan parameters were used: TR = 11.547 ms, TE = 56 ms, FOV = 220 x 220 mm² with an acquisition matrix of 112 x 110, 2 mm slice thickness with no gap between slices, flip angle = 90°, voxel size = 1.96 x 1.96 x 2.00 mm³, number of slices = 75, b-value = 1000 s/mm², and halfscan factor = 0.61.

2.3. DTI processing

Diffusion tensor imaging data were preprocessed using the FMRIB's Diffusion Toolbox (FDT) that is implemented in FMRIB's Software Library (FSL, version 5.0.10, Oxford, United Kingdom).^{19,20} First, images were corrected for distortions caused by eddy

currents and motion artifacts. Then, diffusion tensors were fit to the eddy-current corrected data resulting in fractional anisotropy (FA), radial diffusivity (RD or λ_{\perp}) and axial diffusivity (AD or λ_{\parallel}) maps. RD was defined as the average of the second and third eigenvalues of the diffusion tensor ($(\lambda_2 + \lambda_3) / 2$), while AD corresponded to the first eigenvalue (λ_1).

The FA, RD, and AD maps from each participant were further analyzed using voxel-wise tract-based spatial statistics (TBSS) analysis, part of FSL.²¹ Here, FA images from all participants were nonlinearly registered to a standard space target image (FMRIB58_FA image) to form an averaged registered FA image. Then, a skeleton of white matter was generated by thresholding the averaged FA image, in which only voxels with a mean FA value of 0.2 or higher were included. Consequently, this mean FA skeleton represents the center of the white matter fibers throughout the whole brain. The skeleton projection was then applied to RD, and AD images, to create a separate skeleton for each diffusion measure. All data was visually checked for distortions or incorrect registration.

The anterior and posterior thalamic radiations (including the optic radiations) tracts were used as a mask of the visual pathway and mean FA, RD, and AD values within this mask were extracted. These tracts were identified using the Johns Hopkins University white matter tractography atlas implemented in FSL.

2.4. Visual-evoked potentials (VEP)

Electrical activity of the brain in response to visual stimuli was measured using a pattern-reversal VEP (Medelec Synergy, Oxford Instruments, version 11.0) at the department of Clinical Neurophysiology in the LUMC.

The left and right eyes were stimulated separately in two sessions (a total of four sessions), and were then averaged to form one trace per eye. A high-contrast full-field black-and-white checkerboard was used that flashed at a frequency of 2 Hz with an individual square check size of 0.45 degrees of arc. Participants were seated facing the checkerboard screen at a viewing distance of 2 meter in a dark room and were asked to fixate their gaze on the center of the screen with one eye covered. The EEG signal was recorded using an active mid-occipital (Oz) electrode and referenced to Cz, according to the international 10/20 system. A total of 100 trials were recorded. Trials containing artifacts were manually removed before further analyses.

Four major components (N75, P100, N140 and P200) were measured to analyze brain activity in the occipital cortex. For each component, the latency was calculated to indicate the time from stimulus onset to the component, whereas the amplitude was measured from peak to baseline (i.e. peak amplitude) and from peak to peak (i.e.

peak-to-peak amplitude), as described in the guidelines of the International Society for Clinical Electrophysiology of Vision (ISCEV).²²

2.5. Statistics

Group differences in demographic characteristics were analyzed using analysis of variance (ANOVA), independent T-test or chi-square test when applicable. Group differences between the extracted mean FA, RD, and AD values of the white matter tracts of interest were analyzed using ANOVA with Sidak correction to correct for multiple comparisons.

Post-hoc group differences on all diffusion outcome measures were performed using the general linear model (GLM) tool implemented in FSL. Age and gender were included as covariates in all statistical designs. FSL-randomise was used for voxel-wise non-permutation testing with 5000 permutations.²³ The Threshold-Free Cluster Enhancement technique was used, and family wise error was used to correct for multiple comparisons across voxels.²⁴

Group differences for all VEP outcome measures were analyzed using Kruskal-Wallis test. If this analysis yielded significant results, post-hoc analysis was performed using the Mann-Whitney U test.

Separate univariate linear regression analyses were performed in HD gene carriers (i.e. both premanifest and manifest HD) to assess the associations between diffusion outcome measures and clinical assessments, and between neurophysiological outcome measures and clinical assessments. Only outcome measures that showed significant group differences compared to controls were included in the regression analyses. Age, gender and HD group were included as covariates and entered in one block with the predictor variable. The significant threshold was set at a p -value of < 0.05 . Statistical analyses were performed using the Statistical Package for Social Sciences (SPSS for Mac, version 23, SPSS Inc.).

3. RESULTS

Demographic characteristics for each group are presented in Table 1. Premanifest HD gene carriers were younger compared to both controls and manifest HD ($F(2,55) = 10.81, p = 0.026$ and $p < 0.001$ respectively). Manifest HD had a higher disease burden score compared to premanifest HD ($t(37) = 4.6, p < 0.001$). In addition, manifest HD had more motor impairments compared to controls and premanifest HD on the UHDRS – total motor score ($F(2,55) = 48.06, \text{both } p < 0.001$) and UHDRS - oculomotor

score ($F(2,55) = 67.00$, both $p < 0.001$). Gender and CAG repeat length did not differ between groups.

To study structural integrity of the visual pathway, mean indices of diffusion parameters were measured along the anterior and posterior thalamic radiation tracts. Reduced FA ($F(2,55) = 9.35$, $p = 0.005$), increased RD ($F(2,55) = 16.66$, $p < 0.001$) and increased AD ($F(2,55) = 8.61$, $p = 0.001$) were found in manifest HD compared to controls (Figure 1A). No differences in diffusion parameters were observed between premanifest HD and controls.

Voxel-wise analysis showed that these reduced FA and increased RD values in manifest HD were primarily located posterior in the optic radiation and thalamus (Figure 1B). Reduced mean AD was found in the frontal lobe, particularly in the anterior limb of the internal capsule and thalamus.

All diffusivity parameters showed significant associations with clinical assessments (Table 2). The UHDRS total motor score, UHDRS oculomotor score and disease burden score all showed the strongest association with radial diffusivity, meaning that higher clinical scores were correlated with increased radial diffusivity.

To study functional integrity of the visual pathway, brain activity after visual stimulation

TABLE 1 Demographic group characteristics

	Controls	Premanifest HD	Manifest HD
N	17	21	20
Age (years)	46.5 ± 10.9 (24.1 – 61.3)	37.4 ± 9.0 (23.2 – 52.9)	52.1 ± 10.8 (28.5 – 64.8)
Gender (m/f)	7/10	11/10	11/9
CAG repeat length	–	41.8 ± 2.2 (38 – 45)	42.8 ± 2.4 (40 – 48)
Disease burden score	–	228.6 ± 88.1 (89.9 – 368.0)	362.4 ± 93.1 (185.0 – 538.8)
UHDRS – Total motor score	1.8 ± 1.3 (0 – 5)	2.8 ± 1.0 (1 – 5)	27.2 ± 15.5 (8 – 52)
UHDRS - Oculomotor	0.4 ± 0.7 (0 – 2)	1.6 ± 1.1 (0 – 4)	8.4 ± 3.7 (3 – 15)

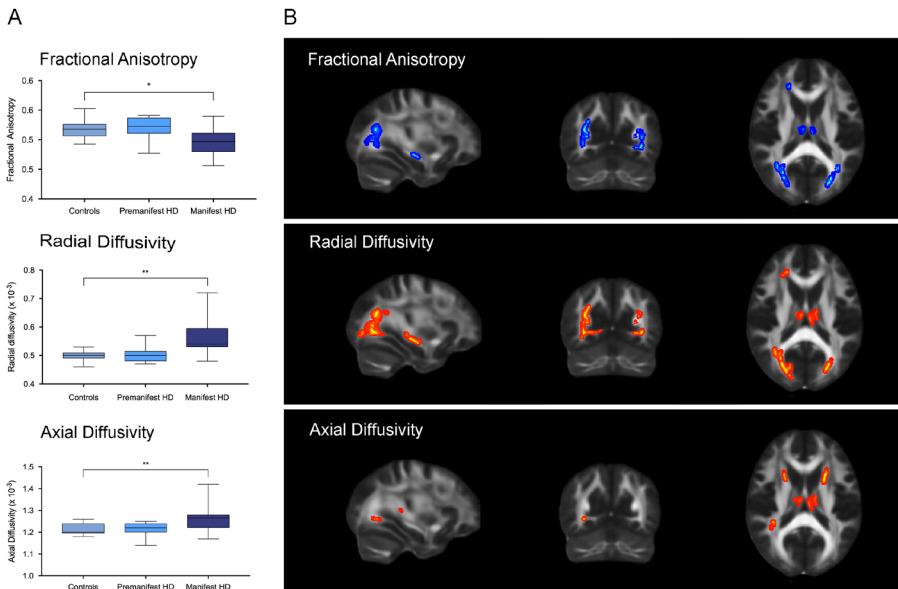
Demographic data are showed (mean ± SD (range), except for gender (numbers)). Disease burden score was calculated with the formula: age x [CAG repeat length – 35.5] by Penney et al., 1997. CAG = cytosine-adenosine-guanine, UHDRS = Unified Huntington's Disease Rating Scale.

TABLE 2 Correlations between diffusion parameters and clinical assessments in HD gene carriers

	Fractional anisotropy			Axial diffusivity			Radial diffusivity		
	R ²	β_{std}	<i>p</i> -value	R ²	β_{std}	<i>p</i> -value	R ²	β_{std}	<i>p</i> -value
UHDRS – Total Motor	0.426	-0.517	0.012	0.374	0.605	0.005	0.534	0.634	0.001
UHDRS – Oculomotor	0.403	-0.486	0.027	0.316	0.501	0.033	0.474	0.535	0.010
Disease burden score	0.484	-0.585	0.001	0.347	0.454	0.012	0.583	0.620	< 0.001

Separate univariate linear regression analyses were performed adjusted for age, gender and HD group (i.e. premanifest and manifest HD). Standardized Beta coefficients (β_{std}) represent the SD change in diffusion parameters per every SD increase in the clinical assessments. As age is already included in the disease burden score (age x [CAG repeat length – 35.5] by Penney et al., 1997), these regression analyses were performed without age as covariate. Significant *p*-values < 0.05 are presented in bold.

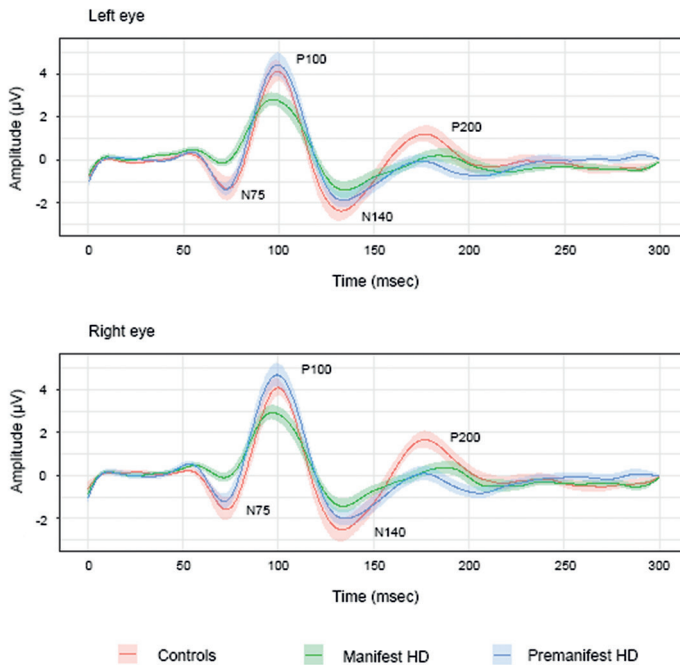
FIGURE 1 Diffusion parameters



Diffusion parameters measured using tract-based spatial statistics (TBSS) analysis showed microstructural changes in manifest HD. A) Fractional anisotropy (FA), radial diffusivity (RD), and axial diffusivity (AD) values within the anterior and posterior thalamic radiation tracts are presented per group. Significant differences between manifest HD and controls are displayed, * *p* < 0.05 and ** *p* ≤ 0.001. B) Voxel-based brain regions that showed significant differences in diffusion parameters between manifest HD and controls. Blue: decreased diffusivity in manifest HD compared to controls. Red: increased diffusivity in manifest HD compared to controls. Age and gender were included as covariates in the statistical model. Regions are overlaid on sagittal, coronal, and transversal slices of a standard FMRIB FA image. A family wise error corrected threshold of *p* < 0.05 was used.

was analyzed, using mean peak latencies and amplitudes of four major pattern-reversal VEP components (Figure 2 and Table 3). Four patients with HD had no recognizable signal due to motion artifacts and were therefore not included in the analyses. Significant lower peak amplitudes of the N75 and P200 components, and reduced N75-P100 peak-to-peak amplitude were found in manifest HD compared to controls ($U = 206, p = 0.011$; $U = 37, p = 0.025$; and $U = 65, p = 0.010$ respectively). In addition, the P200 component was also reduced in premanifest HD compared to controls ($U = 66, p = 0.014$). There were no significant differences between groups in mean peak latencies for any component. In addition, there were no significant associations between N75 and P200 amplitudes and clinical outcome measures (Table 4).

FIGURE 2 Visual evoked potentials



Mean pattern reversal visual evoked potentials per group measured from electrode Oz after left and right eye stimulation separately. In the manifest HD group, four participants had no recognizable signal due to motions artifacts and were not included in further analyses. The four major components, N75, P100, N140, and P200 are displayed, showing significant decreased N75 and P200 amplitudes in manifest HD compared to controls and significant decreased P200 amplitude in premanifest HD compared to controls.

TABLE 3 Mean latencies and amplitudes of pattern-reversal VEP

	Peak latency (msec)				Peak amplitude (mV)				Peak-to-peak amplitude (mV)			
	N75	P100	N140	P200	N75	P100	N140	P200	N75-P100	P100-N140	N140-P200	
Controls	75.2 ± 5.9 (65.3 – 85.4)	99.9 ± 5.7 (86.9 – 110.2)	132.5 ± 6.1 (123.2 – 142.5)	171.6 ± 11.8 (142.4 – 186.3)	-2.3 ± 2.2 (-8.3 – 0.7)	4.7 ± 2.0 (1.5 – 10.5)	-3.1 ± 2.5 (-8.0 – -0.2)	2.3 ± 1.4 (0.5 – 4.2)	7.0 ± 3.4 (1.6 – 14.0)	7.7 ± 3.9 (3.1 – 18.4)	5.5 ± 3.0 (1.5 – 10.4)	
Pre-HD	73.9 ± 4.8 (66.4 – 86.0)	99.2 ± 6.1 (90.1 – 116.0)	134.4 ± 9.8 (121.7 – 158.9)	175.1 ± 14.5 (151.1 – 200.3)	-1.9 ± 1.6 (-4.8 – 1.0)	5.3 ± 2.5 (1.7 – 12.2)	-2.7 ± 1.6 (-5.3 – -0.0)	0.9 ± 1.3 (-2.3 – 3.0)	7.0 ± 3.6 (2.0 – 17.0)	8.1 ± 3.7 (2.9 – 16.6)	3.7 ± 1.7 (1.0 – 6.8)	
Mani-HD	74.3 ± 4.6 (67.1 – 81.3)	101.0 ± 6.8 (90.5 – 112.1)	137.0 ± 10.3 (122.0 – 159.2)	169.2 ± 16.4 (143.4 – 193.8)	-0.7 ± 0.9 (-2.5 – 0.5)	3.9 ± 1.5 (2.2 – 6.9)	-2.4 ± 1.3 (-6.1 – -1.0)	1.1 ± 1.3 (-0.1 – 3.6)	4.5 ± 1.7 (2.1 – 8.5)	6.3 ± 1.8 (4.0 – 9.7)	3.7 ± 2.5 (1.1 – 9.6)	

Neurophysiological data are showed (mean ± SD (range)) measured from electrode Oz. Left and right eyes were averaged for each outcome measure. Significant differences compared to controls are displayed in bold ($p < 0.05$).

TABLE 4 Correlations between visual evoked potentials and clinical assessments in HD gene carriers

	N75 amplitude			P200 amplitude			N75-P100 amplitude		
	R ²	β_{std}	p-value	R ²	β_{std}	p-value	R ²	β_{std}	p-value
UHDRS – Total Motor	0.199	-0.154	0.527	0.256	0.154	0.557	0.191	-0.219	0.345
UHDRS – Oculomotor	0.189	-0.352	0.212	0.246	-0.035	0.896	0.295	-0.290	0.223
Disease burden score	0.159	0.001	0.999	0.163	0.280	0.191	0.209	-0.271	0.165

Separate univariate linear regression analyses were performed adjusted for age, gender and HD group (i.e. premanifest and manifest HD). Standardized Beta coefficients (β_{std}) represent the SD change in amplitude per every SD increase in the clinical assessments. As age is already included in the disease burden score (age x [CAG repeat length – 35.5]) by Penney et al., 1997), these regression analyses were performed without age as covariate.

4. DISCUSSION

This study revealed alterations in structural and functional integrity of the visual pathway in manifest HD compared to controls. Altered microstructure was primarily present in the optic radiations of posterior brain regions and to a lesser extent in the anterior brain regions. In addition, reduced amplitudes with normal latencies were observed in response to visual stimulation using pattern-reversal visual evoked potentials as a measure of functional integrity.

Diffusion markers are thought to reflect the structural integrity of neural tracts in the brain by detecting the extent and coherence of water diffusion.^{25,26} Our diffusion tensor imaging analyses showed reduced axial diffusivity (i.e., axonal degeneration) in manifest HD compared to controls in the anterior limb of the internal capsule in the frontal lobe. In contrast, reduced fractional anisotropy (i.e., overall fiber density) and increased radial diffusivity (i.e. axonal myelination and diameter) were observed more widespread in fibers located in the thalamus and optic radiations in the occipital lobe. Our findings suggest that neurodegeneration of the visual pathway predominantly occurs in fibers that project to the posterior cerebral cortex due to loss of axonal fibers, which is in line with postmortem studies that observed neuronal cell loss and a reduction of axonal connections in the occipital lobe.^{8,9}

Microstructural changes in tracts to the prefrontal cortex, sensorimotor cortex and corpus callosum were found in previous studies that assessed cortico-striatal and deep white matter pathways across the entire brain in patients with HD.²⁷ Diffusivity changes of posterior cerebral tracts have also been found in HD, particularly located in the frontal white matter projections to the occipital lobe.²⁸⁻³⁰ In these studies, however, alterations in the occipital cortex have not been the primary focus of interest.

Although striatal atrophy can be detected in premanifest HD a decade before the onset of motor symptoms,⁵ we did not detect microstructural white matter changes in our group of premanifest HD gene carriers. It is possible that axonal loss in the white matter tracts to the cortex only occurs in manifest disease stages and that microstructural changes during premanifest stages are more variable and dynamic over time.³¹ In contrast, a longitudinal study did observe changes in diffusivity over time in the fronto-occipital tracts in premanifest HD, most prominently in the individuals close to estimated disease onset.²⁸ However, the premanifest HD group in this study already showed motor symptoms, suggesting that the distinction between manifest and premanifest was based on different criteria than our study, making direct comparisons difficult.

We additionally examined correlations between clinical functional assessments and diffusion outcome measures. The strongest association was found between disease burden score and radial diffusivity, indicating that higher disease severity is correlated with increased axonal fiber loss. This finding suggests that diffusion measurements within the visual pathway can be used as a marker of disease severity.

While diffusion markers reflect the structural integrity of white matter tracts, visual-evoked potentials are frequently used to measure the functional integrity of the retinal-cortical pathway. The neural generators of the main components of the evoked potential wave (before 150 milliseconds) are considered to originate in the primary visual cortex, while late components (after 150 milliseconds) reflect activity in the associative occipital and parietal cortical areas.³² In our study, normal latencies of both main and late components were observed in HD gene carriers, which imply preserved pre-chiasmatic function and normal conduction velocities to the primary cortex in early disease stages, since prolonged latencies are generally found in demyelination disorders.³³ We did observe reduced amplitudes for both main and late components (N75 and P200 respectively) in manifest HD compared to controls. Therefore, in addition to our findings of altered structural integrity, we provide evidence of changed functional integrity in the optic tracts in patients with HD as well. There are no previous studies that examined both visual-evoked potentials and microstructural brain changes of the visual pathway in HD. In line with our findings, several previous neurophysiological studies also reported reduced amplitudes in HD patients with normal latencies of the main components in response to light flashes or checkerboard pattern-reversal stimulation.^{34–37} Other pattern-reversal VEP studies, however, report no significant differences in both amplitudes and latencies of the main components in manifest HD compared to controls.^{38,39} Nonetheless, these studies were conducted before genetic testing became available and different criteria were used to define patients with HD. Recent neurophysiological studies focused on the late components to investigate higher level visual processing using more challenging visual processing tasks, such as a word recognition task,⁴⁰ attentional categorization tasks,^{41,42} or a facial emotion expression task.³⁷ These studies all found reduced amplitudes for late components.^{37,41,42} Since reduced main component amplitudes are frequently reported in manifest HD, it is hypothesized that early visual processing is already impaired, thus making subsequent visual processing more difficult.³⁷ We did observe reduced amplitudes in main and late components in manifest HD, but future studies with a larger sample size and different stimulation types could elucidate this hypothesis more thoroughly.

In our study, reduced amplitudes in premanifest HD gene carriers were additionally observed for the late component (P200). Only two other studies assessed the response to visual-evoked potentials in premanifest HD gene carriers, before the onset of overt motor symptoms.^{41,42} One study also observed reduced amplitudes of the late component in premanifest HD in response to a visual attentional processing task, while another study did not find neurophysiological impairments in early perceptual processing in premanifest HD.^{41,42} As the latter study involved more complex stimulation tasks, a direct comparison to our pattern-reversal VEP is not possible.

We did not observe a significant relationship between neurophysiological measures and clinical assessments in HD gene carriers, possibly because of the heterogeneity seen in the waveforms of all participants or the effects of gender and age on evoked-potential components.⁴³ To address the issue of heterogeneity of VEP responses, longitudinal studies could be performed with larger sample sizes to measure individual change over time as a marker for disease progression.

This study examined the microstructure of regional white matter tracts of the visual pathway and the response on pattern-reversal visual-evoked potentials in premanifest and manifest HD gene carriers.

In conclusion, changes in structural integrity were most prominently present in the thalamus and optic radiations in early manifest HD, and were associated with functional scores, such as disease burden and oculomotor scores, suggesting that microstructural changes in the optic tracts are related with clinical disease severity. In addition, reduced amplitudes with normal latencies were observed in response to visual stimulation in manifest HD patients.

Our findings show that the posterior brain regions undergo structural alterations in early stages of the neuropathological process in HD. These data provide more knowledge on the pathophysiological processes in the cerebral cortex and might aid in the identification of other regions than the striatum that can be used as a potential marker of disease severity for future clinical trials.

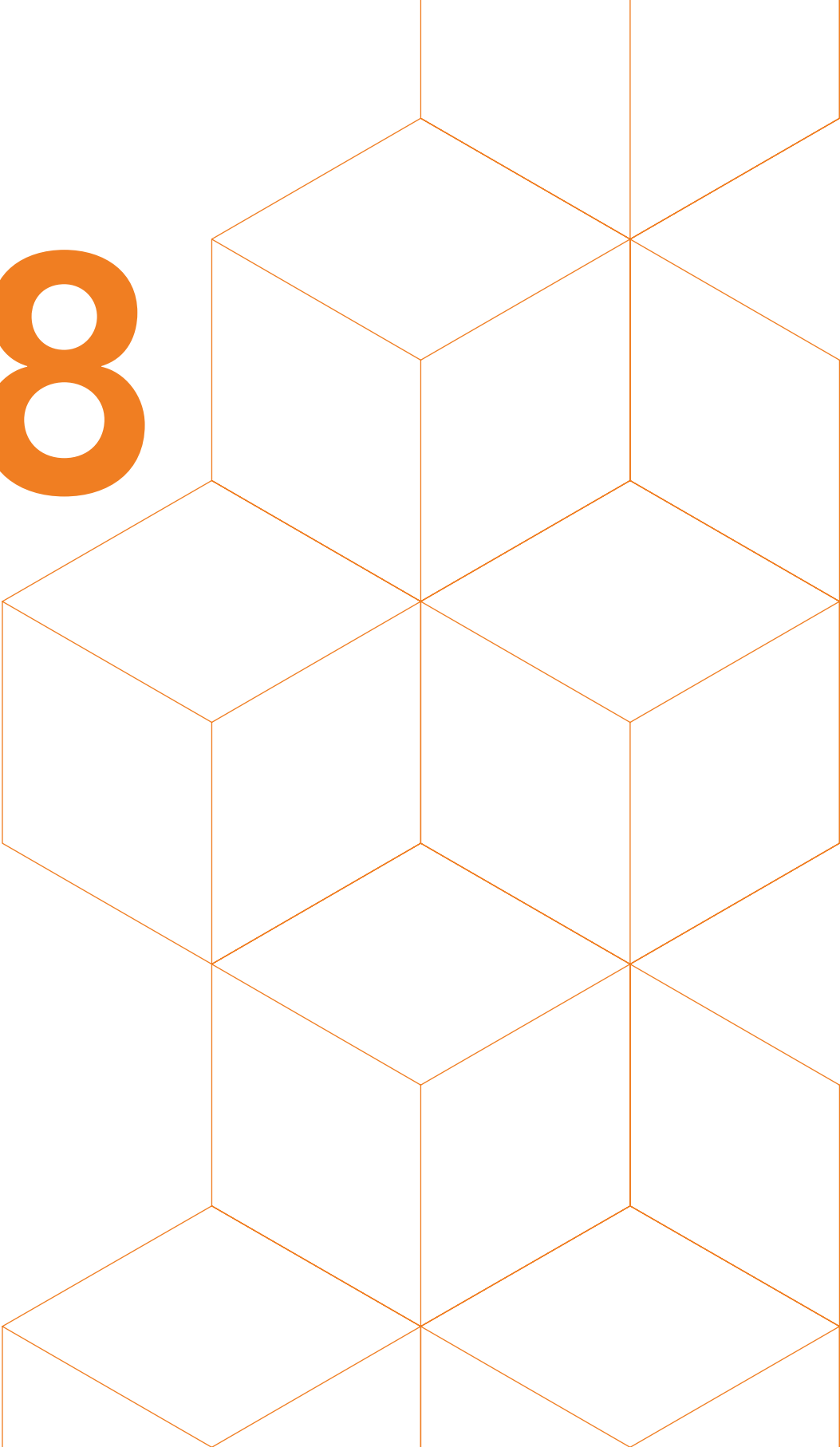
REFERENCES

1. Bates GP, Dorsey R, Gusella JF, et al. Huntington disease. *Nat Rev Dis Prim*. 2015;1:1-21.
2. The Huntington's Disease Collaborative Research Group. A novel gene containing a trinucleotide repeat that is expanded and unstable on Huntington's disease chromosomes. *Cell*. 1993;72(6):971-983.
3. Vonsattel JP, Myers RH, Stevens TJ, Ferrante RJ, Bird ED, Richardson EP. Neuropathological classification of Huntington's disease. *J Neuropathol Exp Neurol*. 1985;44(6):559-577.
4. Reiner A, Albin RL, Anderson KD, D'Amato CJ, Penney JB, Young AB. Differential loss of striatal projection neurons in Huntington disease. *Proc Natl Acad Sci U S A*. 1988;85(15):5733-5737.
5. Aylward E, Sparks B, Field K, et al. Onset and rate of striatal atrophy in preclinical Huntington disease. *Neurology*. 2004;63:66-72.
6. Tabrizi SJ, Scahill RI, Owen G, et al. Predictors of phenotypic progression and disease onset in premanifest and early-stage Huntington's disease in the TRACK-HD study: Analysis of 36-month observational data. *Lancet Neurol*. 2013;12(7):637-649.
7. Coppens EM, van der Grond J, Hart EP, Lakke EAJF, Roos RAC. The visual cortex and visual cognition in Huntington's disease: An overview of current literature. *Behav Brain Res*. 2018;351:63-74.
8. Rüb U, Seidel K, Vonsattel JP, et al. Huntington's disease (HD): Neurodegeneration of Brodmann's primary visual area 17 (BA17). *Brain Pathol*. 2015;25(6):701-711.
9. Nana AL, Kim EH, Thu DCV, et al. Widespread heterogeneous neuronal loss across the cerebral cortex in Huntington's disease. *J Huntingtons Dis*. 2014;3:45-64.
10. Lange H. Quantitative changes of telencephalon, diencephalon, and mesencephalon in Huntington's chorea, postencephalitic, and idiopathic parkinsonism. *Verh Anat Ges*. 1981;75:923-925.
11. Johnson EB, Rees EM, Labuschagne I, et al. The impact of occipital lobe cortical thickness on cognitive task performance: An investigation in Huntington's Disease. *Neuropsychologia*. 2015;79:138-146.
12. Coppens EM, Jacobs M, van den Berg-huysmans AA, van der Grond J, Roos RAC. Grey matter volume loss is associated with specific clinical motor signs in Huntington's disease. *Park Relat Disord*. 2018;46:56-61.
13. Tabrizi SJ, Langbehn DR, Leavitt BR, et al. Biological and clinical manifestations of Huntington's disease in the longitudinal TRACK-HD study: cross-sectional analysis of baseline data. *Lancet Neurol*. 2009;8(9):791-801.

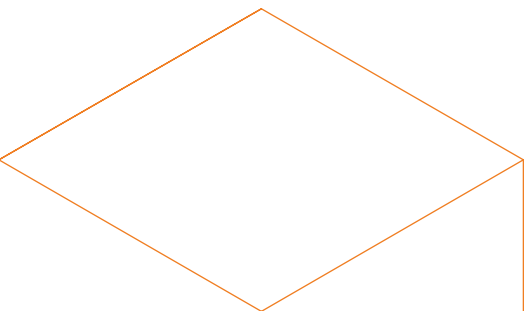
14. Coppen EM, van der Grond J, Hafkemeijer A, Rombouts SARB, Roos RAC. Early grey matter changes in structural covariance networks in Huntington's disease. *NeuroImage Clin.* 2016;12:806-814.
15. Rosas HD, Salat DH, Lee SY, et al. Cerebral cortex and the clinical expression of Huntington's disease: complexity and heterogeneity. *Brain.* 2008;131(4):1057-1068.
16. Huntington Study Group. Unified Huntington's disease rating scale: reliability and consistency. *Mov Disord.* 1996;11(2):136-142.
17. Marder K, Zhao H, Myers RH, et al. Rate of functional decline in Huntington's disease. *Neurology.* 2000;54:452-458.
18. Penney J, Vonsattel JP, MacDonald ME, Gusella JF, Myers RH. CAG repeat number governs the development rate of pathology in Huntington's disease. *Ann Neurol.* 1997;41(5):689-692.
19. Smith SM, Jenkinson M, Woolrich MW, et al. Advances in functional and structural MR image analysis and implementation as FSL. *Neuroimage.* 2004;23:S208-S219.
20. Behrens TEJ, Woolrich MW, Jenkinson M, et al. Characterization and propagation of uncertainty in diffusion-weighted MR imaging. *Magn Reson Med.* 2003;50(5):1077-1088.
21. Smith SM, Jenkinson M, Johansen-Berg H, et al. Tract-based spatial statistics: voxelwise analysis of multi-subject diffusion data. *Neuroimage.* 2006;31(4):1487-1505.
22. Vernon Odom J, Bach M, Brigell M, et al. ISCEV standard for clinical visual evoked potentials: (2016 update). *Doc Ophthalmol.* 2016;133:1-9.
23. Winkler AM, Ridgway GR, Webster MA, Smith SM, Nichols TE. Permutation inference for the general linear model. *Neuroimage.* 2014;92:381-397.
24. Smith SM, Nichols TE. Threshold-free cluster enhancement: addressing problems of smoothing, threshold dependence and localisation in cluster inference. *Neuroimage.* 2009;44(1):83-98.
25. Rees EM, Scahill RI, Hobbs NZ. Longitudinal neuroimaging biomarkers in Huntington's disease. *J Huntingtons Dis.* 2013;2:21-39.
26. Alexander AL, Lee JE, Lazar M, Field AS. Diffusion Tensor Imaging of the Brain. *Neurotherapeutics.* 2007;4(3):316-329.
27. Liu W, Yang J, Burgunder JM, Cheng B, Shang H. Diffusion imaging studies of Huntington's disease: A meta-analysis. *Park Relat Disord.* 2016;32:94-101.
28. Harrington DL, Long JD, Durgerian S, et al. Cross-sectional and longitudinal multimodal structural imaging in prodromal Huntington's disease. *Mov Disord.* 2016;31(11):1664-1675.
29. Matsui JT, Vaidya JG, Wassermann D, et al. Prefrontal cortex white matter tracts in prodromal Huntington disease. *Hum Brain Mapp.* 2015;36(10):3717-3732.
30. Faria AV, Ratnanather JT, Tward DJ, et al. Linking white matter and deep gray matter alterations in premanifest Huntington disease. *NeuroImage Clin.* 2016;11:450-460.
31. Poudel GR, Stout JC, Domínguez D. JF, et al. Longitudinal change in white matter microstructure in Huntington's disease: The IMAGE-HD study. *Neurobiol Dis.* 2015;74:406-412.

32. Di Russo F, Pitzalis S, Spitoni G, et al. Identification of the neural sources of the pattern-reversal VEP. *Neuroimage*. 2005;24(3):874-886.
33. Breceelj J. Visual electrophysiology in the clinical evaluation of optic neuritis, chiasmal tumours, achiasmia, and ocular albinism: an overview. *Doc Ophthalmol*. 2014;129:71-84.
34. Ellenberger C, Petro DJ, Ziegler SB. The visually evoked potential in Huntington Disease. *Neurology*. 1978;28:95-97.
35. Josiassen R, Shagass C, Mancall E, Roemer R. Auditory and visual evoked potentials in Huntington's disease. *Electroencephalogr Clin Neurophysiol*. 1984;57:113-118.
36. Oepen G, Doerr M, Thoden U. Visual (VEP) and somatosensory (SSEP) evoked potentials in Huntington's chorea. *Electroencephalogr Clin Neurophysiol*. 1981;51:666-670.
37. Croft RJ, McKernan F, Gray M, Churchyard A, Georgiou-Karistianis N. Emotion perception and electrophysiological correlates in Huntington's disease. *Clin Neurophysiol*. 2014;125(8):1618-1625.
38. Ehle AL, Stewart RM, Lellelid NA, Leventhal NA. Evoked potentials in Huntington's disease. A comparative and longitudinal study. *Arch Neurol*. 1984;41(4):379-382.
39. Rosenberg C, Nudleman K, Starr A. Cognitive evoked potentials (P300) in early Huntington's disease. *Arch Neurol*. 1985;42(10):984-987.
40. Munte TF, Ridao-Alonso ME, Preinfalk J, et al. An electrophysiological analysis of altered cognitive functions in Huntington Disease. *Arch Neurol*. 1997;54:1089-1098.
41. Antal A, Beniczky S, Kincses TZ, Jakab K, Benedek G, Vecsei L. Perceptual categorization is impaired in Huntington's disease: An electrophysiological study. *Dement Geriatr Cogn Disord*. 2003;16(4):187-192.
42. Beste C, Saft C, Andrich J, Gold R, Falkenstein M. Stimulus-response compatibility in Huntington's disease: A cognitive-neurophysiological analysis. *J Neurophysiol*. 2008;99:1213-1223.
43. de Freitas Dotto P, Berezovsky A, Sacai PY, Rocha DM, Salomão SR. Gender-based normative values for pattern-reversal and flash visually evoked potentials under binocular and monocular stimulation in healthy adults. *Doc Ophthalmol*. 2017;135:53-67.

8



Summary, discussion and future perspectives



Although promising disease-modifying drugs are currently under investigation, there are unfortunately no effective treatment options available to date to delay or prevent the clinical onset of Huntington's disease (HD). Therefore, more knowledge about the pathophysiologic mechanisms in HD is still needed. Magnetic Resonance Imaging (MRI) is a non-invasive and objective approach to study the human brain. In the last decades, the increased use of brain imaging in HD research made it possible to better understand the natural course of the disease. MRI research in HD has been particularly focused on evaluating the onset and rate of striatal atrophy but the contribution of cortical changes remains less understood.

The aim of this thesis was therefore to investigate alterations in the cerebral cortex in HD gene carriers and assess the relationships with clinical signs of HD. Neuroimaging, neurophysiological, and cognitive measurements were used to examine structure and function of the cerebral cortex in premanifest and early manifest HD gene carriers. In this chapter, the main findings described in this thesis are summarized, discussed and recommendations for future research are provided.

SUMMARY

Brain structure

Macrostructural changes of the cerebral cortex are generally examined with volumetric MRI using different methodological techniques. Voxel-based morphometry (VBM) analysis is such a neuroimaging technique that is frequently used in brain research.^{1,2} VBM involves a voxel-by-voxel comparison of the local grey matter density across the entire brain between different groups, therefore making it a sensitive approach to detect disease-specific cortical changes in regional volume.¹

VBM analysis in our cohort of 79 early manifest HD gene carriers and 30 healthy controls showed that grey matter volume loss in HD is located in the sensorimotor cortex in the frontal and parietal lobes, and the associative visual cortices in the temporal and occipital lobes (**chapter 2**). In a smaller cohort of manifest HD gene carriers, consistent grey matter volume reductions were described in the sensorimotor and lateral occipital cortices (**chapter 3**). On the contrary, premanifest HD gene carriers only showed limited volume changes compared to controls in a small region involving the insular cortex and parietal operculum, near the sensorimotor cortex (**chapter 3**), which is consistent with previous studies.^{3,4} The findings from our studies suggest that there is an decrease in cortical volume somewhere during or close after clinical disease onset, however, future longitudinal analysis is warranted to investigate this hypothesis.

Voxel-based methods measure densities per voxel separately within a brain region. Opposed to this technique, network-based analysis provides information about inter-regional changes in grey matter voxels.⁵ Structural covariance networks of spatially independent grey matter regions were identified based on the co-variation of grey matter using independent component analysis (**chapter 3**). This technique is commonly used in resting-state functional MRI (fMRI) studies to assess functional connectivity.⁶ When used on volumetric MRI, this technique defines spatial components based on the co-variation of grey matter patterns among an entire cohort, which can be expressed in a network integrity score.⁶ Network integrity is described as the strength of an individuals' expression in an anatomical network and indirectly provides information regarding network-based grey matter alterations.

Structural covariance networks involving the precuneus, anterior cingulate, sensorimotor and parahippocampal cortices showed reductions in network integrity for both premanifest and manifest HD compared to controls (**chapter 3**). This indicates that this novel technique is sensitive to detect early grey matter changes in the cerebral cortex. The affected regions are generally involved in the planning, control, and execution of voluntary movements, visuospatial processing, and cognitive attention and control.^{7,8} Domains that were all impaired in manifest HD (**chapter 3, 5, and 6**). However, since the grey matter changes were already found in premanifest HD gene carriers, our results suggest that cortical changes occur prior to clinical disease onset, in addition to striatal atrophy.⁹

Interestingly, another network comprising of the cuneus, lateral occipital cortex and lingual gyrus only showed decreased network integrity in manifest HD and not in premanifest HD (**chapter 3**), which indicates that there is an increase in cortical alterations from the premanifest phase to the manifest phase, in particular in the posterior cerebral cortex (**chapter 5**).

Subtle local volumetric differences between groups might not be detected when assessing global volumes. Measuring the thickness of the cortex with an automated method that parcellates the gyri and sulci into many small distinct regions is a frequently used method to distinguish subtle group differences.^{10,11}

Rosas et al. were the first that used this technique in a small cohort of HD gene carriers to evaluate the degree of cortical thinning and reported that the earliest and most severely affected regions in HD are the primary motor, sensory, and visual cortical regions (including the superior parietal and frontal cortices).^{12,13} We conducted a study in 74 HD patients in early disease stages (HD stage 1 and 2) and observed cortical thinning throughout the entire brain in HD stage 2 patients, with most severe thinning

in the parietal and occipital lobes (**chapter 4**). Our findings are therefore consistent with previous studies reporting relative sparing of the frontal and parietal brain regions early in the disease.^{10,13,14} Still, in our study, HD patients in the most early clinical disease stage (HD stage 1) only showed a trend towards thinning of parietal and occipital cortices, while extensive striatal atrophy was observed in both disease stages, with up to 35% volume loss of the caudate nucleus. This implies that the rate of striatal atrophy stabilizes after clinical disease onset, whereas the degree of cortical atrophy increases. More interestingly, no associations were found between cortical thinning and striatal volume loss, suggesting that striatal and cortical degeneration might occur as two separate neurodegenerative processes (**chapter 4**).

To better understand the extent of neurodegeneration in the posterior cerebral cortex, we conducted a cross-sectional observational study with the visual cortex as region of interest. Volumetric MRI was performed to examine macrostructural alterations of the visual cortex (**chapter 6**) and diffusion tensor imaging (DTI) was used to assess the microstructure of pathways towards the visual cortex (**chapter 7**). Microstructural characteristics of fiber tracts in the brain can generally be examined based on the diffusion properties of water molecules in tissues.¹⁵ It is proposed that changes in diffusion parameters in HD can be explained by axonal degeneration or demyelination,¹⁶ although the specific cellular mechanism remains unclear.

Measurement of diffusion parameters along the anterior and posterior thalamic radiation tracts in manifest HD gene carriers showed signs of axonal fiber loss in the thalamus and optic radiation tract in the occipital lobe, and to a lesser degree in anterior fiber tracts in the frontal lobe (**chapter 7**). Remarkably, volumetric analysis of visual cortical regions showed reduced volumes and cortical thinning in the associative visual cortex, while the primary visual cortex did not show signs of atrophy (**chapter 6**). This latter finding is consistent with previous studies that report early involvement of associative visual brain regions, such as the fusiform gyrus, lingual gyrus, lateral occipital cortex, and cuneus in manifest HD gene carriers (**chapter 5**). Premanifest HD gene carriers, however, did not show any macro- or microstructural alterations in the posterior cerebral cortex (**chapter 6 and 7**), again suggesting that neurodegenerative changes in the posterior brain regions occur after clinical disease onset.

Brain function

The structural imaging analyses described in this thesis showed that the posterior cerebral cortex is affected in early manifest stages. Besides brain structure, we examined brain function in premanifest and manifest HD gene carriers compared to healthy controls (**chapter 6**).

In general, brain function can be measured using the different magnetic properties of oxygenated and deoxygenated blood. Activated neurons demand an increased use of energy leading to an increased blood flow in the surrounding microvasculature, which results in higher levels of oxygenated hemoglobin.¹⁷ The change in oxygenated and deoxygenated blood levels causes alterations in MRI signal intensity, which is referred to as the Blood Oxygenation Level Dependent (BOLD) signal. Therefore, this regional hemodynamic response indirectly reflects neuronal activity in response to a task or stimulus, or at rest when measuring spontaneous fluctuations in the BOLD signal within predefined resting-state networks.^{17,18} After visual stimulation using a black-and-white checkerboard stimulus, neuronal activity of the primary visual cortex was not different in premanifest and manifest HD gene carriers compared to controls (**chapter 6**). However, decreased functional connectivity at rest was present in the associative visual cortex (primarily the lingual and fusiform gyri) in manifest HD gene carriers. Our findings indicate preserved basic visual processing function and altered brain function in regions involved in higher level visual processing.

Besides the fact that we did not find structural changes of the posterior cerebral cortex in premanifest HD gene carriers, brain function also remained unaffected in this disease stage (**chapter 6**), supporting our suggestion that alterations (both structurally and functionally) in the posterior cerebral cortex only occur in the manifest disease stage.

Another approach to examine brain function is measurement of pattern-reversal visual-evoked potentials (VEP). A VEP comprises of a high contrast black-and-white checkerboard that is used as visual stimulus and the neurophysiological evoked signal is recorded with electrodes spanning the occipital region. Amplitudes (height) and latencies (length) of early components (waves) are usually considered to originate in the primary visual cortex, while late responses are thought to reflect brain activity in the associative visual cortical areas.¹⁹

Normal latencies were observed in premanifest and manifest HD gene carriers, indicating a preserved pre-chiasmatic function and normal conduction velocities towards and in the primary visual cortex (**chapter 7**). The reduced amplitudes that were found in HD gene carriers could suggest that axonal loss in the visual pathways due to neurodegeneration causes a reduction in signal intensity. However, we did not observe a relationship between the evoked potential measurements and clinical assessments in HD gene carriers, which might be explained by the heterogeneity in waveforms that is commonly seen due to the effects of age and gender.²⁰

Clinical features

The clinical diagnosis of HD is based on the presence of motor symptoms which are measured using the total motor score of the Unified Huntington's Disease Rating Scale.²¹ For this scale, motor symptoms can be divided in separate domains such as chorea, dystonia, gait disturbances, rigidity, and oculomotor dysfunction, with higher scores indicating more dysfunction.^{21,22}

We related the clinical motor phenotype of 79 manifest HD gene carriers to changes in grey matter brain regions (**chapter 2**). Higher chorea scores were associated with volume loss of the striatum and pallidum, whereas higher eye movement scores were related with cortical volume loss in occipital regions. The lack of relationships between other motor symptoms, such as dystonia and gait disturbances, and changes in subcortical or cortical volumes can be explained by the fact that this cohort of early manifest HD gene carriers scored relatively low on these items. This is not unexpected, since dystonia, hypokinesia and related balance problems are often seen in more advanced stages and our cohort consisted of early stage manifest HD gene carriers.^{22,23} Increased motor symptoms in HD gene carriers were also associated with reduced network integrity scores in the structural covariance network comprising of the striatum, precuneus, and anterior cingulate cortex (**chapter 3**), regions that are known to be involved in motor planning and execution.⁸

Besides motor symptoms are visual processing deficits also frequently reported in HD.²⁴⁻²⁶ A review of the current literature showed that impairments are present in several visual cognitive domains, such as visual object perception, facial emotion recognition, visuospatial processing, and working memory, while visual hallucinations and ophthalmic disorders are rarely described in HD (**chapter 5**). Studies have unfortunately used heterogeneous cognitive test batteries to measure visual cognitive function, making direct comparisons between study findings difficult.

In our study, we used specific cognitive tasks with a large visual component that have been used previously and observed impaired visual object perception and visuospatial function in manifest HD gene carriers (**chapter 6**). However, only worse performance on visual perceptual tasks was related with reduced cortical thickness of parieto-occipital brain regions. These visual perceptual tasks required minimal motor involvement and processing speed, which implies that these tasks are a sensitive assessment of visual cognitive function.

CONCLUSIONS

This thesis provides evidence for distinct changes in cortical brain structure and brain function in early symptomatic HD disease stages. Although striatal atrophy is more extensively present in HD, changes in the cerebral cortex can also be detected in the pre-symptomatic stage. Different methodological approaches used in our studies all showed a consistent pattern of cortical atrophy making volumetric MRI a reliable and effective tool to assess early *in-vivo* cortical brain changes, even in a rare neurodegenerative disorder such as HD. Voxel-based morphometry analyses, structural covariance network analysis, and cortical thickness analyses all revealed signs of cortical atrophy in manifest HD gene carriers located in the precuneous, sensorimotor cortex, secondary and associative visual cortex, and anterior cingulate cortex. In premanifest HD gene carriers, cortical atrophy was limited to the precuneous and sensorimotor cortex. It seems that striatal volume loss stabilizes after clinical disease onset, whereas cortical atrophy becomes more pronounced. Our findings additionally imply that cortical atrophy occurs simultaneous with the onset of striatal atrophy as an independent neurodegenerative process, since the presence of cortical thinning in HD gene carriers was not related with striatal volume loss, and cortical changes were already observed in premanifest HD gene carriers close to estimated disease onset. Still, cortical changes seem to be limited to the sensorimotor areas in premanifest HD, whereas manifest HD gene carriers showed more widespread cortical alterations, with the posterior cerebral cortex as main affected brain region.

The findings of this thesis further suggest that cortical degeneration plays an important role in the presence of clinical features of HD, such as oculomotor dysfunction and visual cognitive processing deficits, while the severity of chorea, the most recognized clinical symptom in HD, is related to striatal volume loss.

We additionally examined brain function in HD using functional neuroimaging and neuro-physiological measurements, which showed that basic visual function remains preserved, even in manifest disease stages. The associative visual cortex did show changes in brain activity at rest in manifest HD gene carriers, which is consistent with our findings of impaired higher level visual cognitive functioning. The structural and functional neurodegenerative changes of the posterior cerebral cortex seems to originate in the associative visual cortices in the parietal, temporal and occipital lobes, with sparing of the primary visual cortex in the early manifest stages. Nevertheless, functional alterations of the higher-level visual cortex appear to be less pronounced and widespread than structural changes, which even extend to the inferior temporal and superior parietal cortices. Based on these findings, we can therefore conclude that structural cortical alterations contribute to the clinical signs of HD and likely precede functional brain changes in early HD.

IMPLICATIONS AND FUTURE PERSPECTIVES

Striatal atrophy is the hallmark of the disease and is linked to main clinical features of HD such as choreiform movements. Indeed, extensive volume loss was observed early in the disease, but the influence of cortical changes on other clinical signs that occur in HD should not be overlooked.

Our results demonstrate that volume loss and thinning of the cerebral cortex, especially the posterior brain regions, is detectable in early manifest stages and contributes to the presence of specific motor signs and cognitive impairments. We believe that clinical intervention trials could therefore benefit from using cortical volumes as outcome measures to assess treatment efficacy or disease progression, instead of using striatal volumes as outcome measure alone.

We described deficits in several visual cognitive domains, such as visual perceptual dysfunction and an impaired visual scanning and attention. The awareness of visual stimuli and processing of visual information is important because it is needed in daily life, for example when driving a car, during walking and in communication with others. Moreover, visual perceptual deficits might negatively impact complex cognitive task performance. While these higher-level visual processing deficits in HD are not well-recognized clinical signs of HD, it is remarkable that early involvement of the cerebral cortex seems to originate in the associative visual cortices, the regions that are generally involved in higher-level processing.

This thesis focused on the pattern of cortical changes in HD and the relation with motor and cognitive symptoms. Still, it is also important to investigate the underlying brain changes of behavioral symptoms. There are only limited studies available that assessed the neuronal correlates of behavioral changes in HD,^{27,28} which is surprising since irritability, apathy, and mood disturbances are frequently reported signs in HD.²⁹ The presence of apathy in HD seems to be related to atrophy of the thalamus,²⁷ while depressive symptoms were associated with smaller volumes of the cingulate cortex.²⁸

Novel disease-modifying therapeutic agents, such as huntingtin lowering drugs, are currently under development and could be promising for the treatment of HD. The study design of large multicenter longitudinal clinical trials that examine the efficacy of such drugs should therefore make use of structural and functional MRI for the assessment of both subcortical and cortical structure and function. In addition, an extensive cognitive test battery including visual cognitive tasks can be used to measure improvement of cognitive functioning. We recommend including visual cognitive tasks that are independent of other cognitive or motor processes, such as the Visual Object

and Space Perception (VOSP) tasks, in the standard cognitive battery.

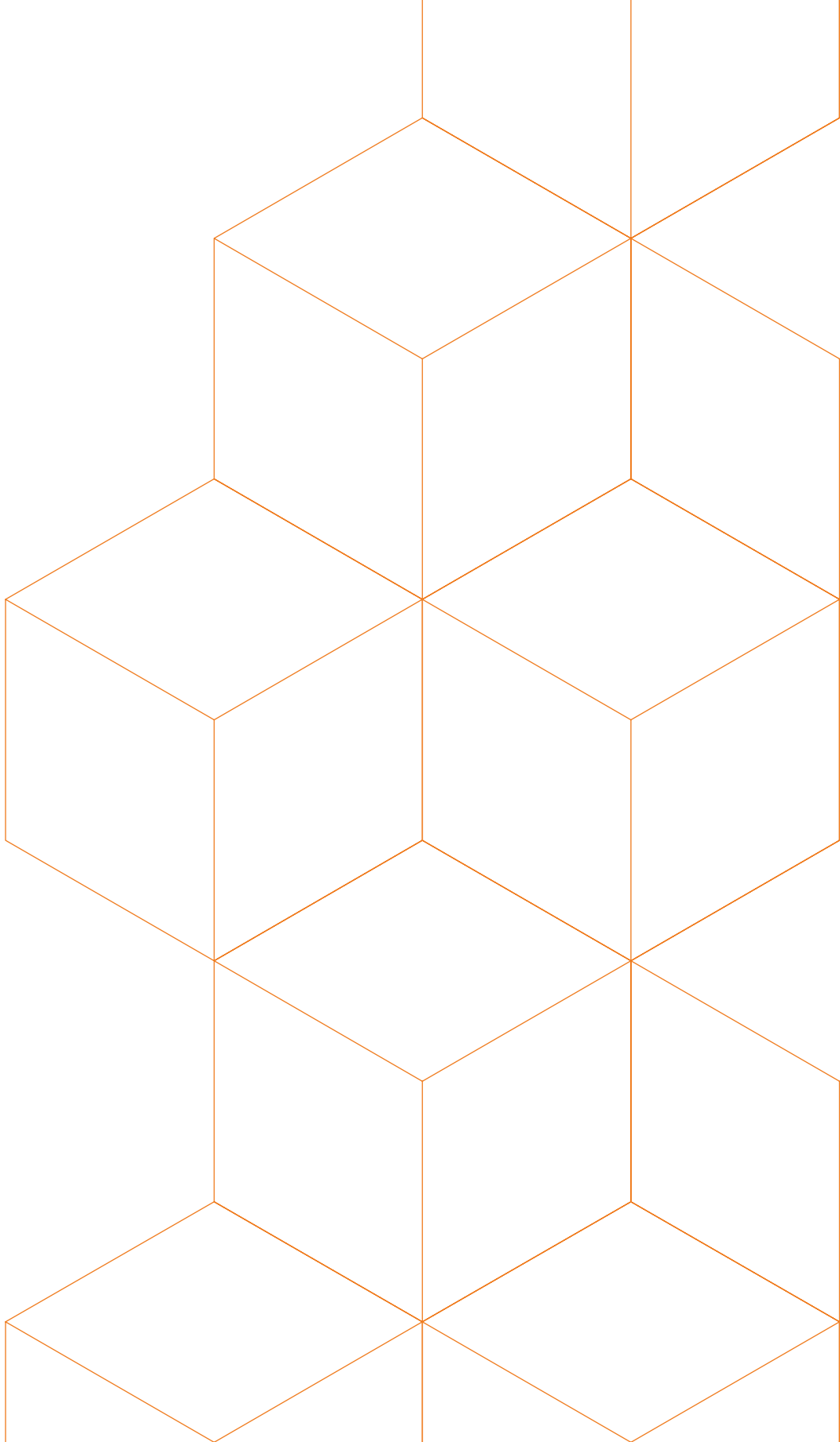
Since atrophy of the posterior cerebral cortex, and in particular the visual cortex, seems to occur early in the disease, we also suggest to include volumetric assessments of the visual cortex as outcome measure in clinical intervention trials, in addition to the more standard measurements of striatal volume.

Future observational studies are continuously necessary to better understand the pathophysiologic mechanisms of the disease and the relationship with clinical signs. For a better understanding of brain function in HD, and in particular to further investigate impairments in higher-level visual processing, functional MRI using more complex visual processing tasks should be performed in future trials. In addition, it would be interesting to examine simultaneous recordings of visual-evoked potentials with functional MRI for high temporal and spatial resolution.^{30,31} This way, the neural correlates of the evoked response can be better interpreted, which provides more information about functional brain changes in the posterior cerebral cortex in HD. Especially large groups of premanifest HD gene carriers (divided based on the estimated time to clinical diagnosis) should be observed over time, since this group can have considerable benefit from disease-modifying drugs.

REFERENCES

1. Ashburner J, Friston KJ. Voxel-Based Morphometry—The Methods. *Neuroimage*. 2000;11(6):805-821.
2. Kurth F, Luders E, Gaser C. Voxel-Based Morphometry. *Brain Mapp An Encycl Ref*. 2015;1:345-349.
3. Hobbs NZ, Henley SMD, Ridgway GR, et al. The progression of regional atrophy in premanifest and early Huntington's disease: a longitudinal voxel-based morphometry study. *J Neurol Neurosurg Psychiatry*. 2010;81(7):756-763.
4. Gómez-Ansón B, Alegret M, Muñoz E, et al. Prefrontal cortex volume reduction on MRI in preclinical Huntington's disease relates to visuomotor performance and CAG number. *Park Relat Disord*. 2009;15(3):213-219.
5. Evans AC. Networks of anatomical covariance. *Neuroimage*. 2013;80:489-504.
6. Hafkemeijer A, Möller C, Dopfer EGP, et al. Differences in structural covariance brain networks between behavioral variant frontotemporal dementia and Alzheimer's disease. *Hum Brain Mapp*. 2016;988:978-988.
7. Cavanna AE, Trimble MR. The precuneus: a review of its functional anatomy and behavioural correlates. *Brain*. 2006;129(3):564-583.
8. Wenderoth N, Debaere F, Sunaert S, Swinnen SP. The role of anterior cingulate cortex and precuneus in the coordination of motor behaviour. *Eur J Neurosci*. 2005;22(1):235-246.
9. Aylward E, Sparks B, Field K, et al. Onset and rate of striatal atrophy in preclinical Huntington disease. *Neurology*. 2004;63:66-72.
10. Nopoulos PC, Aylward EH, Ross CA, et al. Cerebral cortex structure in prodromal Huntington disease. *Neurobiol Dis*. 2010;40(3):544-554.
11. Fischl B, Dale AM. Measuring the thickness of the human cerebral cortex from magnetic resonance images. *Proc Natl Acad Sci U S A*. 2000;97(20):11050-11055.
12. Rosas HD, Liu AK, Hersch S, et al. Regional and progressive thinning of the cortical ribbon in Huntington's disease. *Neurology*. 2002;58(5):695-701.
13. Rosas HD, Salat DH, Lee SY, et al. Cerebral cortex and the clinical expression of Huntington's disease: complexity and heterogeneity. *Brain*. 2008;131(4):1057-1068.
14. Tabrizi SJ, Langbehn DR, Leavitt BR, et al. Biological and clinical manifestations of Huntington's disease in the longitudinal TRACK-HD study: cross-sectional analysis of baseline data. *Lancet Neurol*. 2009;8(9):791-801.
15. Alexander AL, Lee JE, Lazar M, Field AS. Diffusion Tensor Imaging of the Brain. *Neurotherapeutics*. 2007;4(3):316-329.

16. Poudel GR, Stout JC, Domínguez D. JF, et al. Longitudinal change in white matter microstructure in Huntington's disease: The IMAGE-HD study. *Neurobiol Dis.* 2015;74:406-412. doi:10.1016/j.nbd.2014.12.009.
17. Norris DG. Principles of magnetic resonance assessment of brain function. *J Magn Reson Imaging.* 2006;23:794-807.
18. Beckmann CF, DeLuca M, Devlin JT, Smith SM. Investigations into resting-state connectivity using independent component analysis. *Philos Trans R Soc.* 2005;360:1001-1013.
19. Di Russo F, Pitzalis S, Spitoni G, et al. Identification of the neural sources of the pattern-reversal VEP. *Neuroimage.* 2005;24(3):874-886.
20. de Freitas Dotto P, Berezovsky A, Sacai PY, Rocha DM, Salomão SR. Gender-based normative values for pattern-reversal and flash visually evoked potentials under binocular and monocular stimulation in healthy adults. *Doc Ophthalmol.* 2017;135:53-67.
21. Huntington Study Group. Unified Huntington's disease rating scale: reliability and consistency. *Mov Disord.* 1996;11(2):136-142.
22. Jacobs M, Hart EP, van Zwet EW, et al. Progression of motor subtypes in Huntington's disease: a 6-year follow-up study. *J Neurol.* 2016;263(10):2080-2085.
23. Roos RAC. Huntington's disease: a clinical review. *Orphanet J Rare Dis.* 2010;5(1):40.
24. Lawrence AD, Watkins LH, Sahakian BJ, Hodges JR, Robbins TW. Visual object and visuospatial cognition in Huntington's disease: implications for information processing in corticostriatal circuits. *Brain.* 2000;123:1349-1364.
25. Dumas E, Say M, Jones R, et al. Visual working memory impairment in premanifest gene-carriers and early Huntington's disease. *J Huntingtons Dis.* 2012;1:97-106.
26. Johnson EB, Rees EM, Labuschagne I, et al. The impact of occipital lobe cortical thickness on cognitive task performance: An investigation in Huntington's Disease. *Neuropsychologia.* 2015;79:138-146.
27. Baake V, Coppen EM, van Duijn E, et al. Apathy and atrophy of subcortical brain structures in Huntington's disease: A two-year follow-up study. *NeuroImage Clin.* 2018;19(March):66-70.
28. Hobbs NZ, Pedrick AV, Say MJ, et al. The structural involvement of the cingulate cortex in premanifest and early Huntington's disease. *Mov Disord.* 2011;26(9):1684-1690.
29. van Duijn E, Craufurd D, Hubers AAM, et al. Neuropsychiatric symptoms in a European Huntington's disease cohort (REGISTRY). *J Neurol Neurosurg Psychiatry.* 2014;85(12):1411-1418. doi:10.1136/jnnp-2013-307343.
30. Kevin W, Doug W, Matthias S, Gerhard S. Correspondence of visual evoked potentials with fMRI signals in human visual cortex. *Brain Topogr.* 2008;21(2):86-92.
31. Henning S, Merboldt KD, Frahm J. Simultaneous recordings of visual evoked potentials and BOLD MRI activations in response to visual motion processing. *NMR Biomed.* 2005;18(8):543-552.

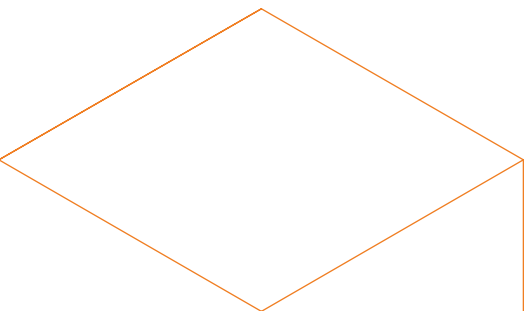


Nederlandse
samenvatting

List of publications

Dankwoord

Curriculum Vitae



SAMENVATTING

De ziekte van Huntington (Huntington's disease, HD) is een zeldzame autosomale dominante neurodegeneratieve aandoening. De ziekte wordt veroorzaakt door een abnormale CAG (cytosine-adenine-guanine) expansie in het huntingtine gen op chromosoom 4, coderend voor het huntingtine eiwit. Hoewel de exacte functie van het normale huntingtine eiwit niet geheel bekend is, is het eiwit betrokken bij de embryonale ontwikkeling en speelt het een belangrijke rol bij axonaal transport, regulatie van gentranscriptie en overleven van zenuwcellen. Het afwijkende huntingtine eiwit bij HD aggregereert in verschillende delen van zenuwcellen en veroorzaakt progressieve hersenschade.

In Nederland zijn er ongeveer 1.700 mensen met genetisch bevestigd HD en zijn er 6.000 tot 9.000 mensen potentieel drager van de genmutatie die zich nog niet hebben laten testen.

Klinisch kenmerkt de ziekte zich door een progressief beloop, zich uitend in bewegingsstoornissen (chorea, dystonie, rigiditeit, balansstoornissen), cognitieve achteruitgang (executieve functiestoornissen, geheugenstoornissen), en gedragsveranderingen (depressie, irritatie, apathie, en obsessief-compulsieve stoornissen). Hoewel symptomen tussen patiënten kunnen variëren in aard en ernst, en psychiatrische of cognitieve klachten al vroeg aanwezig kunnen zijn, wordt de ziekte gedefinieerd als klinisch manifest zodra er motorische symptomen zichtbaar zijn. De ziekte begint meestal rond een leeftijd van 30 tot 50 jaar met een gemiddelde ziekte duur van 17 tot 20 jaar. Ondanks de ontdekking van de chromosomale lokalisatie in 1983 en de specifieke genmutatie in 1993, is er momenteel nog geen genezing of remming van het ziekteproces mogelijk. De symptomatische behandeling is gericht op het verbeteren van de kwaliteit van leven van de patiënt en naasten en bestaat vaak uit medicamenteuze behandeling in combinatie met psychologische en paramedische ondersteuning.

Magnetic resonance imaging (MRI) is een niet-invasieve en objectieve methode om *in-vivo* veranderingen in hersenstructuur en -functie te onderzoeken. Eerdere MRI-studies in HD hebben aangetoond dat volume verlies in het striatum, het belangrijkste neuropathologische kenmerk van HD, al aantoonbaar is in de premanifeste fase, de fase wanneer er nog geen klinische motorische symptomen aanwezig zijn. Naast atrofie in het striatum zijn er ook aanwijzingen voor vroege veranderingen in de cerebrale cortex, maar dit is minder uitgebreid onderzocht (**hoofdstuk 1**).

Het doel van dit proefschrift was de neurodegeneratieve veranderingen in de cerebrale cortex in kaart te brengen in zowel de premanifeste als manifeste fase van de ziekte van Huntington. Met behulp van verschillende MRI-maten en neurofysiologisch onderzoek bieden wij meer inzicht in de structuur en functie van de hersenen in genmutatiedragers met HD ten opzichte van gezonde controles. Daarnaast hebben wij onderzocht of de mate van cerebrale atrofie in HD gerelateerd is aan stoornissen in de motoriek en cognitie.

Macrostructurele veranderingen in het volume van de cortex kunnen onderzocht worden middels diverse methodologische technieken. Standaard volume analyses zijn uitgevoerd met behulp van structurele T1 MRI-scans in een cohort van 79 HD patiënten in een vroeg stadium van de ziekte en 30 gezonde controles (**hoofdstuk 2**). Dit onderzoek toonde aan dat grijze stof veranderingen zichtbaar zijn in de somatosensible en motorische cortex in de frontoparietal kwabben, en in de associatieve visuele cortex in de temporo-occipitaal kwabben. Een toename van chorea was geassocieerd met een afname in volume van het striatum en pallidum, terwijl een toename van oogbewegingsstoornissen was gerelateerd aan afname in volume in corticale gebieden in de occipitale kwab. Dystonie en balansstoornissen waren niet gerelateerd aan volume verlies. Dit kan verklaard worden door het feit dat dystonie, hypokinesie en daaraan gerelateerde balansstoornissen vaker aanwezig zijn in meer vergevorderde stadia van de ziekte, terwijl ons cohort bestond uit patiënten in een vroeg ziektestadium.

Netwerkanalyse is een nieuwe methode om volume veranderingen in de hersenen te bestuderen en kijkt in tegenstelling tot de standaard volume analyse niet op regionaal niveau, maar naar interregionale hersengebieden. Structurele netwerken zijn opgebouwd uit hersengebieden die overeenkomsten in structuur vertonen, waardoor men meer inzicht kan krijgen in ziekte-specifieke veranderingen in de hersenen. Netwerken bestaande uit de precuneus, cortex cingularis anterior, somatosensibele cortex en motorische cortex, lieten een verminderde integriteit zien in premanifest HD (n=30) en manifest HD (n=30) ten opzichte van gezonde controles (n=30) (**hoofdstuk 3**). Verminderde netwerk integriteit van het visuele netwerk (cuneus, gyrus lingualis, cortex occipitalis lateralis) was alleen aanwezig in manifest HD en niet in premanifest HD. Dit betekent dat de overgang van de premanifest naar de manifeste fase wordt gekenmerkt door een toename in corticale veranderingen, met name in de posterior cerebrale cortex.

Globaal dagelijks functioneren wordt in HD onderzoek gemeten middels de totale functionele capaciteit (TFC) score. Op basis van deze score kunnen patiënten in de manifeste fase van de ziekte worden ingedeeld in verschillende ziektestadia, waarbij stadia 1 (HD1) en 2 (HD2) de vroege stadia zijn, en stadia 4 (HD4) en 5 (HD5) de meest gevorderde stadia.

In onze studie met 18 gezonde controles, 31 HD1 patiënten en 43 HD2 patiënten was in beide ziektestadia reeds uitgebreid volume verlies in het striatum aanwezig, met name in de nucleus caudatus (**hoofdstuk 4**). In vergelijking met gezonde controles was er een afname in volume van de nucleus caudatus met 31.1% en 31.4% voor respectievelijk HD1 en HD2 patiënten. Daarnaast toonde analyse van de corticale dikte een afname in de gemiddelde dikte van alle hersenkwabben in HD2 patiënten, met de grootste reductie in corticale dikte in de pariëtale en occipitale kwabben. HD1 patiënten lieten echter geen veranderingen in corticale dikte zien. In de gecombineerde HD1 en HD2 groep was er tevens geen associatie aantoonbaar tussen de mate van atrofie in het striatum en de cortex. Deze bevindingen suggereren dat degeneratie van het striatum onafhankelijk is van corticale degeneratie en dat er sprake is van twee afzonderlijke neurodegeneratieve processen.

Een overzicht van de bestaande literatuur toonde aan dat volumeveranderingen in de posterior cerebrale cortex al vroeg in het ziekte proces ontstaan terwijl fronto-temporale hersengebieden relatief gespaard blijven (**hoofdstuk 5**). Neuropathologische studies hebben aangetoond dat er specifiek verlies is van neuronen in het visuele systeem in het posterieure deel van de hersenen. Dit wordt bevestigd door MRI-studies, die uitgebreide atrofie en verminderde hersenfunctie in de posterior cerebrale cortex in HD laten zien, met name in de cuneus, gyrus lingualis en gyrus fusiformis.

Recente studies tonen tevens aan dat stoornissen van het visuele systeem frequent voorkomen in patiënten met HD, naast de veelvoorkomende symptomen zoals stoornissen in de motoriek, cognitieve achteruitgang en gedragsproblemen. Deze visuele stoornissen kunnen aanwezig zijn in verschillende ziektestadia en bestaan uit visuomotor en visuospatiële dysfunctie, gestoorde visuele attentie en stoornissen in het herkennen van visuele objecten.

Het visuele systeem in de hersenen is echter bij patiënten met HD niet eerder systematisch onderzocht. Daarom hebben wij een exploratieve, observationele studie uitgevoerd in 18 gezonde controles, 22 premanifest HD en 22 manifest HD om meer inzicht te krijgen in de structurele en functionele veranderingen van het visuele systeem. Uitkomsten van structurele en functionele MRI, neurofysiologisch onderzoek en visuele cognitieve neuropsychologische taken zijn verzameld en de bevindingen van deze studie zijn besproken in **hoofdstukken 6 en 7**.

Volume verlies en afname in corticale dikte in manifest HD was aanwezig in de secundaire visuele cortex en associatieve visuele cortex en niet in de primaire visuele cortex. Daarnaast was afname in corticale dikte in de associatieve visuele cortex geassocieerd met een verminderde visuele object perceptie. Structurele integriteit van de axonenbundels in de vezelbanen naar de visuele cortex werden gemeten met behulp van Diffusion Tensor Imaging (DTI). In manifest HD waren aangedane vezelbanen met name gelokaliseerd naar de thalamus en radiatio optica in de occipitaal kwab. Neurofysiologisch onderzoek middels Visual-Evoked Potentials (VEP) liet in premanifest en manifest HD normale geleidingsnelheden (latenties) maar lagere signaalintensiteiten (amplituden) zien na visuele stimulatie. DTI en VEP-onderzoek wijst dus op tekenen van axonale schade in de banen naar de visuele cortex in patiënten met HD.

Een opvallende bevinding was dat in alle groepen een normale neuronale activiteit van de primaire visuele cortex werd gemeten na visuele stimulatie middels functionele MRI, terwijl er afgenomen neuronale activiteit in manifest HD werd waargenomen in de associatieve visuele cortex in rust. De resultaten uit deze studie wijzen derhalve op een normale basale visuele functie ondanks tekenen van axonale schade in de vezelbanen naar de visuele cortex en een gestoorde visuele aandacht en object perceptie in HD patiënten.

Tot slot worden de belangrijkste bevindingen en implicaties voor toekomstige studies besproken in **hoofdstuk 8**. Samenvattend laten de studies beschreven in dit proefschrift zien dat er naast uitgebreide atrofie van het striatum ook corticale atrofie in vroege ziekte stadia kan worden aangetoond met behulp van verschillende methodologische technieken. Corticale atrofie lijkt met name gelokaliseerd in de somatosensibele en motorische cortex in de vroege (pre)klinische ziektestadia, waarna atrofie in het posterieure deel van de cortex meer uitgesproken wordt. Corticale degeneratie blijkt daarnaast ook bij te dragen aan klinische symptomen van HD, zoals oculomotor stoornissen en visueel cognitieve stoornissen. Systematisch onderzoek van de posterior cerebrale cortex toonde tevens dat neurodegeneratieve veranderingen in manifest HD zich met name lokaliseren in de associatieve visuele cortex waarbij de functie en structuur van de primair visuele cortex intact blijft.

Naar aanleiding van onze bevindingen vinden wij dat corticaal volume gebruikt moet worden als uitkomstmaat in klinische HD studies (zoals observationeel en placebo-gecontroleerd medicatie onderzoek), mede omdat de cortex in belangrijke mate bijdraagt aan specifieke stoornissen in de motoriek en cognitie. Naast motorische symptomen kunnen visuele cognitieve stoornissen van grote invloed zijn op algemeen

dagelijks functioneren. Visuele cognitieve achteruitgang kan mogelijk ook een negatief effect hebben op prestaties bij algemeen cognitief onderzoek. Daarom adviseren wij visueel cognitieve taken toe te voegen aan de standaard cognitieve taken die vaak gebruikt worden in klinisch onderzoek naar HD.

Dit onderzoek heeft zich met name gericht op veranderingen in de cerebrale cortex en de invloed daarvan op stoornissen in de motoriek en cognitie in HD. De onderliggende hersenveranderingen van gedragsproblemen in HD is echter niet onderzocht. Gezien de potentieel effectieve huntingtine verlagende geneesmiddelen die momenteel onderzocht worden, is meer observationeel onderzoek uiterst zinvol om de complexe pathologische mechanismen van de ziekte beter in kaart te brengen.

LIST OF PUBLICATIONS

Coppen EM, Jacobs M, van der Zwaan KF, Middelkoop HAM, Roos RAC. Visual object perception in premanifest and early manifest Huntington's disease. *Archives of Clinical Neuropsychology* 2019, E-pub ahead of print.

Coppen EM, van der Grond J, Hafkemeijer A, Barkey Wolf JJH, Roos RAC. Structural and functional changes of the visual cortex in early Huntington's disease. *Human Brain Mapping*. 2018;Dec;39(12):4776-4786.

Coppen EM, van der Grond J, Hart EP, Lakke EAJF, Roos RAC. The visual cortex and visual cognition in Huntington's disease: an overview of current literature. *Behavioural Brain Research*. 2018;351,63-74.

Baake V, **Coppen EM**, van Duijn E, Dumas EM, van den Bogaard SJA, Scahill R, Johnson H, Leavitt B, Durr A, Tabrizi S, Craufurd D, Roos RAC. Apathy and atrophy of subcortical brain structures in Huntington's disease: a two-year follow up study. *NeuroImage: Clinical*. 2018;19:66-70.

Coppen EM, van der Grond J, Roos RAC. Atrophy of the putamen at time of clinical motor onset in Huntington's disease: a 6-year follow-up study. *Journal of Clinical Movement Disorders*. 2018;5(2):1-7.

Coppen EM*, Jacobs M*, van der Grond J, van den Berg - Huysmans AA, Roos RAC. Grey matter volume loss is associated with specific clinical motor signs in Huntington's disease. *Parkinsonism and Related Disorders*. 2018;46:56-61.

Coppen EM, Roos RAC. Current pharmacological approaches to reduce chorea in Huntington's disease. *Drugs*. 2017;77:29-46.

Coppen EM, van der Grond J, Hafkemeijer A, Rombouts SARB, Roos RAC. Early grey matter changes in structural covariance networks in Huntington's disease. *NeuroImage: Clinical*. 2016;12:806-814.

* these authors contributed equally

Submitted articles

Jacobs M, **Coppen EM**, Roos RAC. Reasons for unemployment and driving cessation in Huntington's disease gene carriers. – Submitted

Coppen EM, Hafkemeijer A, Barkey Wolf JJH, van der Grond J, Roos RAC. Patterns of corticostriatal degeneration in early Huntington's disease patients. – Submitted

Coppen EM, Hafkemeijer A, van der Grond J, Reijntjes RHAM, Tannemaat MR, Roos RAC. The visual pathway in Huntington's disease: a diffusion tensor imaging and neurophysiological study. – Submitted

van Diemen MPJ, Kan H, van der Grond J, van Beelen I, Hart EP, **Coppen EM**, Winder JY, den Heijer J, Webb A, Roos RAC, Groeneveld GJ. There is no correlation between mitochondrial function in the brain and skeletal muscle in Huntington's disease. – Submitted

van Diemen MPJ, Hart EP, Kan H, van der Grond J, Bergheanu S, Abbruscato A, Mead L, **Coppen EM**, Winder JY, van Beelen I, Webb A, Roos RAC, Groeneveld GJ. A two-part study to assess the safety, pharmacokinetics and pharmacodynamics of SBT-020 in patients with early stage Huntington's disease. – Submitted

DANKWOORD

Mijn grootste dank gaat uit naar alle patiënten en hun familieleden die hebben deelgenomen aan onze onderzoeken. Ik hoop dat er in de toekomst een behandeling komt voor deze vreselijke ziekte.

Professor Roos, dank dat u uw jarenlange kennis over de ziekte van Huntington met mij wilde delen. Uw geduld en begrip voor patiënten zijn waardevolle eigenschappen die ik mee zal nemen in mijn verdere carrière.

Jeroen, onze wekelijkse overleggen waren niet alleen leerzaam, maar ook gezellig. Dank voor je adviezen, interesse, feedback en inperken van mijn uiteenlopende ideeën voor nieuwe artikelen.

Paranimfen Milou en Anne, dank voor alle gezelligheid aan het eiland en het harde samenwerken bij de MRI scan en op het lab! Milou, dank dat je mijn artikelen van jouw scherpe mening wilde voorzien. Dankzij jou heb ik SPSS leren begrijpen en waarderen. Ik ben er trots op dat ons gezamenlijke paper in mijn boekje terecht is gekomen. Anne, jouw enthousiasme en betrokkenheid voor het Huntington onderzoek hebben aanstekelijk op mij gewerkt. Dank voor de support, alle bijzondere momenten en het vele lachen. Ik ga jullie missen als collega's, maar ben ontzettend blij dat we samen mijn promotie kunnen afronden. Ciao-ciao!

J3-162 kamergenoten! Dank voor alle steun, de lekkere snoep-pot en het aanhoren van al mijn irritaties over de NS, printer issues en administratieve eigenaardigheden. Kasper, succes met je eigen onderzoek! Jessica, ik hoop je nog vaak te zien bij de nascholing.

HD-onderzoekers Marye, Marit, Stephanie en Jantine, dank voor de fijne samenwerking en veel succes bij de interessante studies die gaan komen. Alle onderzoekers, neuropsychologen, KNF-laboranten en neurologen van J3, dank voor alle gezellige momenten in de koffiekamer en tijdens de KNF uitjes.

Co-auteurs, veel dank voor jullie bijdrage en samenwerking. Annette, jouw pipelines en scriptjes hebben mijn FSL analyses een stuk overzichtelijker gemaakt! Anne, dank voor de vele adviezen over goede registraties, mooie figuren, klustips en alle andere gezellige gesprekken.

Lieve familie en vrienden, dank voor jullie interesse en nodige afleiding de afgelopen jaren. In het bijzonder gaat mijn dank uit naar mijn ouders, dat jullie mij altijd hebben gemotiveerd om door te leren en voor jullie onvoorwaardelijke steun.

Lars en Jaap, dank voor jullie liefde en dat jullie altijd voor mij klaar staan. Lars, de figuren en omslag in dit proefschrift zijn prachtig. Heel veel dank voor je steun, hulp en geduld. Op naar onze toekomst samen in ons mooie nieuwe huis!

CURRICULUM VITAE

Emma Coppen werd geboren op 15 oktober 1987 te Amsterdam. Na het behalen van haar VWO diploma in 2005 aan het Amstelveen College, begon zij aan de studie geneeskunde aan de Universiteit van Amsterdam. Als onderdeel van het doctoraal examen volgde zij een wetenschapsstage bij het Nederlands Herseninstituut in Amsterdam naar multipotente neuronale stamcellen in de sub-ventriculaire zone bij patiënten met multiple sclerose. Haar enthousiasme voor de neurologie groeide verder tijdens haar coschappen die zij afrondde met een oudste coschap op de afdeling neurologie in het Slotervaartziekenhuis in Amsterdam en een extra coschap op de afdeling neurochirurgie in het dr. Cipto Mangunkusumo ziekenhuis in Jakarta, Indonesië.

Het artsexamen behaalde zij in 2012, waarna zij aansluitend heeft gewerkt in het Diakonessenhuis te Utrecht en in het Groene Hart ziekenhuis te Gouda als arts-assistent neurologie.

Eind 2014 begon zij aan haar promotietraject onder leiding van Prof. dr. R.A.C. Roos in het Leids Universitair Medisch Centrum (LUMC) bij de afdeling neurologie in samenwerking met dr. J. van der Grond van de afdeling radiologie. Tijdens haar promotieonderzoek was zij tevens als onderzoeksarts nauw betrokken bij internationale studies naar de effectiviteit van symptomatische behandelingen en de longitudinale observationele Enroll-HD studie van het European Huntington's Disease Network (EHDN) en de Huntington Study Group (HSG). Na haar promotietraject is zij als arts-assistent neurologie werkzaam geweest in het Reinier de Graaf Gasthuis in Delft. Per april 2019 is zij gestart met de opleiding tot neuroloog in het LUMC.



2019